Harvard University
Department of Mathematics

Lefschetz Fibrations on 4-Manifolds

Author:
Gregory J. Parker
gparker01@college.harvard.edu

Advisor:
Prof. Clifford Taubes

This thesis is submitted in partial fulfillment of the requirements for the degree of Bachelor of Arts with Honors in Mathematics and Physics.

March 20, 2017

Contents

Acknowledgements: First and foremost, I would like to thank my advisor, Clifford Taubes, for his guidance throughout the process of learning this material and writing this thesis. His insights and suggestions have helped me grow as a writer and as a mathematician. Second, I would like to thank Roger Casals for inspiring me to learn these topics and for sharing his expertise on them. In particular, he taught me the material that appears in Chapter 2. I would also like to thank Matt Hedden and Selman Akbulut for helpful conversations regarding the material in Chapter 4. Finally, I would like to thank my friends and family for their support and encouragement over the course of this project.

Recommended Background: Throughout this thesis, it is assumed that the reader is familiar with smooth manifolds, say at the level of [1], and Morse theory both in the language of handle attachments, as in [2], and in the language of gradient flows, as in [3]. The language of homology and cohomology at the level of [4] is also used throughout without exposition. For Chapter 3 in particular, some familiarity with connections and curvature is also helpful [5].

Introduction

Morse theory studies the topology of smooth manifolds by analyzing the critical points of generic smooth functions on them. It is one of the most fruitful tools in differential topology, and since its invention, it has been applied to almost every area of geometry and topology from the classification of compact surfaces to the study of infinite-dimensional manifolds in Floer theory.

The basic premise of Morse theory is to consider a **Morse function** on a manifold, i.e. a function with non-degenerate critical points. A fundamental lemma is:

Lemma 0.1. *Let X be a smooth manifold and $f : X \to \mathbb{R}$ a Morse function . If the interval (a, b) contains no critical values, then the level sets $f^{-1}(c)$ are smooth submanifolds and are diffeomorphic for all $c \in (a, b)$.*

This is proved by flowing along a normalized negative gradient. This lemma implies that the topology of the level sets can only change when crossing a critical value. At the critical value itself, the level set is a not a submanifold, and is instead a **singular** level set.

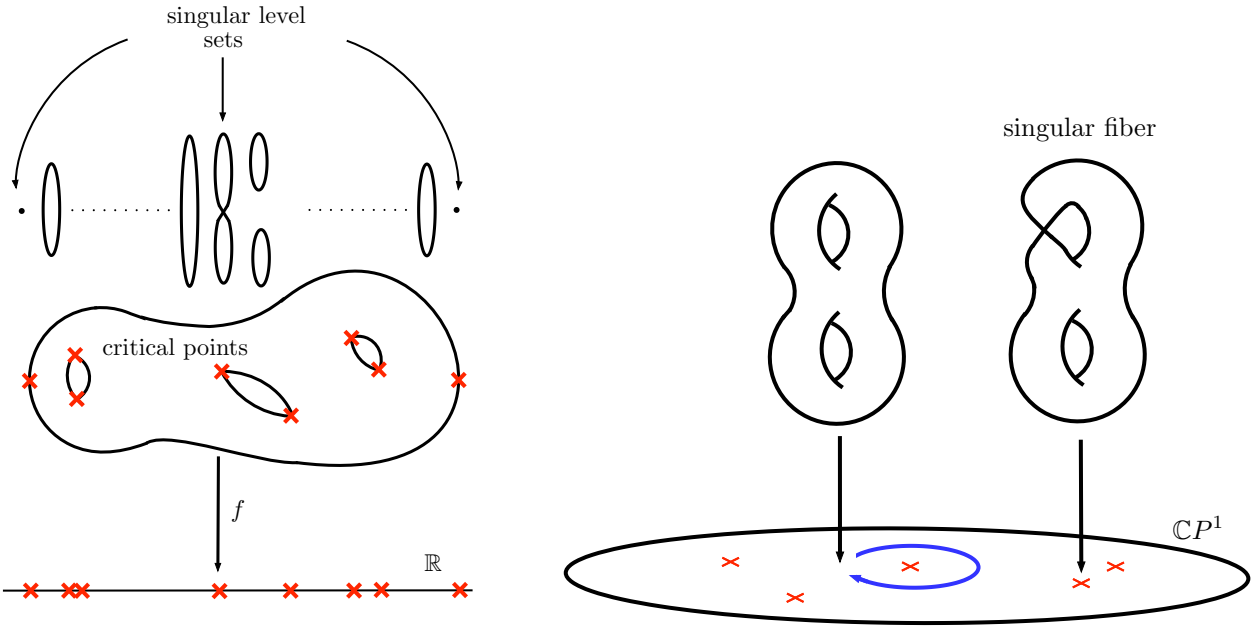

Figure 1: (Left) a smooth manifold with a Morse function f. Critical points and critical values are indicated by crosses (red). The level sets of f (top) are smooth submanifolds except at level sets containing a critical point, which are singular level sets. (Right) a Lefschetz fibration above a region of the Riemann sphere. There can be non-trivial monodromy around loops encircling critical points, such as the one indicated (blue).

Lefschetz fibrations, originally due to Solomon Lefschetz, are the holomorphic analogue of Morse functions and have proved equally fruitful in their application. Here, one takes a holomorphic function to the complex numbers or the Riemann sphere $\mathbb{C}P^1$ with non-degenerate critical points. Similar to the real case, the fibers away from the critical values are all diffeomorphic submanifolds, and there are singular fibers above the critical values. In the holomorphic case, however, one can ask the additional question of what happens when considering the fibers above a path that encircles a critical value. Looping around a path that encircles a critical value will result in a non-trivial twisting of the fiber above the base point of the loop. This action is called the **monodromy** and understanding it is a central question in the study of Lefschetz fibrations.

The goal of this thesis is to give an introduction to the theory and applications of Lefschetz fibrations in smooth topology. Lefschetz fibrations were originally developed in the context of complex algebraic varieties, and have been a standard tool in algebraic geometry for decades. In 1995, however, a startling theorem of Simon Donaldson proved the existence of Lefschetz fibrations on compact symplectic manifolds, which need not have a holomorphic structure. Since then, Lefschetz fibrations and slight generalizations of them called broken Lefschetz fibrations have been defined on arbitrary smooth 4-manifolds. In all these cases, Lefschetz fibrations have a chance to reduce the study of the geometry and topology of compact manifolds to the study of the monodromy around critical points, which is, in principle, a question only about the self-diffeomorphisms of fibers.

For the majority of this exposition, the focus will be on manifolds whose real dimension is 4. There are two main reasons for this. First, Lefschetz fibrations are an especially powerful tool in 4 dimensions. A Lefschetz fibration will, up to the critical fibers, decompose a 4-manifold into a fiber bundle of surfaces over another surface. Explicit understanding of (real) surfaces and their diffeomorphisms can provide significant insight into 4-dimensional topology that is lost in higher dimensions. Second, 4-manifolds are the most interesting case from the perspective of smooth topology. In many ways, 4-manifolds are more complicated than either lower or higher dimensional manifolds. In low dimensions, there are simply not many possibilities for complexity. The Geometrization conjecture and the 3-dimensional Poincaré conjecture were resolved by G. Perelman in 2003, yielding a relatively complete understanding of 3-manifolds [6]. In dimensions strictly greater than 4, there is more fluidity than in 4-dimensions. For example, the "Whitney Trick" allows one to "untangle" submanifolds by moving them past each other in the extra dimensions. S. Smale used this trick to resolve the Poincaré conjecture in dimension $\geqslant 5$ in 1961 [7], showing that certain aspects of high dimensional topology are quite tractable. The smooth Poincaré Conjecture in 4 dimensions remains open, and symbolizes the lack of understanding in this boundary case between the simplicity of low dimensions and the fluidity of high dimensions.

The discovery of exotic smooth structures on 4-manifolds [8] added further complexity to the study of 4-manifolds. Seiberg-Witten theory, developed in the 1980s, gave a fleeting hope that a classification of 4-manifolds would be possible. Since then, however, many new examples of strange and exotic 4-manifolds have been constructed, and Seiberg-Witten theory has thus far been unable to parse the complexity of 4-manifolds. As of 2017, the study of 4-manifold topology remains a quagmire that defies understanding. Lefschetz fibrations have been on both sides of the study of 4-manifolds, at times being used to aid understanding of 4-manifolds, while at others being used in bizarre and counter-intuitive constructions.

This thesis is divided into four chapters. Chapter 1 discusses Lefschetz fibrations in the classical setting of complex algebraic varieties. This includes the basic definitions, the Picard-Lefschetz Theorem, which is the essential result for understanding the monodromy of Lefschetz fibrations, and results relating the monodromy to the topology of the manifold. Chapter 2 introduces a computational process that allows the results of Chapter 1 to be realized concretely on specific varieties. Chapter 3 gives a survey of Donaldson's theorem on the existence and uniqueness of Lefschetz fibrations on compact symplectic manifolds. The majority of this chapter is devoted to the development of "approximately-holomorphic" theory and has a rather more geometric flavor than the other chapters. Chapter 4 discusses more recent results about generalizations of Lefschetz fibrations on arbitrary smooth 4-manifolds, many of which are due to Robion Kirby and David Gay.

Chapter 1

Lefschetz Fibrations on Complex Algebraic Varieties

1.1 Lefschetz Pencils and Fibrations

This section gives the basic definitions and constructions of Lefschetz fibrations on complex algebraic varieties. Lefschetz fibrations in this case arise from preliminary structures called Lefschetz pencils.

The construction of Lefschetz pencils is a holomorphic analogue of a height function on a compact smooth manifold embedded in Euclidean space. Given such a manifold $M \subseteq \mathbb{R}^N$ a "height" function can be constructed on it by choosing a vector v and taking the projection to the span $\mathbb{R}v$. It can be shown that this projection is a Morse function for almost every $v \in \mathbb{R}^N$. Viewed another way, choosing v specifies a smoothly varying family of hyperplanes H_t for $t \in \mathbb{R}$ — the planes perpendicular to v — such that $\bigsqcup_t H_t = \mathbb{R}^N$ and the height function is $f : M \to \mathbb{R}$ is defined by $f(x)$ being the unique t_0 such that $x \in H_{t_0}$. The intersections $M \cap X_t$ are the level sets of f and are submanifolds for all but finitely many values of t, at which there are singular level sets. Lefschetz pencils are constructed the same way: by taking parameterized families of complex hyperplanes or hypersurfaces and projecting to the parameter.

First, pencils are defined on projective spaces. After this, they can be defined on smooth varieties. Throughout, let $[z_0; \ldots; z_N]$ denote projective coordinates (equivalence classes under the action of $\mathbb{C}^\times$) on $\mathbb{C}P^N$. Let $\mathbb{P}(d, N)$ be the projective space of homogenous degree d polynomials in $N+1$ complex variables $z_0, ..., z_N$. These are the polynomials well-defined on $\mathbb{C}P^N$. Consider a degree 1 holomorphic embedding

$$\mathbb{C}P^1 \longrightarrow \mathbb{P}(d, N). \tag{1.1.1}$$

Such an embedding results in a polynomial $P_{[t_0;t_1]}$ for each $[t_0; t_1] \in \mathbb{C}P^1$. In fact, by a choice of basis, one may choose two polynomials P_0 and P_1 such that the embedding takes the form

$$[t_0; t_1] \mapsto t_0 P_0 + t_1 P_1. \tag{1.1.2}$$

Definition 1.1. *A* **pencil of degree** d *on* $\mathbb{C}P^N$ *is a family of hypersurfaces* $H_{[t_0;t_1]} \subseteq \mathbb{C}P^N$ *of degree* d *for* $[t_0; t_1] \in \mathbb{C}P^1$ *where the hypersurfaces* $H_{[t_0;t_1]}$ *are the zero sets of the polynomials* $P_{[t_0;t_1]}$ *resulting from an embedding of the form (1.1.1).*

The first fact about pencils is that for a pencil on $\mathbb{C}P^N$, a point either lies in exactly one of the hyperplanes $H_{[t_0;t_1]}$ or in all of them. More precisely, there is the following dichotomy:

Proposition 1.2. *For each* $[z_0; \ldots; z_N] = z \in \mathbb{C}P^N$ *either* $z \in \bigcap_{[t_0;t_1]} H_{[t_0;t_1]}$ *or there is a unique* $[t_0; t_1]$ *such that* $z \in H_{[t_0;t_1]}$.

Proof. Choose polynomials P_0, P_1 so that the pencil is given by an embedding of the form (1.1.2). Pick an arbitrary $z \in \mathbb{C}P^N$. The first step is to show there is some $[t_0; t_1] \in \mathbb{C}P^1$ so that $z \in H_{[t_0;t_1]}$. This is clear, however, since choosing $[t_0; t_1] = [P_1(z); -P_0(z)]$ gives

$$t_0 P_0(z) + t_1 P_1(z) = 0.$$

Hence $z \in H_{[t_0;t_1]}$ for these values of t_0, t_1.

Now, assume there are two distinct points $[t_0; t_1], [t'_0; t'_1] \in \mathbb{C}P^1$ so that $z \in H_{[t_0;t_1]} \cap H_{[t'_0;t'_1]}$. Then z must solve the system of equations

$$\begin{cases} 0 = t_0 P_0(z) + t_1 P_1(x) \\ 0 = t'_0 P_0(z) + t'_1 P_1(x). \end{cases}$$

For any other $[s_0; s_1] \in \mathbb{C}P^1$, there must be complex numbers $a, b \in \mathbb{C}$ so that $a[t_0; t_1] + b[t'_0; t_1] = [s_0; s_1]$. This is simply because the matrix

$$\begin{pmatrix} t_0 & t'_0 \\ t_1 & t'_1 \end{pmatrix}$$

is non-singular, as it being singular would imply $[t_0; t_1] = [t'_0; t'_1]$, and contradicting the assumption these were distinct. For such a choice of a, b one then has

$$s_0 P_0(z) + s_1 P_1(z) = a P_{[t_0;t_1]}(z) + b P_{[t'_0;t'_1]}(z) = 0.$$

Thus $z \in H_{[s_0;s_1]}$ for all $[s_0; s_1] \in \mathbb{C}P^1$. In fact, choosing $[s_0; s_1] = [1; 0]$ and $[0; 1]$ shows that at any z in more than a single $H_{[t_0;t_1]}$ both $P_0(z)$ and $P_1(z)$ must vanish. □

Definition 1.3. *The intersection $B := \bigcap_{[t_0;t_1] \in \mathbb{C}P^1} H_{[t_0;t_1]}$ is called the* **base locus** *of a pencil. When the pencil is given by two polynomials as in (1.1.2), B is the mutual vanishing locus.*

Example 1.4. In the case of degree $d = 1$, a pencil can be constructed by taking a codimension 2 projective space $\mathbb{C}P^{N-2} \simeq A \subseteq \mathbb{C}P^N$ called the **axis** and letting the pencil of hyperplanes be given by all the hyperplanes containing A, which can be parameterized by $\mathbb{C}P^1$.

For a specific example, take $\mathbb{C}P^3 = \{[z_0; z_1; z_2; z_3]\}$ and $A = \{[0; 0; z_2; z_3]\} \simeq \mathbb{C}P^1$. Then, for each $[t_0; t_1] \in \mathbb{C}P^1$ let $H_{[t_0;t_1]}$ be the hyperplane given by the embedding

$$[w_0; w_1; w_2] \mapsto [w_0 t_0 \ ; \ w_0 t_1 \ ; \ w_1 \ ; \ w_2].$$

Alternatively, $H_{[t_0;t_1]}$ is given as the zero-set of $t_0 P_0 + t_1 P_1$ where $P_0 = -z_1$ and $P_1 = z_0$. These hyperplanes cover all of $\mathbb{C}P^3$ and the base locus is their mutual intersection $A = \{[0; 0; z_2; z_3]\}$. □

Now pencils may be defined on smooth complex varieties. Let $X \subseteq \mathbb{C}P^N$ be a smooth variety of (complex) dimension n. A **pencil on X** is the restriction of a pencil on the ambient space $\mathbb{C}P^N$. Thus if $H_{[t_0;t_1]}$ is a pencil on $\mathbb{C}P^N$, one obtains a codimension 1 subvariety $F_{[t_0;t_1]} := H_{[t_0;t_1]} \cap X$ for each $[t_0; t_1] \in \mathbb{C}P^1$ called the **fiber** above $t = [t_0; t_1]$, and a codimension 2 subvariety $B_X = B \cap X$, which is still called the base. A pencil on X comes with a map $f : X \setminus B \to \mathbb{C}P^1$ that sends each $x \in X$ to the unique $[t_0; t_1]$ such that $x \in H_{[t_0;t_1]}$. In fact, by the proof of Proposition 1.2 this map is $[P_1; -P_0]$ so it is holomorphic.

Definition 1.5. *A pencil on X is said to be a* **Lefschetz pencil** *if the following two conditions are satisfied:*

- *The base $B_X \subseteq X$ is a smooth submanifold of (complex) codimension 2.*
- *The map $f : X \setminus B \to \mathbb{C}P^1$ has non-degenerate critical points with distinct critical values.*

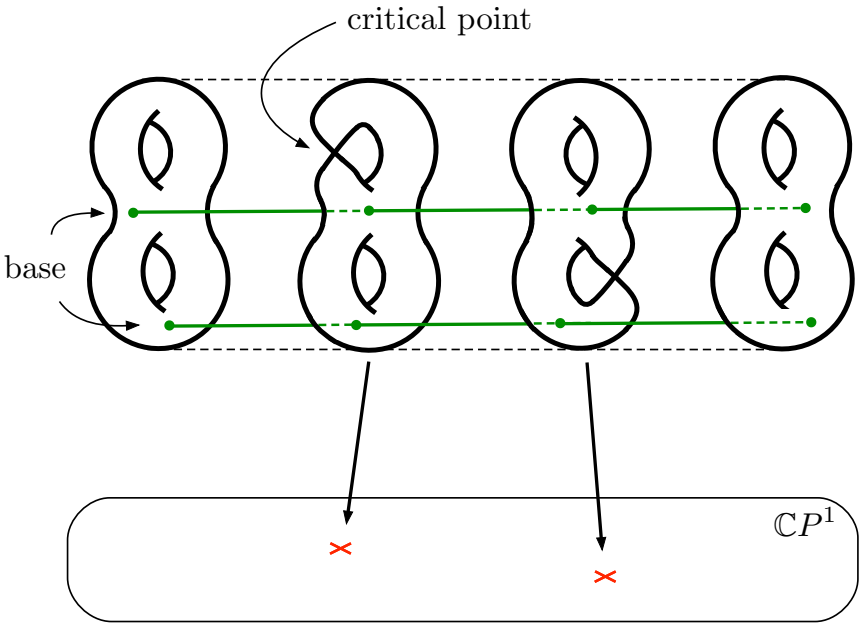

Figure 1.1: A Lefschetz pencil above a region in $\mathbb{C}P^1$. The critical values are indicated by crosses, and the singular fibers lie above them. The base locus (isolated points in this dimension), is the intersection of the fibers. Here, each line (green) represents a single base point that lies in all fibers simultaneously.

By a slight abuse of terminology, the map f itself is often called the Lefschetz pencil. A few things should be noted immediately.

(I) The critical points of f occur exactly where the hyersurfaces $H_{[t_0,t_1]}$ are not transvsere to X. This is because a critical point occurs where the tangent space $TX \subseteq \ker(df) = H_{[t_0;t_1]}$. Since the codimension is 1, if $TX \nsubseteq H_{[t_0;t_1]}$ then it is transverse. For every $t \in \mathbb{C}P^1$ that is *not* a critical value, one has transversality and the pre-image $F_{[t_0;t_1]} = X \cap H_{[t_0;t_1]}$ is a smooth submanifold of (complex) codimension 1. It is closed as a submanifold of X, thus the fibers of $f : X \setminus B \to \mathbb{C}P^1$ are these closed surfaces $F_{[t_0;t_1]}$ with the base B_X removed from each, since f is not defined there.

(II) In fact, if letting $A \subseteq X$ be the set of critical points with critical values $f(A)$:=crit(f), the restriction $f| : X \setminus (B \cup A) \to \mathbb{C}P^1 \setminus \text{crit}(f)$ has mutually isomorphic fibers. Moreover, by a slight extension of Lemma 0.1 called the Ehresmann's fibration lemma (see Lemma 1.17 below), it follows that the restriction $f| : X \setminus (B \cup A) \to \mathbb{C}P^1 \setminus \text{crit}(f)$ is a fiber bundle. The smooth fibers are called **regular fibers**.

(III) Above each point of the finite set crit(f) of critical values there are **singular fibers**. In fact, as will be shown in a later section, the non-degeneracy condition implies these fibers have only simple nodal singularities.

Understanding the topology of a Lefschetz pencil therefore requires understanding two things: the diffeomorphism type of the smooth fibers $F_{[t_0;t_1]}$, and the monodromy of the fiber bundle around the isolated points of crit(f). Section 1.3 will show that knowing these two things results in a relatively complete description of the topology of X. This issue of understanding the topology of X through the topology of fibers and the monodromy around critical points will be a theme throughout the following sections and chapters. We are getting ahead of ourselves, however; it should first note that the objects being studied actually exist. In fact, just as with Morse functions, they are in abundance:

Theorem 1.6. *A generic pencil is Lefshchetz.*

The proof of this theorem would be a rather long excursion into algebraic geometry, so it is omitted here and the reader is referred to [9, 10].

One should note, however, a slight distinction from the case of smooth real-valued Morse functions. There, a smooth function that is *not* Morse can always be perturbed in neighborhoods of the critical points to become Morse. By using a partition of unity to do the perturbation locally, it can be arranged that the function remains unchanged away from these neighborhoods. In the holomorphic setting of Lefschetz pencils, there is no such local freedom. If one encounters a pencil that is not Lefschetz, the entire pencil must be perturbed to make it so.

Example 1.7. Consider the smooth variety $\mathbb{C}P^2 \subseteq \mathbb{C}P^3$ given in projective coordinates by $[z_0; z_1; z_2; 0]$. Example 1.4 showed that the hyperplanes $H_{[t_0;t_1]} = [w_0 t_0 \ ; \ w_0 t_1 \ ; \ w_1 \ ; \ w_2]$ form a pencil on $\mathbb{C}P^3$. Intersecting with $\mathbb{C}P^2$ results in a pencil on $\mathbb{C}P^2$ with fibers

$$F_{[t_0;t_1]} = [w_0 t_0 \ ; \ w_0 t_1 \ ; \ w_1] \subseteq \mathbb{C}P^2$$

which are embedded copies of $\mathbb{C}P^1$. It is relatively easy to check that this function has no critical points, hence this pencil is trivially Lefschetz. There is a single base point at $[0; 0; 1]$, thus the map $f : \mathbb{C}P^2 - \{[0; 0; 1]\} \to \mathbb{C}P^1$ given by $f([z_0 \ ; \ z_1 \ ; \ z_2]) := [z_0; \ z_1]$ has only regular fibers that are (embedded) complex lines with a single point removed, hence in this case f is a fiber bundle.

Example 1.8. (Elliptic Pencils) For a slightly more interesting example, let $\mathbb{C}P^2 \subseteq \mathbb{C}P^3$ as before, but choose two generic cubics C_0 and C_1. Consider the pencil defined by the family of cubic hypersurfaces $H_{[t_0;t_1]} = t_0 C_0 + t_1 C_1$. Each fiber $H_{[t_0;t_1]} \cap \mathbb{C}P^2$ is then a cubic hypersurface inside $\mathbb{C}P^2$, i.e. they are elliptic curves. In general, a pencil whose fibers are elliptic curves is called an elliptic pencil. Two elliptic curves in $\mathbb{C}P^2$ will have 9 points of intersection, since the both represent $3d \in H^2(\mathbb{C}P^2; \mathbb{Z})$ where d is the generator. Thus in this case the base locus B consists of nine points, and one obtains a Lefschetz pencil

$$f : \mathbb{C}P^2 \setminus \{9 \ pts\} \to \mathbb{C}P^1$$

$$[z_0; z_1; z_2] \mapsto [C_1(z); -C_0(z)]$$

Unlike in the previous example, this pencil has critical points. Thus the map f is no longer a true fiber bundle over $\mathbb{C}P^1$, and instead has several singular fibers lying above isolated critical points. In fact, techniques developed in Section 1.3 will show the number of singular fibers is exactly 12.

Example 1.9. Let $C \subseteq \mathbb{C}P^N$ be a complex curve. A Lefschetz pencil on C is the same as branched cover $f : C \to \mathbb{C}P^1$ with only doubly ramified points. Here, the base locus of codimension 2 will generically be disjoint from C, hence a Lefschetz pencil is defined on all of C, giving a holomorphic map $f : C \to \mathbb{C}P^1$. The non-degeneracy condition guarantees the critical points of f, which are the ramification points, are locally modeled by $z \mapsto z^2$, hence there can be only doubly ramified points.

The Blow-up Process

It can be slightly annoying that a Lefschetz pencil comes equipped only with a map not defined on the total space. The blow-up process will convert a Lefschetz pencil into a map on a closed manifold related to the original space. The result of blowing-up a Lefschetz pencil will be a Lefschetz fibration, which is defined precisely below. The blow-up process is a standard tool in algebraic geometry, and a more detailed description can be found in many standard texts, such as [11].

Definition 1.10. *Define the* **Modification** *or* **Blow-up** $\hat{X}$ *of* X *by*

$$\hat{X} = \{(x, t) \mid x \in H_t\} \subseteq X \times \mathbb{C}P^1.$$

The blow-up comes with two natural projections.

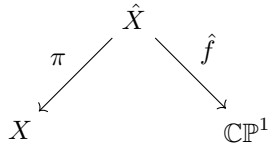

The fiber $\hat{f}^{-1}(t)$ above some $t \in \mathbb{C}P^1$ is $F_t \times \{t\} = \{(x,t) \mid x \in H_t\} \simeq F_t$. In contrast to the pencil f, the fibers are now entire closed surfaces, and the base locus is no longer removed from each. For the other projection, the fiber above some $x \in X$ depends on whether or not $x \in B_X$. If $x \notin B_X$ there is exactly one $t_x \in \mathbb{C}P^1$ so that $x \in H_{t_x}$, hence $\pi^{-1}(x) = \{x\} \times \{t_x\}$. If $x \in B_X$, then $x \in H_t$ for all $t \in \mathbb{C}P^1$ by definition, hence the fiber is $\pi^{-1}(x) = \{x\} \times \mathbb{C}P^1$. Intuitively, the blow-up process replaces each point of the base with the projective space of all lines going through that point, so topologically it attaches a copy of $\mathbb{C}P^1$ at each point of B.

Proposition 1.11. *If a pencil is Lefschetz, then the blow-up $\hat{X}$ is a smooth manifold and has the same dimension as X.*

Proof. (Sketch) consider the subset $W := \{(x,P) \mid x \in P^{-1}(0)\} \subseteq X \times \mathbb{P}(d,N)$ where, recalling that $X \subseteq \mathbb{C}P^N$, $P^{-1}(0)$ is the vanishing locus of the polynomial P on $\mathbb{C}P^N$ intersected with X. W is a codimension 1 variety, since it is cut out by a single condition. The Lefschetz pencil resulted from an embedding $L : \mathbb{C}P^1 \to \mathbb{P}(d,N)$.

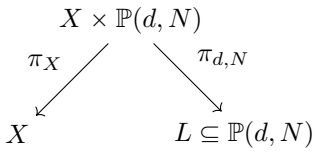

By definition, $\hat{X} = \{(x,P) \mid (x,P) \in W, \ , P \in L\} = W \cap \pi_{d,N}^{-1}(L)$. Thus $\hat{X}$ is smooth exactly when $\pi_{d,N}|_W$ is transverse to L. The proof of Theorem 1.6 [9, 10], however, shows that this transversality condition, which will be satisfied generically, is satisfied for the generic subset of pencils that are Lefschetz. Alternatively, it could have been required in the definition of Lefschetz pencil that $\hat{X}$ is smooth, and the proof and strength of Theorem 1.6 would not change. □

In general, after blowing-up, the fibers of $\hat{f}$ are now closed surfaces. Before blowing-up, each fiber F_t of f was a closed surface with the (complex) codimension 1 base removed. Blowing-up attaches a copy of $\mathbb{C}P^1$ for each $b \in B_X$, and the fibers F_t become disjoint closed surfaces where for each $[t_0;t_1] \in \mathbb{C}P^1$, $F_t \cap B_X$ has been filled in with the points of $(b,t) \in \hat{X}$ for that t. Thus blowing-up turns each shared base point into a projective line, giving one point to fill in each fiber.

Definition 1.12. *The map $\hat{f} : \hat{X} \to \mathbb{C}P^1$ that results from blowing-up a Lefschetz pencil f is called a* **Lefschetz fibration**.

Remark 1.13. (Blow-ups on 4-manifolds) The blow-up process has a particularly nice topological description when $\dim_{\mathbb{R}}(X) = 4$. In this case, the base B_X is a discrete set, and the fibers F_t of f are surfaces punctured where they meet the base.

Let

$$\tau = \{(t,v) \mid v \in t\} \subseteq \mathbb{C}P^1 \times \mathbb{C}^2$$

be the tautological bundle. It comes with a projection to $\mathbb{C}^2$, which restricts to a diffeomorphism

$$\Psi : \tau \setminus \{\text{zero-section}\} \simeq \mathbb{C}^2 - \{0\}$$

with inverse given by $v \in \mathbb{C}^2 \mapsto (\mathbb{C}v, v)$. At a base point $b \in B$ one can define a local diffeomorphism of τ with a region where the blow-up took place. Let $\varphi : B^4 \subseteq \mathbb{C}^2 \to X$ be a chart centered at b. Then consider the map defined on $(\mathrm{Im}(\varphi) \times \mathbb{C}P^1) \cap \hat{X} \longrightarrow \tau$ given by

$$\begin{cases} (x,t) \mapsto \Psi^{-1} \circ \varphi^{-1} \circ proj_X(x,t) & x \notin B \\ (b,t) \mapsto (t,0) \in \tau \end{cases}$$

This map is clearly a bijection with the unit disk bundle $\mathbb{D}(\tau) \subseteq \tau$, and one can readily check that it is smooth. Thus the blow-up process has effectively removed a $B^4 \subseteq \mathbb{C}^2$ region around b whose boundary is S^3 and glued in a copy of the disk bundle $\mathbb{D}(\tau)$, which also has boundary S^3 given by the Hopf fibration. The new zero-section of τ is called the **exceptional sphere** of the blow-up. It provides another generator in $H_2(\hat{X};\mathbb{Z})$ with self-intersection -1 compared to $H_2(X;\mathbb{Z})$.

One can also show that for a neighborhood U of $[0;0;1] \in \mathbb{C}P^2$ one has a diffeomorphism $\overline{\mathbb{C}P^2} \setminus U \simeq \mathbb{D}(\tau)$ given by $[z_0;z_1;z_2] \mapsto ([z_0;z_1], z_2)$, and where $\overline{\mathbb{C}P^2}$ is the same as $\mathbb{C}P^2$ but with the orientation opposite the standard orientation from the complex structure. To see this change of orientation is necessary, one need only check that the bundle orientation of τ (i.e. zero-section $\wedge$ fibers) is opposite the standard orientation on $\mathbb{C}P^2$, and so this diffeomorphism is orientation-reversing. Therefore, the effect of cutting out a B^4 and gluing in $D(\tau)$ is exactly connect summing with $\overline{\mathbb{C}P^2}$. In summary, this gives:

Fact 1.14. *If $\dim_{\mathbb{R}}(X) = 4$ with discrete base locus $B = \{b_1, ..., b_n\}$, the blow-up $\hat{X}$ is*

$$\hat{X} \simeq X \# n(\overline{\mathbb{C}P^2})$$

where each connect sum is done in a neighborhood of each b_i.

It can also now explicitly be seen how blowing-up makes the fibers disjoint. Given two curves C_1, C_2 that intersect transversally at b_i, one can embed $C_j - \{b_i\}$ for $j = 1, 2$ into $\hat{X}$. In $\hat{X}$, the closures $\overline{C_j - \{b_i\}}$ will be disjoint, with the puncture at b_i being filled in respectively by $(t_i, 0)$ in the zero-section of the new copy of τ attached at b_i, where t_i is the complex line tangent to C_i at the puncture. In the case of the curves being the punctured fibers F_t, these closures are the new closed fibers of the fibration $\hat{f}$. □

Example 1.7 Revisited: Blowing-up the Lefschetz pencil with a single base point in Example 1.7 gives a Lefschetz fibration $f : \mathbb{C}P^2 \# \overline{\mathbb{C}P^2} \to \mathbb{C}P^1$. The fibers are closed copies of $\mathbb{C}P^1$, this fibration expresses $\mathbb{C}P^2 \# \overline{\mathbb{C}P^2}$ topologically as an S^2 bundle over S^2. However, it is not $S^2 \times S^2$, since the cup product on cohomology differs from that of the trivial bundle.

Example 1.8 Revisited: Blowing-up the Lefschetz pencil in Example 1.8 results in Lefschetz fibration on the total space $\hat{X} \simeq \mathbb{C}P^2 \# 9(\overline{\mathbb{C}P^2})$ whose fibers are elliptic curves (including some singular ones). This total space is the **Elliptic Surface** $E(1)$ together with an **Elliptic fibration**. A generalization of this construction yields elliptic surfaces $E(n)$ for all $n \geqslant 1$. This family of surfaces has been studied extensively within algebraic geometry, symplectic geometry, and 4-manifold topology.

One can also easily re-obtain a Lefschetz pencil from a fibration. A Lefschetz fibration resulting from a blow-up comes with a set of distinguished sections. For each point $b \in B_X$, blowing-up at b results in a section $s_b : \mathbb{C}P^1 \to \hat{X}$ given by $t \mapsto (b, t)$. The image is exactly the exceptional sphere obtained from the blow-up at b. Given such a set of distinguished sections $s_i : \mathbb{C}P^1 \to \hat{X}$ quotienting by their images results in a Lefschetz pencil. This process is called **blowing-down**. The relationship between Lefschetz pencils and fibrations can therefore be summarized by the following diagram.

$$\left\{ \begin{array}{l} \text{Lefschetz Fibration} \\ \hat{f} : \hat{X} \to \mathbb{C}P^1 \text{ with closed fibers} \\ \text{sections } s_1, ..., s_n \end{array} \right\} \underset{\text{blow-down}}{\overset{\text{blow-up}}{\Longleftrightarrow}} \left\{ \begin{array}{l} \text{Lefschetz Pencil} \\ \text{codimension 2 base } B_X \subseteq X \\ f : X \setminus B_X \to \mathbb{C}P^1 \text{ with punctured fibers} \end{array} \right\} \tag{1.1.3}$$

The essential topological properties of Lefschetz fibrations can be captured in dimension 4 with the following more general definition.

Definition 1.15. *On a 4-manifold X with two discrete sets $A, B \subseteq X$, a* **topological Lefschetz pencil** *on X is a map $f : X \setminus B \to S^2$ so that f has the following local models at A, B.*

- *Around $b \in B$, there are local coordinates (z_1, z_2) on X in which f takes the form $(z_1, z_2) \mapsto z_1/z_2$.*
- *Around $a \in A$ there are local coordinates (z_1, z_2) in which f is holomorphic and has a single non-degenerate critical point at A.*

If B is empty, f is said to be a **topological Lefschetz fibration**.

Clearly, in this definition B plays the role of the base with the local coordinates modeling the projection of $\mathbb{C}^2 - \{0\}$ onto $\mathbb{C}P^1$. The set A likewise plays the role of the critical locus, thus it is clear this definition encompasses the previous one. In later chapters, however, it will be shown that there are many important topological Lefschetz fibrations that do not arise from pencils on complex algebraic varieties.

Remark 1.16. (Affine Lefschetz Fibrations) Essentially every construction in this section applies equally well to affine algebraic varieties by taking a Lefschetz pencil parameterized by $\mathbb{C}$ instead of $\mathbb{C}P^1$. In fact, the affine case is particularly simple in the case of hyperplanes because there is no base locus. For example, given a smooth affine variety $X \subseteq \mathbb{C}^n$, a generic linear projection $(z_1, ..., z_n) \mapsto \sum_i a_i z_i$ will be a Lefschetz fibration with critical points wherever the planes perpendicular to $\sum_i a_i z_i$ coincide with the tangent spaces of X.

1.2 Monodromy and the Picard-Lefschetz Theorem

In this section one of the main tools for studying the topology of Lefschetz fibrations is developed: the Picard-Lefschetz theorem. As advertised in the introduction, this will describe the monodromy of the fibers above a path that encircles a critical value. This and the remaining sections of this chapter will consider primarily Lefschetz *fibrations*. For simplicity, the total space will often be denoted by X rather than $\hat{X}$, although it is understood that this X results from a blow-up as in the previous section.

First, note a fundamental result that is a slight generalization of Lemma 0.1:

Lemma 1.17. (Ehresmann Fibration Lemma) *Let M, N be smooth manifolds, and $f : M \to N$ a proper submersion. Then M is fiber bundle over N with projection given by f.*

To prove this, one essentially chooses a coordinate chart on N and uses the fact that the projection to each coordinate in a Morse function. This gives a gradient flow along each coordinate, resulting in a local trivialization above the coordinate chart.

For a Lefschetz fibration $f : X \to \mathbb{C}P^1$ with critical points $A \subseteq X$ and critical values $f(A) = \text{crit}(f)$, the restriction $f : X \setminus A \to \mathbb{C}P^1 \setminus \text{crit}(f)$ is a submersion by construction and is proper since it is the restriction of a map between compact manifolds. Hence by the above lemma, f is a fiber bundle away from the critical points. To simplify notation, call this bundle E and the generic fiber F. Here, the bundle may be non-trivial because for each $t_1, ..., t_r \in \text{crit}(f)$ a loop encircling t_i (or several of the t_i) can result in a non-trivial gluing of the fibers. This non-trivial gluing is called the monodromy, which is now defined precisely. Given a loop $\gamma : [0, 1] \to \mathbb{C}P^1 \setminus \text{crit}(f)$, one may consider the pullback bundle over $I = [0, 1]$. Since any fiber bundle over the interval is trivial, there exists a trivializing diffeomorphism $\Gamma : I \times F \to \gamma^*(E)$.

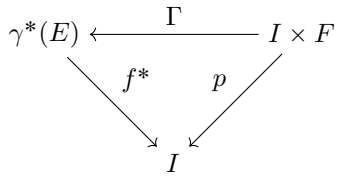

The gluing self-diffeomorphism of the fiber F_0 above the base point $\gamma(0) = \gamma(1)$ is given by

$$\mu_\gamma := \Gamma\mid_{\{1\}\times F} \circ\ \Gamma\mid^{-1}_{\{0\}\times F} : F_0 \longrightarrow F_0. \tag{1.2.1}$$

This self-diffeomorphism may, *a priori*, depend on the choice of trivialization. Recall that two diffeomorphisms f_0, f_1 are **isotopic** if they are smoothly homotopic through maps f_t that are diffeomorphisms for all t. Given two trivializations, $\Gamma_1, \Gamma_2 : I \times F \to \gamma^*(E)$, consider $(\Gamma_2)^{-1} \circ \Gamma_1 : I \times F \to I \times F$. By fixing an association $F \simeq F_0$ and requiring both trivializations restricted to $\{0\} \times F$ to be this, one may assume $(\Gamma_2)^{-1} \circ \Gamma_1$ is the identity on $\{0\} \times F$. Then, the restriction of $(\Gamma_2)^{-1} \circ \Gamma_1$ to $\{1\} \times F$ is plainly isotopic to $Id : \{1\} \times F \to \{1\} \times F$ via, for each t, the isotopy through the family of diffeomorphisms $(\Gamma_2)^{-1} \circ \Gamma_1(s, -)$ for $0 \leqslant s \leqslant t$. This shows that $\Gamma_1|_{\{1\}\times F}$ is isotopic to $\Gamma_2|_{\{1\}\times F}$ hence the self-diffeomorphism (1.2.1) is uniquely determined up to isotopy.

Definition 1.18. *For a loop γ, the isotopy class $[\mu_\gamma]$ of $\mu_\gamma : F \mapsto F$ is called the* **monodromy** *of γ.*

Some authors, call this map the **geometric monodromy**, to distinguish it from the induced map on homology $\mu_* : H_*(F; \mathbb{Z}) \mapsto H_*(F; \mathbb{Z})$ which is called the **algebraic monodromy**.

The monodromy also only depends on the path γ up to homotopy:

Proposition 1.19. *If two paths γ_0, γ_1 are homotopic, then the monodromies $[\mu_{\gamma_0}]$ and $[\mu_{\gamma_1}]$are the same isotopy class.*

Proof. Let $H(t, s) : I \times I \to \mathbb{CP}^1 \setminus \{t_1, ..., t_r\}$ be a homotopy such that $H(t, 0) = \gamma_0$ and $H(t, 1) = \gamma_1$. As any fiber bundle over $I \times I$ is trivial, there is a trivialization:

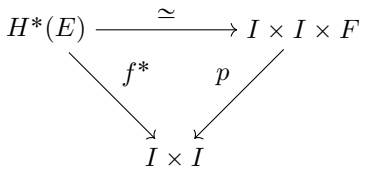

For each $s \in I$ there is a diffeomorphism $\mu_{H(s,-)} : F_0 \simeq F_0$ as in (1.2.1). For $s = 0, 1$ these diffeomorphisms are exactly μ_{γ_0} and μ_{γ_1}, thus these diffeomorphisms for $s \in [0, 1]$ provide an isotopy between them. □

Definition 1.20. *The* **Mapping class group** *of a manifold S is the group (under composition)*

$$Mod(S) := \{\textit{Diffeomorphisms } f : S \to S\} \Big/ \textit{smooth isotopy.}$$

An isotopy class of maps is called a **mapping class**. *If S has a boundary ∂S, then only diffeomorphisms $f : S \to S$ so that $f(x) = x$ for all $x \in \partial S$ are considered.*

Proposition 1.19 and the fact that monodromy is well-defined up to isotopy shows that given a base point $* \in \mathbb{C}P^1 \setminus \{t_1, ..., t_r\}$ with fiber F_*, the monodromy descends to a map

$$\mu : \pi_1(\mathbb{C}P^1 \setminus \{t_1, ..., t_r\}, *) \longrightarrow Mod(F_*) \tag{1.2.2}$$

sending $\gamma \mapsto [\mu_\gamma]$, and which respects composition. One should note, however, that because of the conventions for composing diffeomorphisms versus homotopy classes of loops, it is actually an anti-homomorphism, so that $[\alpha] \cdot [\beta] \mapsto \mu_\beta \circ \mu_\alpha$. A quick application of Van-Kampen's Theorem shows

$$\pi_1(\mathbb{C}P^1 \setminus \{t_1, ..., t_r\}, *) \simeq \langle\, [\gamma_1], ..., [\gamma_r] \;\big|\; [\gamma_1] \cdot \ldots \cdot [\gamma_r] = Id \,\rangle$$

where γ_i is a loop based at $*$ that circles once around the critical point t_i. In particular, the monodromy must satisfy the relation

$$[\mu_{\gamma_r}] \circ \ldots \circ [\mu_{\gamma_1}] = [\mu_{\gamma_1 \cdot \ldots \cdot \gamma_r}] = Id \in Mod(F_*). \tag{1.2.3}$$

This relation can also be seen directly: monodromy must be trivial around a loop enclosing *all* of the critical points, since the same loop also bounds a disk on the other side of the sphere, over which the bundle must be trivial. This relation (1.2.3) will be crucial in relating the topology of X to the monodromy μ.

A Local Model

The next step is to prove the Picard-Lefschetz theorem (1.35) which identifies explicitly the mapping class $[\mu_\gamma]$. The following holomorphic version of the Morse lemma gives a local model that will reduce the problem of understanding the general monodromy to understanding a specific monodromy in local coordinates.

Lemma 1.21. (Morse Lemma) *Let $f : X \to \mathbb{C}$ be a holomorphic function with $z \in X$ a non-degenerate critical point. Then there is a holomorphic coordinate chart $(z_1, ..., z_n)$ centered at z in which f is given by*

$$f(z_1, ..., z_n) \mapsto z_1^2 + \ldots + z_n^2. \tag{1.2.4}$$

Proof. By choosing preliminary coordinates, it may be assumed that $X = U \subseteq \mathbb{C}^n$ is an open neighborhood and $z = 0$. By translation, it may further be assumed that $f(0) = 0$. Thus f vanishes to second order at the origin, and so by Taylor's theorem there are holomorphic functions $h_{i,j}(z)$ so that

$$f(z_1, ..., z_n) = \sum_{i,j}^{n} h_{i,j}(z) z_i z_j.$$

By replacing h_{ij} and h_{ji} by their average $\frac{1}{2}(h_{ij} + h_{ji})$ one may assume that the matrix of h_{ij} is symmetric. Thus f is given by a quadratic form depending holomorphically on z, which is non-degenerate in a neighborhood of the origin by assumption. It is a standard fact that for any non-degenerate quadratic form over $\mathbb{C}$, there exists a linear change of coordinates $z \mapsto Az$ after which it appears as the standard quadratic form $\sum_i z_i^2$. It is possible to check, via the proof of this fact, that the change of coordinates depends holomorphically on the functions $[h_{ij}(z)]$, hence one obtains a linear coordinate change $A(z)$ for all $z \in U$. Define new coordinates $z' := A(z)z$. By the inverse function theorem, this is a biholomorphism in a neighborhood of 0, and in the z' coordinates f has the desired form. □

In particular, since the critical points of a Lefschetz fibration $f : X \to \mathbb{C}P^1$ are non-degenerate by definition, there exist local coordinate charts about each $a \in A$ and $f(a) \in \mathrm{crit}(f)$ so that f has the standard form (1.2.4). The fibers of f intersect this coordinate chart as the hypersurfaces (now with boundary)

$$F_t \cap U = \{z_1^2 + \ldots z_n^2 = t\} \cap B^{2n}$$

This shows (as was promised earlier) that the singular fibers only have singularities modeled on $z_1^2 + \ldots z_n^2 = 0$. This is a **nodal singularity**, the simplest type of singularity that can occur in algebraic geometry.

The following coordinate change identifies the fibers $F_t \cap U$ in the coordinate chart with a rather more familiar hypersurface.

Lemma 1.22. *For each $t \neq 0$, the hypersurface $\{z_1^2 + \ldots z_n^2 = t\} \cap B^{2n} \subseteq \mathbb{C}^n$ is diffeomorphic to the unit disk bundle $\mathbb{D}(T^*S^{n-1})$.*

Proof. The map f in coordinates is a proper submersion away from 0, so the fibers are mutually diffeomorphic by the Ehressman fibration lemma (Lemma 1.17). It therefore suffices to prove the claim for $t = \frac{1}{2} \in \mathbb{R}$, for which an explicit diffeomorphism can be written.

In real coordinates, $z_j = x_j + iy_j$ the fiber $f^{-1}(\frac{1}{2}) = \{\sum z_i^2 = \frac{1}{2}\}$ is

$$\{(x, y) \in \mathbb{R}^n \times \mathbb{R}^n \mid |x|^2 - |y|^2 = \frac{1}{2} \ , \ x \cdot y = 0 \ , \ |x|^2 + |y|^2 \leqslant 1\}. \tag{1.2.5}$$

Now define a change of coordinate by

$$x' := \sqrt{\frac{1}{\frac{1}{2} + |y|^2}} \cdot x \qquad y' := 2y.$$

This is simply a scaling of both coordinates, so it is a diffeomorphism. In these new coordinates,

$$|x'|^2 = \frac{|x|^2}{\frac{1}{2} + |y|^2} = 1 \qquad |y'|^2 = 4|y|^2 \leqslant 1$$

where the second equality follows from subtracting the two equation of (1.2.5), which gives $2|y|^2 \leqslant 1 - \frac{1}{2}$. Clearly the vectors remain orthogonal in the new variables so that in (x', y') coordinates, the fiber is

$$\{(x', y') \in \mathbb{R}^n \times \mathbb{R}^n \mid |x'|^2 = 1 \ , \ x' \cdot y' = 0 \ , \ |y'|^2 \leqslant 1\} \simeq \mathbb{D}(T^*S^{n-1}) \tag{1.2.6}$$

□

In the local coordinates, the zero-section $\{(x, 0) \mid |x|^2 = t\} \subseteq \mathbb{D}(T^*S)$ gives an embedded sphere $S_t^{n-1} \subseteq F_t$ for $t \geqslant 0$. As $t \to 0$, this sphere shrinks and collapses to a point. See Figure 1.2 on the next page. Note as $t \to 0$ from different directions, these embedded spheres are isotopic in B^{2n}.

Definition 1.23. *For a critical point $a \in A$ the isotopy class of S_t^{n-1} (as an embedded sphere) is called the* **vanishing cycle** *of the critical point a and denoted ν_a. The collection $\{S_t^{n-1} \mid t \geqslant 0\} \simeq B^n$ is called the* **Lefschetz thimble** *of the vanishing cycle.*

Some authors define the vanishing cycles as homology classes in $H_{n-1}(F_t; \mathbb{Z})$ that are in the kernel of the inclusion of the fiber $\iota_* : H_{n-1}(F_t; \mathbb{Z}) \to H_{n-1}(X; \mathbb{Z})$. In the total space, the sphere S_t^{n-1} bounds the thimble, making in null-homologous there, so this definition captures the same idea. The isotopy class of S_t^{n-1}, however, contains more information than only the homology class, so the stronger definition of vanishing cycle is sometimes preferable. One should also note that, *a priori*, there is no reason that a vanishing cycle should be non-trivial in $H_{n-1}(F_t; \mathbb{Z})$. A vanishing cycle is said to be **non-separating** if it is homologically non-trivial, and **separating** otherwise. The name results from the fact that for a homologically trivial sphere, removing the neighborhood $U \cap F_t \simeq \mathbb{D}(T^*S^{n-1})$ will result in a disconnected (i.e. separated) manifold, whereas the homologically non-trivial case will leave the fiber connected.

The vanishing cycles of all the critical points $a \in A$ can be taken to all lie in a single fiber as follows. Let $* \in \mathbb{C}P^1$ be a base point. Draw paths $\delta_i : [0, 1] \to \mathbb{C}P^1$ from $*$ to each critical point t_i. The vanishing cycle ν_{t_i} is defined in the fibers near t_i via the local coordinates, and in particular, in a fiber above $\delta_i(s)$ for $s = 1 - \varepsilon$ where ε is small. Trivializing the bundle above $\delta_i([1 - \varepsilon])$ gives a diffeomorphism of the fiber where the vanishing cycle is defined to the fiber above $*$, so the vanishing cycle ν_{t_i} may be considered in the fiber F_*. Thus, the vanishing cycle $\nu_i \in F_*$ contracts to a point, that is to say vanishes, when it is transported along δ_i (via a trivialization for $t \in [0, 1 - \varepsilon)$ and local coordinates for $t \in [1 - \varepsilon, 1]$).

Definition 1.24. *A path δ_i as above is called a* **vanishing path** *for the critical value t_i.*

A choice of a collection of vanishing paths $\delta_1, \ldots, \delta_r$ determines a generating set $[\gamma_1], \ldots, [\gamma_r]$ of the fundamental group $\pi_1(\mathbb{C}P^1 \setminus \{t_1, ..., t_r\}, *)$ as follows. Take each γ_i to be a path that traces δ_i to within a small radius of t_i, then circle t_i once, and returns to $*$ tracing δ_i the other direction. The collection of paths $[\gamma_1], ..., [\gamma_r]$ given in this way is called the **generating set determined by** $\delta_1, ..., \delta_r$. See Figure 1.3.

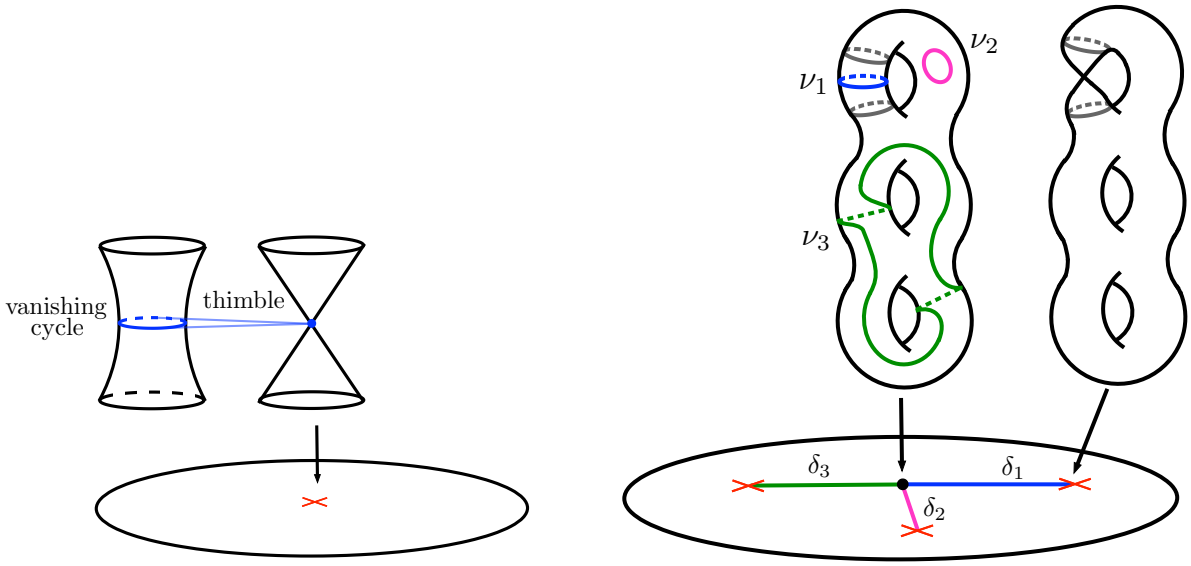

Figure 1.2: (Left) The vanishing cycle and thimble (blue) of a critical point in local coordinates for $\dim_{\mathbb{R}}(X) = 4$. (Right) three vanishing cycles ν_1, ν_2, ν_3 depicted in a generic fiber F_*. The cylindrical neighborhood (gray) of ν_1 collapses according to the local model when moving along the vanishing path δ_1 (blue), resulting in the singular fiber on the right. The vanishing cycle ν_2 (magenta) is a separating vanishing cycle, and ν_3 (green) is an example of a rather more complicated vanishing cycle.

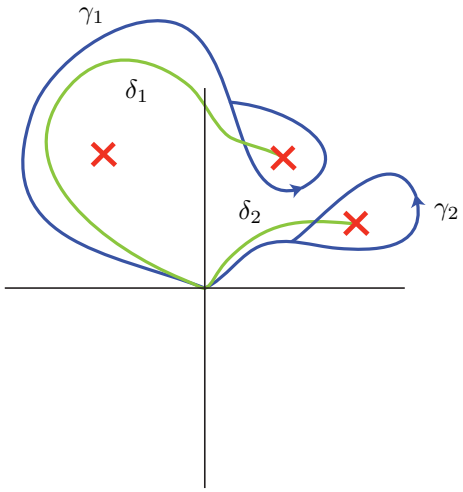

Figure 1.3: Two vanishing paths δ_1, δ_2 (green) and the corresponding generators of the fundamental group γ_1, γ_2 (blue).

Note 1.25. *A priori*, the collection of vanishing cycles $\nu_{t_1}, ..., \nu_{t_r}$ in F_* may depend on the choice of vanishing paths $\delta_1, ..., \delta_r$.

Up to this point, everything that has been done is valid in any dimension. Moving forward, however, only (real) dimension 4 will be considered, in which case the fibers are closed surfaces. As discussed in the introduction, this is a particularly interesting case and one that can often be described more explicitly. The reason for the latter is that the mapping class groups of high-dimensional manifolds are often hopelessly

complicated, whereas the mapping class groups of surfaces are quite well-understood and can frequently be given explicitly by generators and relations [12].

Mapping Class Groups and Dehn Twists

Before proving the Picard-Lefschetz Theorem, it is useful to go over a few facts about mapping class groups. This subsection introduces Dehn Twists and their actions on branched covers. These notions will make the description of the monodromy very simple, and will result in an easy proof of the Picard-Lefschetz theorem.

Consider the following mapping class $[\tau] \in Mod(S^1 \times [0,1])$. In coordinates (θ, r) on $S^1 \times [0,1]$, $[\tau]$ is represented by $\tau(\theta, r) = (\theta + 2\pi r, r)$. Intuitively, this mapping class is the result of grabbing one boundary circle and twisting it completely around once. It turns out, however, that this diffeomorphism is not isotopic to the identity through maps that fix the boundary.

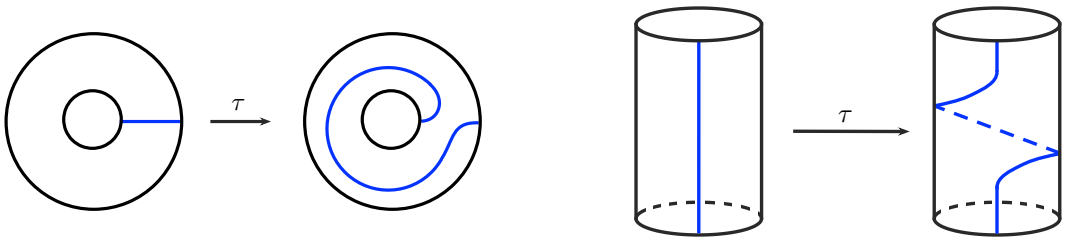

Figure 1.4: The Dehn twist on $S^1 \times [0,1]$ shown as the annulus (left) and the cylinder (right).

Definition 1.26. *The mapping class* $[\tau]$ *is called a* **right-handed Dehn twist**. *Its inverse is called a* **left-handed Dehn twist**.

Although it will not be needed, it is worth noting for completeness that:

Fact 1.27. **[12]** The mapping class group of the cylinder is $Mod(S^1 \times [0,1]) = \langle [\tau] \rangle \simeq \mathbb{Z}$ where the latter is the free abelian group generated by $[\tau]$.

In general, for any surface S and a simple closed curve $\alpha \subseteq S$ one can define the **Dehn Twist around** α, denoted $[\tau_\alpha]$ as follows. Choose a tubular neighborhood $U \simeq S^1 \times [0,1]$ of α so that $\alpha = S^1 \times \{1/2\} \subseteq U$ and let

$$\tau_\alpha(x) = \begin{cases} \tau(\theta, r) & x \in U \\ Id & x \in S \setminus U. \end{cases}$$

The Dehn Twist $[\tau_\alpha]$ is defined to be the mapping class of the above diffeomorphism. Note that if two curves α_0, α_1 are isotopic through a family of curves α_t, then as mapping classes, $[\tau_{\alpha_0}] = [\tau_{\alpha_1}]$, as the family τ_{α_t} provides an isotopy between them. It therefore makes sense to consider $[\tau_{[c]}]$ where $[c]$ is an isotopy class of simple closed curves, rather than a single such curve.

It is clear from the definition that the Dehn twists around two curves that have disjoint tubular neighborhoods commute, since they fix points outside these tubular neighborhoods. Specifically, if two curves α, β have intersection $[\alpha] \cdot [\beta] = 0$ in $H_1(S; \mathbb{Z})$, then the Dehn twists commute, since disjoint tubular neighborhoods always exist in this case. Moreover, if $[\alpha] \cdot [\beta] = 0$ then β is fixed by the action of $[\tau_a]$, as it lies outside the tubular neighborhood. In particular, since $[\alpha] \cdot [\alpha] = 0$ for any simple closed curve $\alpha \subseteq S$, it is always the case that $\tau_\alpha(\alpha) = \alpha$. Any other representative of $[\tau_\alpha]$ applied to α results in a curve isotopic to α. If β *does* intersect α then the twist τ_α sends β to a curve that follows its original path, but right before it crosses a, turns and follows α along its length, crossing it half way, and coming back on the other side to rejoin the original β after the crossing as shown in Figure 1.5. When choosing different representatives of $[\tau_\alpha]$, this curve is again well-defined up to isotopy.

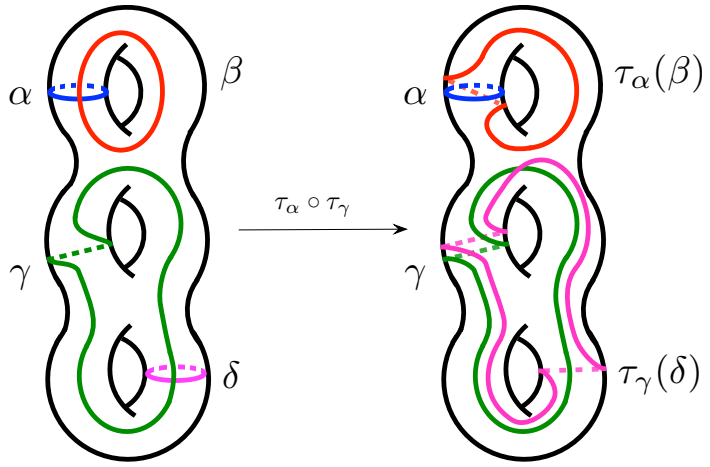

Figure 1.5: Curves in a surface of genus 3 under the action of $\tau_\alpha \circ \tau_\gamma$. Since the pairs are disjoint $\tau_\alpha \circ \tau_\gamma(\alpha) = \alpha,\ \tau_\alpha \circ \tau_\gamma(\beta) = \tau_\alpha(\beta)$ and likewise for γ, δ.

The action of a Dehn twist on homology is rather apparent:

Proposition 1.28. *The result of a Dehn twist around α on homology is*

$$[\tau_a(\beta)] = [\beta] + ([\alpha] \cdot [\beta])\ [\alpha]$$

where brackets here denote homology classes of the simple closed curves in $H_1(S;\mathbb{Z})$.

Proof. Under $\beta \mapsto \tau_\alpha(\beta)$, a segment of β that represents the generator of relative homology $H_1(U, \partial U)$ in the tubular neighborhood U of α is wrapped once around α. In the whole surface S, where β represents a non-relative class, this sends $[\beta] \mapsto [\beta] + [\alpha]$. If β intersects α n times, then this happens independently for n segments of β each representing the relative class in U. This process respects the orientation of the curves, since the new loop in U inherits the orientation of β. □

Example 1.29. The mapping class group $Mod(D^2)$ of the disk is trivial. Given a diffeomorphism $\varphi :\ D^2 \to\ D^2$ there is an isotopy

$$I(x,t) := \begin{cases} (1-t)\varphi\left(\frac{x}{1-t}\right) & 0 \leqslant |x| \leqslant 1-t \\ x & 1-t \leqslant |x| \leqslant 1 \end{cases}$$

to the identity through homeomorphisms. One can then argue that this can be smoothed so that the radial derivative is smooth ([12], Chapter 2).

Example 1.30. (Mapping Class group of the punctured disk) Let $S = D^2 - \{p_1, ..., p_k\}$ be the k-times punctured disk. Then $Mod(S) = \mathcal{B}_k$, where $\mathcal{B}_k$ is the braid group on k strands. Recall that the braid group $\mathcal{B}_k$ is the set of configurations of k strands in $D^2 \times I$ with fixed ends considered up to isotopy, where composition is given by placing two configurations end to end. In terms of generators and relations, the group is given by

$$\mathcal{B}_k \ = \ \langle \sigma_1, \ldots, \sigma_{k-1} \mid \sigma_i\sigma_{i+1}\sigma_i = \sigma_{i+1}\sigma_i\sigma_{i+1}\ ,\ \sigma_i\sigma_j = \sigma_j\sigma_i \rangle$$

where σ_i is the configuration in which the i^{th} strand crosses under the $i+1^{st}$ (see Figure 1.6). The fact that $Mod(S) = \mathcal{B}_k$ can now be deduced from the previous example as follows. A diffeomorphism $\varphi : S \to S$ can be extended to a diffeomorphism of D^2 by some permutation of the punctured points, after which it is isotopic to the identity via an isotopy $I(t,-)$ by Example 1.29 . The punctured points $p_1, ..., p_k$ are moved by this isotopy through paths $I(t, p_i) \in D^2 \times I$ to the identity. These paths will wander around the disk

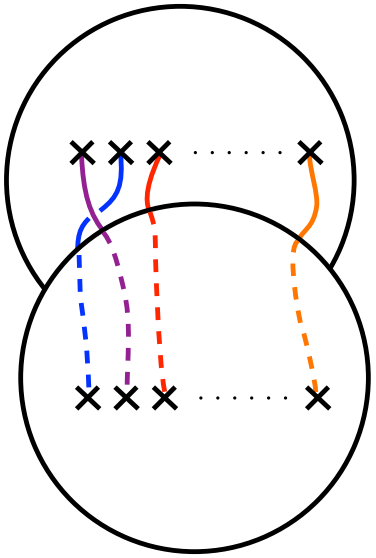

Figure 1.6: A braid resulting from an isotopy of the disk coming from a mapping class in $Mod_k(D^2)$. During the isotopy, the far left point passes over the one second from the left, resulting in the crossing of the two leftmost strands (blue, purple).

for $t \in [0,1]$. Drawing them in $D^2 \times I$ associates to each mapping class a braid. See Figure 1.6. This correspondence can be shown to be an isomorphism ([12], Chapter 9). Notice that the mapping class group of $D^2 - \{p_1, ..., p_k\}$ is the same as the mapping class group of D^2 with k marked points. That is, the group of diffeomorphisms of D^2 permuting the marked points up to isotopy, denoted $Mod_k(D^2)$. The isomorphism $Mod_k(D^2) \simeq Mod(D^2 - \{p_1, ..., p_k\})$ is given by restricting to the complement of the marked points.

Definition 1.31. *The image of the generators $\sigma_i \in \mathcal{B}_k$ under the above isormorphism are called* **half Dehn twists**.

Thus the action of the half Dehn twist of that is the image of σ_i is to flip the two points p_i, p_{i+1} passing the right point over the left. Of course, this diffeomorphism is isotopic to the identity through an isotopy that allows the punctures $\{p_j\}$ to move, but not through one in which the punctures stay fixed. To see the action of the half-twist on points near $\{p_j\}$, it is helpful to draw the vertical line between the punctures and imagine it as a string lying on the disk. The action of the half-twist on the string is the effect of placing two fingers on the punctures and rotating by 180°, pushing the string along as you rotate. See Figure 1.7. The diffeomorphism is compactly supported in a neighbhorhood of the two punctures.

For non-adjacent points indexed by i, j the braid that has a single crossing of the i^{th} strand under the j^{th} one is the element $\sigma_{i,j} = \sigma_{j-1} \circ \ldots \circ \sigma_i$. The image of this element under the isomorphism is a mapping class that flips p_i and p_j, and is compactly supported in a stretched disk containing these two punctures. The effect on a vertical line in this disk is the same as in the case where the points are adjacent (see Figure 1.7). Extending Definition 1.31 slightly, this element (as a mapping class) is called a half Dehn twist about two punctures p_i, p_j. By a slight abuse of notation, it is denoted by $[\sigma_{i,j}]$.

Recall now that a **branched cover** over the disk is a map $p : S \to D^2$ from a surface S that is an even covering away from finitely many points. At these finitely many points, the map must conform to the local model $z \mapsto z^n$ for some n. These points are called **ramification points** and their images are called **branch points**. Generically, branched covers will have only double branch points, so that $n = 2$ in the local model. Throughout what follows, it is assumed that all branched covers are generic in this sense. Since p is a local diffeomorphism where it is an even covering, the critical points of the map p are exactly the ramification points.

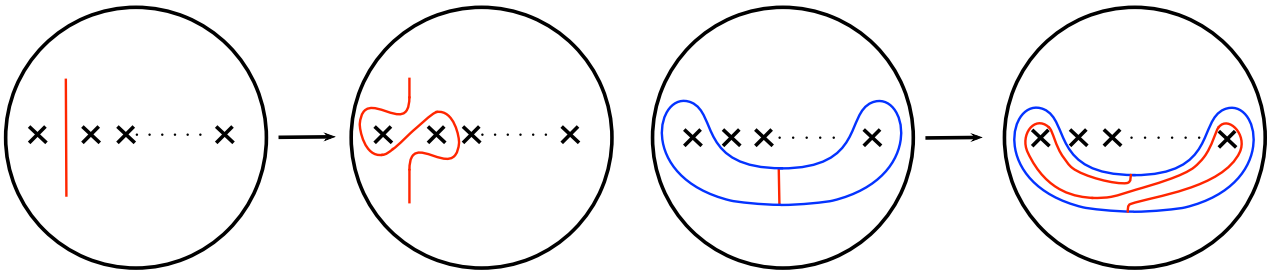

Figure 1.7: The image of a vertical line between two punctures under the half Dehn twists around two adjacent (left) and non-adjacent (right) punctures. On the right, the Dehn twist is supported in the stretched disk indicated (blue).

Definition 1.32. *Let $p : S \to D^2$ be a branched cover of the disk with branching points $t_1, \dots, t_n$ where S is a surface with boundary. Consider $t_1, ..., t_n$ as a set of n marked pints in D^2. A diffeomorphism $\phi : D^2 \to D^2$ that permutes the marked points is said to be* **liftable** *with respect to p if there exists a diffeomorphism $\tilde{\phi} : S \to S$ fixing the boundary ∂S of S pointswise such that the following diagram commutes:*

$$\begin{array}{ccc} S & \xrightarrow{\tilde{\phi}} & S \\ \downarrow{\scriptstyle p} & & \downarrow{\scriptstyle p} \\ D^2 & \xrightarrow{\phi} & D^2 \end{array}$$

the map $\tilde{\phi}$ is called the **lift**.

The following is a fundamental fact about lifts.

Lemma 1.33. *If a lift of a diffeomorphism exists, then it is unique. Moreover, if ϕ_0, and ϕ_1 represent the same mapping class in $Mod_n(D^2)$ and ϕ_0 is liftable, then ϕ_1 is also liftable and the lift $\tilde{\phi}_1$ of ϕ_1 represents the same mapping class in $Mod(S)$ as the lift $\tilde{\phi}_0$ of ϕ_0.*

Proof. Suppose two diffeomorphisms $\tilde{\phi}, \tilde{\psi}$ were both lifts of ϕ. Then $\tilde{\psi}^{-1} \circ \tilde{\phi}$ is a deck transformation covering the identity on D^2. By the theory of covering spaces, any non-trivial deck transformation must permute the boundary, but $\tilde{\psi}, \tilde{\phi}$ fixes the boundary by assumption, hence $\tilde{\psi}^{-1} \circ \tilde{\phi} = id$ and $\tilde{\phi} = \tilde{\psi}$.

For the second statement, notice that by considering $\phi_1^{-1} \circ \phi_0$, it suffices to prove the statement in the case that $\phi_0 = Id$ and ϕ_1 is isotopic to it through diffeomorphisms ϕ_t preserving marked points. Since the marked points are discrete and ϕ_t varies smoothly in t, the marked points must remain fixed throughout the isotopy. Away from the marked points, p is an even covering. A lift $\tilde{\phi}_1$ isotopic to $\tilde{\phi}_0$ can now be constructed as follows. For each points $x \in S$, let $\tilde{\phi}_t(x)$ be the unique lift of the path $\phi_t(p(x))$ beginning at x. One can check that this defines a family of diffeomorphisms $\tilde{\phi}_t$ isotopic the identity on S (which is clearly the unique lift of the identity on D^2) ending in a diffeomorphism $\tilde{\phi}_1$ that covers ϕ_1 (see [13]). □

In light of Lemma 1.33 it makes sense to consider lifts on mapping classes. That is, mapping class $[\tilde{\phi}] \in Mod(S)$ is the lift of a mapping class $[\phi] \in Mod_n(D^2)$ if there exists a represetative of $[\phi]$ whose lift is in $[\tilde{\phi}]$. The lemma guarantees that if such a lift exists for one representative, it exists for all and defines the same mapping class $[\tilde{\phi}] \in Mod(S)$.

The second fundamental fact abut lifts is the relation between Dehn Twists and half Dehn twists that the reader might have guessed already:

Lemma 1.34. *Let $p : S \to D^2$ be a branched cover of a surface with boundary that has only double branch points. Suppose $\alpha \in S$ is a simple closed curve that projects to a path $\gamma \subseteq D^2$ between two branch points p_i and p_j. Then the Dehn twist $[\tau_\alpha]$ is the unique lift of the half Dehn twist $[\sigma_{i,j}]$.*

Proof. By the previous Lemma 1.33, it suffices to show the Dehn twist is a lift of the half Dehn twist, as uniqueness then follows. To begin, the statement is proved in the case that $S = S^1 \times [0,1]$. There is a branched cover $p : S^1 \times [0,1] \to D^2$ with two branch points given as follows. Let ι be rotation by 180° around an axis perpendicular to the $[0,1]$ factor that passes through the cylinder twice (see Figure 1.8). The quotient by the action of ι gives a degree 2 branched cover of D^2. The pre-image of a point in a tubular neighborhood of ∂D^2 is a pair of points, each in a tubular neighborhood of one of the boundary components of $S^1 \times [0,1]$, that are taken to each other by the rotation ι. For example, in Figure 1.8, the pre-images of the blue and green radial lines are each the two segments of the corresponding colors. Said a different way, this is the branched cover obtained by taking two copies of D^2 with two marked point, cutting along the line between the marked points, and gluing together by associating each edge to the opposite edge in the other copy of D^2.

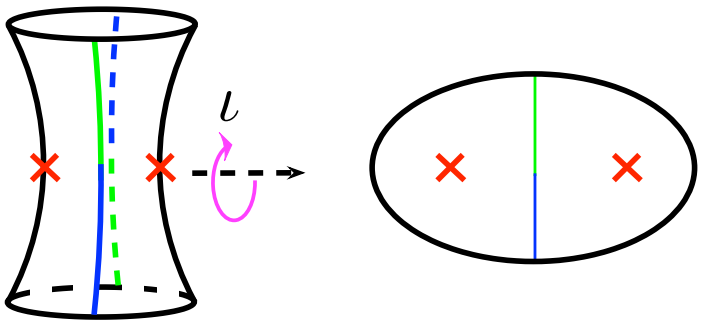

Figure 1.8: The quotient by action of ι gives a branched cover with two critical points (red crosses). The action associates opposite points on the cylinder (green/dashed green, blue/dashed blue).

After coming to terms with the action of ι, it is straightforward to see that τ covers a diffeomorphism of the disk. Since the action of τ is symmetric, pairs points associated by ι are taken to pairs of points still associated by ι, thus τ descends to a diffeomorphism of the disk. Clearly, τ flips the ramification points, hence also the branch points. Thus the diffeomorphism τ covers must be either $[\sigma_{1,2}]$ or $[\sigma_{1,2}]^{-1}$. To distinguish amongst these, consider the line $\Delta = \theta_0 \times [0,1] \subseteq S^1 \times [0,1]$. Under the action of τ, the image $p(\Delta)$ is sent to the path that begins at the top of the disk, goes inward increasing its angular coordinate to π passing around the branch point to the center of the disk, and then goes out by the reverse, as shown in Figure 1.9. As in Figure 1.7, this is (up to isotopy) the action of the half Dehn twist, rather than its inverse (the inverse passes the line $p(\Delta)$ over the right branch point first). This shows the result for the case of $S = S^1 \times [0,1]$.

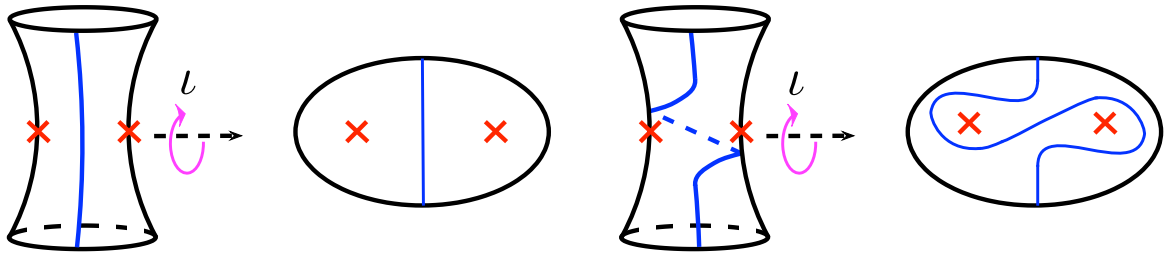

Figure 1.9: The branched cover of $S^1 \times [0,1]$ before (left) and after (right) the action of τ. The path Δ and its image $p(\Delta)$ are shown (blue).

For a general surface and branched cover $p : S \to D^2$ of degree n, let α be a curve whose image is a path between two branched p_i and p_j. Take a neighborhood U of $p(\alpha)$ containing no branched points other than p_i and p_j. For α to be a simple closed curve rather than a path, the branching at p_i and p_j must be between the same pair of sheets. Thus $p^{-1}(U)$ is a single copy of the cylinder $S^1 \times [0,1]$ covering the disk as above (up to diffeomorphsim, as the branching is the same), and $n-2$ disjoint copies of U. Restricted to the copy of $S^1 \times [0,1]$ the projection of the Dehn twist is a half Dehn twist by the above argument. On the $n-2$ disjoint copies of U, the action of the half-twist can be lifted by diffeomorphism. This makes the Dehn twist and the half twist commute with the projection to the disk. In the $n-2$ copies of U (which don't have ramification points) this is isotopic to the identity, hence the total isotopy class is still $[\tau_\alpha]$, and so $[\tau_\alpha]$ is the unique lift of the half Dehn twist around p_i and p_j.

□

The Picard-Lefschetz Theorem

These facts about the mapping class group are now applied in the context of Lefschetz fibrations to prove the Picard-Lefschetz Theorem.

Theorem 1.35. (Picard-Lefschetz) *Let $f : X \to \mathbb{C}P^1$ be a Lefschetz fibration with distinct critical values $t_1, ..., t_r$. Choose a basepoint $*$ and let $\delta_1, ..., \delta_r$ be a collection of vanishing paths determining a collection of vanishing cycles $[\nu_1], ..., [\nu_r]$ and a generating set $[\gamma_1], ..., [\gamma_r]$ of $\pi_1(\mathbb{C}P^1 \setminus \{t_1, ..., t_r\}, *)$. Then the action of the monodromy*

$$\mu : \pi_1(\mathbb{C}P^1 \setminus \{t_1, ..., t_r\}, *) \longrightarrow Mod(F_*)$$

is

$$[\gamma_i] \mapsto [\tau_{\nu_i}].$$

In words, the monodromy around each critical value is a (right-handed) Dehn twist around the vanishing cycle.

Corollary 1.36. (Picard-Lefschetz Formula) *The algebraic monodromy is*

$$\mu_*([\beta]) = [\beta] + ([\nu_i] \cdot [\beta])[\nu_i]$$

Proof. This is immediate from the theorem and Proposition 1.28. □

Proof. (Picard-Lefschetz Theorem) Let t_i be one of the critical points and γ_i the loop encircling it. Choose coordinates neighborhood $U \subseteq X$ and $V \subseteq \mathbb{C}P^1$ around t_i on which f has the standard form $(z_1, z_2) \mapsto z_1^2 + z_2^2$. It suffices to assume γ_i is the loop $\gamma_i(t) = \frac{1}{2}e^{2\pi i t} \subseteq \mathbb{C}$ in coordinates on V, since this point may be connected to $*$ via the vanishing path δ, and by choosing a trivialization of the bundle above δ the monodromy and vanishing cycle can be transported back to F_*.

Thus it suffices to find the monodromy as a self-diffeomorphism of the fiber $F_{1/2}$ above $1/2 \in \mathbb{C}$. First, the monodromy must be trivial outside U. To see this, observe that the restriction of f to $f^{-1}(D^2_{1/2}) \setminus U$ (where $D^2_{1/2}$ is the disk of radius $1/2$) has no critical points. By the Ehressman fibration lemma (Lemma 1.17) it is therefore a fiber bundle over the disk, and so is trivial. In particular, the monodromy around the boundary is trivial up to isotopy. By extending an isotopy of $F_{1/2} \setminus (F_{1/2} \cap U)$ to all of $F_{1/2}$ and composing with this, it may be assumed that the monodromy is the identity outside of and on the boundary of U.

Now consider the monodromy of the restriction of the fibers to the local coordinates $\tilde{F}_t := \{z_1^2 + z_2^2 = \frac{1}{2}e^{2\pi i t}\} \subseteq B^4$ around the path γ_i. A triviailiation of $\{\tilde{F}_t \mid t \in S^1\} \simeq S_0 \times I$ is given explicitly as follows. For each t, define a map $\psi_t : \tilde{F}_0 \to \tilde{F}_t$ by

$$z_1 \mapsto z_1 e^{i\pi\chi(|z|)t} \qquad z_2 = \pm\sqrt{\frac{1}{2} - z_1^2} \mapsto \pm\sqrt{\frac{1}{2}e^{2\pi i t} - z_1^2(t)}$$

where χ is a smooth bump function that takes value 1 in a neighborhood of the origin and falls to 0 smoothly by, say, 3/4. It is clear ψ_t is a diffeomorphism for each t, since replacing t with $-t$ provides an inverse. The monodromy is, by definition, ψ_1.

Now the result is deduced by observing the action on a branched cover. Project to the z_1 coordinate. This is a branched cover $\tilde{F}_t \to D^2$ for each $t \in [0,1]$. By construction, points with the same z_1 coordinate are taken to points that still have the same z_1 coordinate by ψ_t, so ψ_t descends to a well-defined diffeomorphism of the disk. Since $\chi(|z|) = 0$ on the boundary, both ψ_t and the diffeomorphism of the disk are fixed on the boundary. For all $t \in [0,1]$ there are two branched points when $z_2 = 0$ so that the branched points solve $z_1^2 = \frac{1}{2}e^{2\pi i t}$ and thus are given by $(z_1, z_2) = \pm\left(\frac{1}{\sqrt{2}}e^{i\pi t}, 0\right)$. The diffeomorphism of the disk that ψ_t covers therefore rotates the branch points by a half circle, hence it must be either a half Dehn twist or its inverse (up to isotopy of $D^2 - \{p_1, p_2\}$ fixing the branched points). However, the family of diffeomorphisms that ψ_t covers for $t \in [0,1]$ give an isotopy (that moves the branch points) between the two under which the branch points undergo a half rotation counterclockwise, thus the diffeomorphism of the disk is the half Dehn twist, not its inverse. By Lemma 1.34, it follows that the monodromy ψ_1 is a Dehn twist about the simple closed curve $\tilde{F}_0 \cap \mathbb{R}^2 = \{x_1^2 + x_2^2 = \frac{1}{2}\}$ which is the vanishing cycle.

□

1.3 The Topology of Lefschetz Fibrations

This section covers how to extract topological information about a manifold X from a Lefschetz fibration $f : X \to \mathbb{C}P^1$. It begins with a discussion of how some classical invariants of X like the Euler characteristic can be recovered. This is followed by a discussion of how to obtain a handle-body presentation of X from a Lefschetz fibration, just as one can be obtained from a standard Morse function. The section concludes by stating a theorem of Kas and Matsumoto relating the topology of X to the monodromy of the fibration f, which is one of the most important results in the study of Lefschetz fibrations.

Classic Invariants of Lefschetz Fibrations

A few standard topological invariants and useful facts about the topology of Lefschetz fibrations can be deduced from singular homology. To avoid a rather unilluminating detours into homological algebra, proofs are only given for a few results in this section.

Proposition 1.37. (Euler Characteristic Formula) *Let $X \subseteq \mathbb{C}P^N$ be a smooth variety of (complex) dimension n. If $f : X \setminus B \to \mathbb{C}P^1$ is a Lefchetz pencil with base B, generic fiber F_*, and r critical points. Then the Euler characteristics are related by*

$$\chi(X) = 2\chi(F_*) - \chi(B) + (-1)^n \cdot r$$

$$\chi(\hat{X}) = 2\chi(F_*) + (-1)^n \cdot r,$$

where $\hat{X}$ is the blow-up of X as in Section 1.1.

This can be deduced from long exact sequences of pairs and standard tools like excision. The full details can be found in [14], Section 5.2.

Example 1.38. (Singular fibers in E(1)) If one already knows the Euler characteristic $\chi(X)$, then this formula can be used to deduce the number of critical points r, which is also the number of singular fibers. For example, the elliptic surface $E(1)$ in Example 1.8, was constructed by taking $X = \mathbb{C}P^2 \subseteq \mathbb{C}P^3$ with a pencil $t_0P_0 + t_1P_1$ where P_0, P_1 were homogenous cubic polynomials. Since the zero of a cubic represents $3x \in H_2(\mathbb{C}P^2)$ where x is the generator, the base locus $B = P_0^{-1}(0) \cap P_1^{-1}(0)$ will consist of 9 points for generic P_0, P_1. Additionally, since since the zero-set of a cubic is topologically a torus, one has $\chi(F_*) = 0$. From the Euler characteristic formula for X, it therefore follows that the elliptic fibration on $E(1)$ has exactly $r = 12$ critical points and singular fibers.

Given a Lefschetz fibration $\hat{f} : \hat{X} \to \mathbb{C}P^1$ (assume again $\dim_{\mathbb{R}}(X) = 4$), it is often useful to know the genus of the generic fiber F_*. The following formula answers this question for pencils of degree 1 on hypersurfaces in $\mathbb{C}P^3$.

Proposition 1.39. (Genus Formula) *If $X \subseteq \mathbb{C}P^3$ is smooth hypersurface of degree d and $f : X \setminus B \to \mathbb{C}P^1$ is a pencil of degree 1. Then the genus g of the generic fiber F_* is given by*

$$g = \frac{(d-1)(d-2)}{2}$$

Proof. For a pencil of degree 1, the generic fiber is the intersection of X with a $\mathbb{C}P^2$ hyperplane in $\mathbb{C}P^3$. By choosing an isomorphism of this hyperplane with $\mathbb{C}P^2$ itself, it may be assumed that the intersection is given by a curve of degree d in $\mathbb{C}P^2$. It therefore suffices to prove the formula for a complex curve $C \subseteq \mathbb{C}P^2$ of degree d. Let ι denote the inclusion map of C. There is a splitting of vector bundles

$$\iota^*(T\mathbb{C}P^2) = TC \oplus N$$

where N is the normal bundle. Taking the first chern class c_1 and applying it to the fundamental class $[C] \in H_2(C;\mathbb{Z})$ yields

$$c_1(\iota^* T\mathbb{C}P^2)[C] = c_1(TC)[C] + c_1(N)[C]. \tag{1.3.1}$$

It is known that $c_1(T\mathbb{C}P^2) = 3x \in H^2(\mathbb{C}P^2;\mathbb{Z})$ where x is the generator (see [15], Proposition 14.10). Hence, by the naturality of pullback and because C is degree d, the left side of (1.3.1) is $3d$. On the right side, $c_1(TC) = e(TC)$ is the Euler class, so the first term is the Euler characteristic $2-2g$. Likewise, $c_1(N) = e(N)$ is the Euler class. The Euler number $e(N)[C]$ is also the number of zeroes in a generic section of the normal bundle, i.e. the self-intersection number. But since C is of degree d, it has d^2 self-intersections. Altogether, (1.3.1) becomes

$$3d = (2-2g) + d^2$$

and solving for g yields the formula.

□

The following result is a classic and celebrated theorem of Lefschetz himself. It is really only useful in higher dimensions, but it is worth stating nevertheless.

Theorem 1.40. (Lefschetz Hyperplane Theorem) *Suppose $X \subseteq \mathbb{C}P^N$ is a smooth variety of (complex) dimension n. Let $f : X \setminus B \to \mathbb{C}P^1$ be a Lefschetz pencil of degree 1 with base B. For every regular fiber F_t, the inclusion of the closed fiber $F_t \cup B \subseteq X$ induces an isomorphism*

$$H_k(F_t \cup B;\mathbb{Z}) \longrightarrow H_k(X;\mathbb{Z})$$

for $k < n-1$ and is surjective if $k = n-1$. In particular, the fibers of a Lefschetz fibration are always connected if X is.

Proof. See [2] Section 1.7 or [14] Section 5.2. □

Handle Attachments

It is a classic result [2] that a Morse function on a manifold gives rise to a handle-body decomposition. This subsection describes how to obtain a handle-body decomposition from a given Lefschetz fibration $f : X \to \mathbb{C}P^1$.

Consider a Lefschetz fibration restricted to a disk $D^2 \subseteq \mathbb{C}P^1$. If there are no critical points in D^2, then the fibration is the trivial $F_* \times D^2$. Now, one can imagine increasing the radius of the disk and seeing at what point the diffeomorphism type of the total space changes. This is analogous to looking at the submanifolds $g^{-1}[0,c)$ of a Morse function g and increasing c. In that case, Lemma 0.1 shows the topology changes only

when c passes a critical value. In the case of a Lefschetz fibration, expanding the disk does not change the diffeomorphism type of the pre-image provided the boundary of the disk does not cross any critical values. This follows from the Ehresmann Fibration Lemma (Lemma 1.17). Similar to the Morse case, the diffeomorphism type of the fibration restricted to the pre-image of a growing disk changes only when the disk expands to include a critical point.

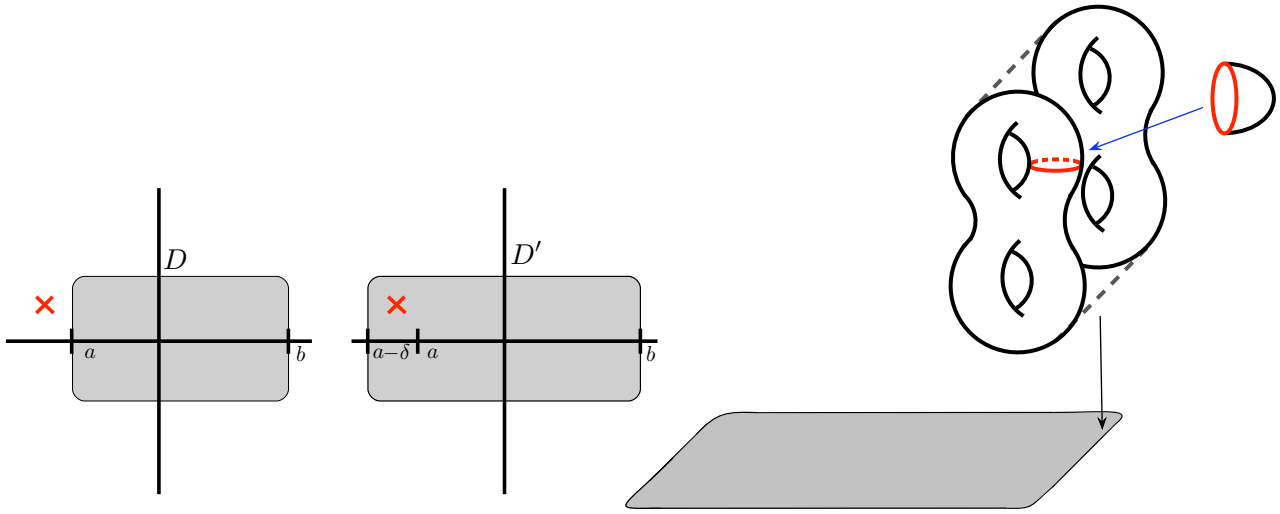

Figure 1.10: (Left) expanding the disk $D = [-1,1] \times [a,b]$ to $D' = [-1,1] \times [a-\delta, b]$ as in the proof of Proposition 1.41. The new disk D' contains the critical value t_i (red cross). (Right) A 2-handle attached along the vanishing cycle of a critical point to a fiber over the boundary ∂D.

The following proposition gives the precise change in the diffeomorphism type in the language of handle attachments. Recall that an n-dimensional k-handle is a copy of $D^k \times D^{n-k}$ attached to a framed sphere $S^{k-1} \subseteq X$.

Proposition 1.41. *Let $f : X \to \mathbb{C}P^1$ be a Lefschetz fibration. Suppose $D \subseteq D'$ are disks such that D' contains exactly one more critical value t_i than D. Then $f^{-1}(D')$ is obtained from $f^{-1}(D)$ (up to diffeomorphism) by a two-handle attachment along the vanishing cycle ν_i of the critical point in $f^{-1}(t_i)$.*

Notice here that ν_i is technically an isotopy class of embedded spheres, so attaching a two-handle requires choosing a representative. Isotopic attaching maps, however, result in the same manifold up to diffeomorphism ([16], Chapter 4), hence the choice of representative of the vanishing cycle does not matter.

Proof. By a choice of local coordinates on $\mathbb{C}P^1$, it may be assumed that D is a square $[-1,1] \times [a,b]$ and $D' = [-1,1] \times [a-\delta, b]$ so that the disk expands only horizontally (as in Figure 1.10, Left). Consider the negative of the projection to the real axis $f_{\mathbb{R}} := -Re(f)$, which has a single critical point with critical value $-Re(t_i) \in (-a, -a+\delta)$. In fact, this projection $f_{\mathbb{R}}$ is a Morse function, because by Lemma 1.21 there is a coordinate chart in which f is given by $(z_1, z_2) \mapsto z_1^2 + z_2^2$ so in real coordinates $z_j = x_j + iy_j$ the negative real part is $-Re(f) = -x_1^2 + y_1^2 - x_2^2 + y_2^2$, hence the critical point is non-degenerate. In terms of this Morse function, the total spaces are $f^{-1}(D) = f_{\mathbb{R}}^{-1}([-b, -a])$ and $f^{-1}(D') = f_{\mathbb{R}}^{-1}[-b, -a+\delta]$, thus the the latter is obtained from the former by a single $k-$handle attached to the descending sphere $\mathcal{D}_i$ of the critical point. Consider the descending sphere D_i in a subcritical level set, say $f_{\mathbb{R}}^{-1}(-(Re(t_i) + \varepsilon)$. Since in the above coordinates, $-Re(f) = -x_1^2 + y_1^2 - x_2^2 + y_2^2$, the single critical point has index 2. In fact, these coordinates are already standard Morse coordinates for the critical point, in which the descending sphere, $\mathcal{D}_i = \{(x_1, y_1, x_2, y_2) \mid x_1^2 + x_2^2 = \varepsilon \ , \ y_i = 0\}$ is, by definition, the vanishing cycle. □

This result is rather intuitive, since topologically, a nodal fiber is obtained from the generic fiber by attaching a disk bounded by the vanishing cycle, and contacting it.

It is now straightforward to obtain a complete handle-body decomposition of X. Above a disk D' without critical points, the pre-image is the trivial bundle $D^2 \times F$ for the generic fiber F a surface of genus g. This is diffeomorphic to a handle-body with a single 0-handle, $2g$ 1-handles, and a single 2-handle. Then one expands the disk, adding a 2-handle each time the disk D' expands to include another critical point. Once all the critical points are included, the result is a handle-body X^+ that is a union of 0, 1, and 2-handles. The pre-image of the complement is again a trivial bundle $D^2 \times F$ since the complementary disk does not include any critical point. The pre-image of the complement therefore has the same handle-body decomposition as the original $D^2 \times F$, call it X^-. The handle-body decomposition of X is obtained by gluing these two handle-bodies along their shared boundaries, $f^{-1}(\partial D')$. Alternatively, by considering a negative Morse function, X^- may be viewed as the union of the 3, 4−handles and one more 2-handle, which complete the handle-body decomposition begun with X^+.

There is one subtlety regarding framings. In dimension 4, one has to keep track of framing data for 2-handles ([16], Chapter 4). As before, let $D \subseteq \mathbb{C}P^1$ be a disk, and consider the restriction of the fibration to the pre-image $f^{-1}(D)$. When expanding D to include one more critical point, the attaching sphere can be taken to lie in a single fiber F_* of $\partial D \times F$. In the local coordinates used in the proof of Proposition 1.41, one could take F_* to be the fiber above $a + 0i$. A vanishing cycle lying in a single fiber has a canonical framing as follows. Let $\nu : [0,1] \to F_*$ parameterize the vanishing cycle. Then there is a canonical choice of a single normal vector given by $w_i(t) := i(D\nu(t)) \in TF_*$. Then, taking a second normal $w_2(t)$ along the ∂D factor in the boundary $\partial D \times F$ yields a framing $\varphi : S^1 \times D^2 \to N(\nu)$ of the normal bundle of ν by $(t, e_1, e_2) \mapsto (\nu(t), w_1(t), w_2(t))$.

Proposition 1.42. *The 2-handle for at the critical point with value t_i is attached with a -1 framing relative to this canonical framing.*

Proof. In Morse coordinates, the 2-handle is attached to the descending sphere of the critical point $\mathcal{D} = \{(x_1, y_1, x_2, y_2) \mid x_1^2 + x_2^2 = \varepsilon \ , \ y_i = 0\}$ by the obvious framing of the normal bundle of S^1_ε in Euclidean space. To determine how the canonical framing differs from this one given by the Morse coordinates, it suffices to count how many times the vector $w_1(t)$ rotates in the coordinates. In the (complex) local coordinates, the descending sphere (which is also the vanishing cycle) is parameterized by $t \mapsto (\sqrt{\varepsilon}\cos(t), \sqrt{\varepsilon}\sin(t))$. The tangent vector is $(-\sqrt{\varepsilon}\sin(t), \cos(t))$. Hence $w_1(t) = (-i\sqrt{\varepsilon}\sin(t), i\sqrt{\varepsilon}\cos(t))$. One therefore sees that the vector $w_1(t)$ rotates once (counterclockwise) for $t \in [0, 2\pi]$ with respect to the framing from the Morse coordinates which is given by $e_1 = (i, 0), e_2 = (0, i)$. The canonical framing given by the surface F_* therefore differs by 1 from the framing provided by the Morse coordinates, which is the framing of the attached handle. A careful check of orientations shows -1 is the correct signed framing of the handle relative to the canonical framing given by the surface (see ([16], pgs. 292-93). □

This description via handle attachments gives an easy algorithm to draw a handle-body diagram for the 4-manifold X. From there, one can employ "handle-body calculus" (also called "Kirby calculus") to analyze X or compare it to a handle-body diagram for another manifold X' to attempt to prove or disprove the two are the same. The reader not familiar with the calculus of handle-body diagrams is referred to [16] or [17]. The reader not concerned with handle-body calculus can proceed to the next subsection.

A handle-body diagram of X can be constructed from a Lefschetz fibration $f : X \to \mathbb{C}P^1$ as follows. First, choose a basepoint $* \in \mathbb{C}P^1$, viewed as $\mathbb{C}$ as it may be assumed that infinity is not a critical value. Label the critical values $t_1, ..., t_r$ counterclockwise, and choose a collection of vanishing paths $\delta_1, ..., \delta_r$. As in 1.24 and 1.25, this gives a vanishing cycle $[\nu_i]$ in F_* for each $i = 1, ..., r$. Different choices of a set of vanishing paths can result in different handle-bodies for X, which will necessarily be equivalent by a sequence of "handle-body moves" (it is a standard result, see [16], that any two handle-body diagrams for the same manifold differ by such a sequence). The effect of different choices of sets of vanishing cycles is discussed in greater detail in the next subsection.

To construct a handle-body for X, begin with the standard handle-body diagram for $D^2 \times F$ for F a genus g surface. This includes $2g$ 1-handles and a single 0-framed (see [16] for conventions) 2-handle running

over all of them, as in Figure 1.11. Given vanishing cycles $\nu_1, ..., \nu_n$ in F_*, draw the attaching circles (in order!) starting with ν_1 in the diagram as if drawing each of them in a 2-dimensional handle-body. All these 2-handles are given a -1 framing. See Figure 1.12. There is one final 2-handle to attach, coming from $X^- \simeq D^2 \times F$. Seeing how to attach this final handle, and what framing it should have, is rather tricky and involves keeping track of how the boundary $\partial D \times F$ appears in the diagram after adding all the 2-handles. By a standard result in handle-body calculus ([16], pg. 116), after attaching the 2-handles there is a unique way to attach 3 and 4-handles.

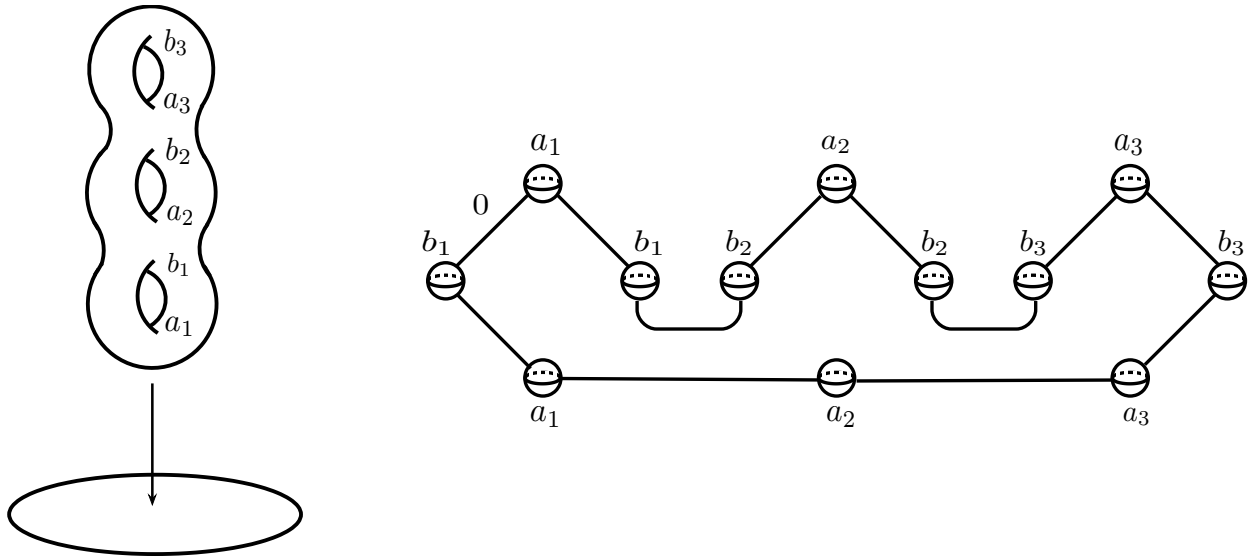

Figure 1.11: (Left) the trivial bundle $D^2 \times F$ where F is the surface of genus 3. The 1-handles are labelled $a_1, ..., b_3$. (Right) the corresponding handle-body diagram with the 1-handles labelled. A single 0-framed 2-handle passed over all of them.

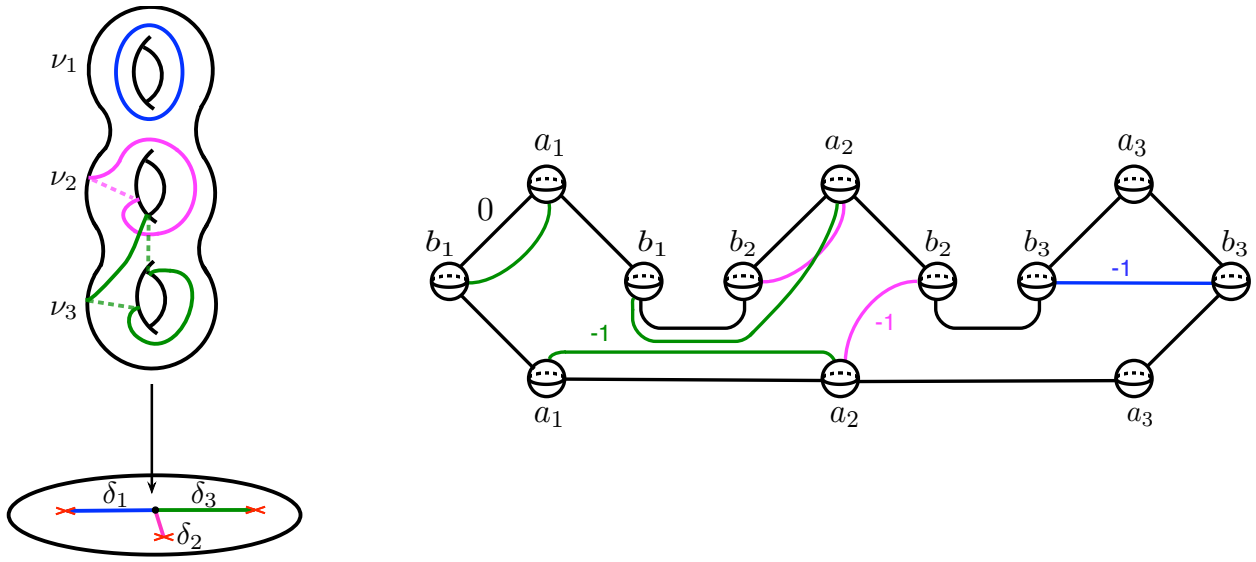

Figure 1.12: (Left) Expanding the fibration to include three critical points with vanishing paths δ_i and vanishing cycles ν_i shown. (Right) each vanishing cycle adds a -1-framed 2-handle to the diagram of Figure 1.11.

Once the handle-body diagram is drawn, one can freely use handle moves and Reidemeister moves to simplify it or show it is equivalent to another handle-body. One should note that choosing a rotated chart will result in a cyclic permutation of the vanishing cycles $\nu_1, ..., \nu_n$ that will move the bottommost attaching circle to the top. These two handle-bodies will be equivalent, though at times via an extensive sequence of moves. It is often worthwhile, therefore, to search for an angle at which to start the indexing of the vanishing cycles that gives a more tractable diagram.

Example 1.43. It is possible, though not very straightforward, to find the vanishing cycles for the elliptic surface $E(1)$ introduced in Example 1.8 of Section 1.1. By Example 1.38, a Lefschetz fibration on $E(1)$ will have 12 vanishing cycles in a generic fiber, which is diffeomorphic to a torus. The torus has two non-trivial isotopy classes of simple closed curves as shown on the left in Figure 1.13 below. One can show that for paths $\gamma_1, ..., \gamma_{12}$ the vanishing cycles alternate between the two isotopy classes. These 12 vanishing cycles result in 12 corresponding 2-handles, each attached with a -1 framing, giving the handle-body diagram in Figure 1.13. It is also possible to show that the final 2-handle should be attached around the original 0-framed 2-handle with a framing of -1. These calculation are worked out in more detail in [16] (Example 8.2.11) and [18].

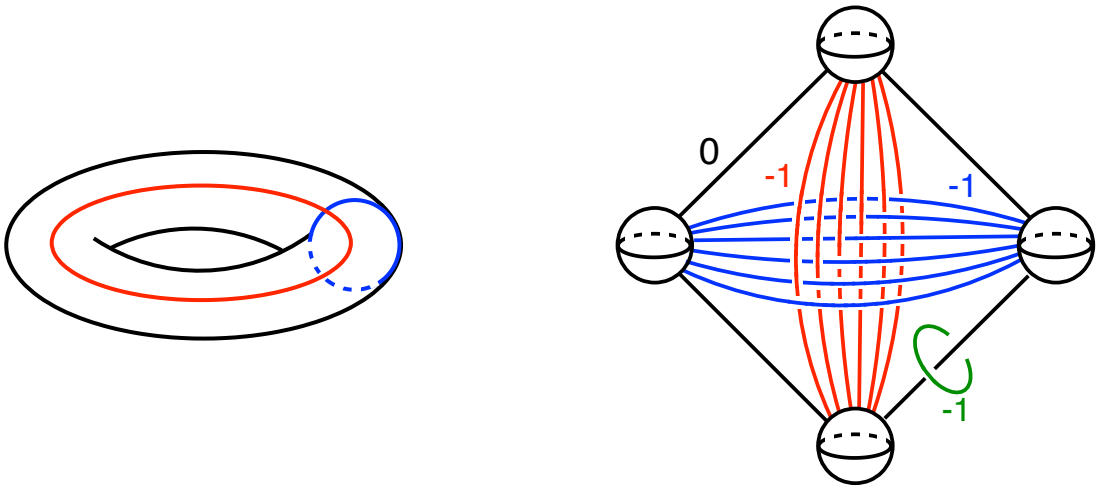

Figure 1.13: (Left) the torus with its two non-trivial isotopy classes of curves indicated (red, blue). (Right) the handle-body diagram for the surface $E(1)$. 12 2-handles alternating between the two isotopy classes are attached with framing -1. The extra 2-handle from the second copy of $D^2 \times T^2$ is indicated in green.

Remark 1.44. Lefschetz fibration are a quite powerful tool for obtaining handle-body diagrams. In theory, any Morse function on a 4-manifold can be used to obtain a handle-body, however it is rarely possible to calculate the framings for complicated manifolds. For example, if one chooses Morse coordinates, the framing information is hidden in the transition maps to nearby coordinate charts. The fact that the 2-handles in a Lefschetz fibration are always attached with a -1 framing makes them significantly more practical for drawing handle-body diagrams than general Morse functions.

Relations in $Mod(S_g)$ and Classification of Lefschetz Fibrations

This subsection introduces equivalence relations between collections of vanishing paths. This leads to an important theorem of Kas and Matsumoto.

As discussed in Section 1.2, the monodromy of a Lefschetz fibration $f : X \to \mathbb{C}P^1$ gives a (anti)-homomorphism,

$$\mu : \pi_1(\mathbb{C}P^1 \setminus \{t_1, ..., t_r\}, *) \longrightarrow Mod(F_*).$$

Specifying a collection of vanishing paths $\delta_1, ..., \delta_r$ determines a set of generators $[\gamma_1], ..., [\gamma_r]$ for the fundamental group $\pi_1(\mathbb{C}P^1 \setminus \{t_1, ..., t_r\}, *)$ which satisfy the relation $[\gamma_1] \cdot \ldots \cdot [\gamma_r] = 1$. By the Picard-Lefschetz Theorem (Theorem 1.35) there is a corresponding relation of mapping classes

$$[\tau_{\nu_1}] \circ \ldots \circ [\tau_{\nu_r}] = Id, \tag{1.3.2}$$

where τ_{ν_i} is the Dehn twist around each vanishing cycle ν_i. Thus, by choosing a diffeomorphism $\psi : F_* \to S_g$ with the standard genus g surface, a Lefschetz fibration on X and a choice of vanishing paths determine an ordered collection of Dehn twists in $Mod(S_g)$ whose product is the identity.

Conversely, given an ordered collection of Dehn twists along simple closed curves $[\tau_{\nu_1}], ..., [\tau_{\nu_r}] \in Mod(S_g)$ whose product is the identity, one can construct a Lefschetz fibration with generic fiber S_g. This fibration is constructed as follows. Begin with a trivial fibration $f : D^2 \times S_g \to D^2$ given by projection. Choose a fiber on the boundary $\partial D^2 \times S_g$ and attach a 2-handle h_1 along a simple closed curve representing the isotopy class ν_1 with a framing -1 relative to the canonical framing determined by the fibers as in Proposition 1.42. As before, the choice of curve within the isotopy class ν_1 does not matter when considering the space up to diffeomorphism. It is possible to extend the fibration f over the handle h_1 with a single critical point in the core of the 2-handle. This yields a new fibration with a single critical point. Up to a diffeomorphism of the base, it may be assumed that this new fibration is also over the disk with the single critical point in the interior. By the Picard-Lefschetz theorem, the monodromy around the boundary $f^{-1}(\partial D)$ is now $[\tau_{\nu_1}]$. Now repeat the procedure, attaching a 2-handle h_i along the curve ν_i in a boundary fiber at each successive step. After attaching the handle h_i, the monodromy around the boundary ∂D will be $[\tau_{\nu_1}] \circ \ldots \circ [\tau_{\nu_i}]$. After all the 2-handles are attached, the result is a fibration over the disk whose monodromy around the boundary is trivial up to isotopy by the assumption that $[\tau_{\nu_1}] \cdot \ldots [\tau_{\nu_r}] = Id$. The the boundary is therefore the trivial fibration $S^1 \times S_g$. A closed $4-$manifold with a Lefschetz fibration over $\mathbb{C}P^1 \simeq S^2$ is obtained by gluing $S_g \times D^2$ by the identity on their common boundary. In this way, a relation of Dehn Twists of the form (1.3.2) in the mapping class group determines a 4-manifold with a Lefschetz fibration.

Two relations of the form (1.3.2) can result in the same Lefschetz fibration. This can occur in two ways (and in combination). First, choices of the diffeomorphism $\psi : F_* \to S_g$ can differ yet yield the same fibration. Second, different collections of vanishing paths can describe the same fibration. These two equivalences are now described in detail.

I. (Simultaneous Conjugation)

Given an $r-$tuple of Dehn-twists $([\tau_{\nu_1}], \ldots, [\tau_{\nu_r}])$ whose product is the identity in $Mod(S_g)$ and any other mapping class $[\phi] \in Mod(S_g)$ consider conjugating each Dehn twist by $[\phi]$.

$$([\tau_{\nu_1}], \ldots, [\tau_{\nu_r}]) \longrightarrow \left([\phi] \circ [\tau_{\nu_1}] \circ [\phi]^{-1} \ , \ \ldots \ , \ [\phi] \circ [\tau_{\nu_r}] \circ [\phi]^{-1}\right). \tag{1.3.3}$$

This yields a new tuple whose product is still the identity. Recall that to obtain a relation in $Mod(S_g)$ from a Lefschetz fibration, a diffeomorphism $\psi : F_* \to S_g$ associating the base fiber with the standard genus g surface had to be chosen. This choice, however, is not canonical and two different choices ψ_1, ψ_2 will result in two different tuples of Dehn twists that differ by conjugation by $[\phi] = [\psi_2 \circ \psi_1^{-1}] \in Mod(S_g)$. The difference in the two r-tuples here is an artifact of the choice of ψ and does not reflect anything about the topology of X. This shows that r-tuples of Dehn twists that differ by conjugation by some ϕ can yield the same Lefschetz fibration.

II. (Hurwitz Equivalence)

Given an r-tuple of Dehn-twists one may also consider the operation

$$([\tau_{\nu_1}], \ldots, [\tau_{\nu_r}]) \longrightarrow \left([\tau_{\nu_1}] \ , \ \ldots \ , \ [\tau_{\nu_i}] \circ [\tau_{\nu_{i+1}}] \circ [\tau_{\nu_i}]^{-1} \ , \ [\tau_{\nu_i}] \ , \ \ldots \ , \ [\tau_{\nu_r}]\right) \tag{1.3.4}$$

for each $i = 1, ..., r$. By inspection, it is clear the product is still the identity. Again, r-tuples of differ by this operation can correspond to the same Lefschetz fibration. Geometrically, (1.3.4) results from the following operation when choosing a collection of vanishing paths. Replace an adjacent pair (δ_i, δ_{i+1}) with $(\sigma_{i,i+1}(\delta_i), \sigma_{i,i+1}(\delta_{i+1}))$ where $\sigma_{i,i+1}$ is the half Dehn twist flipping the two points t_i, t_{i+1} (considered up to

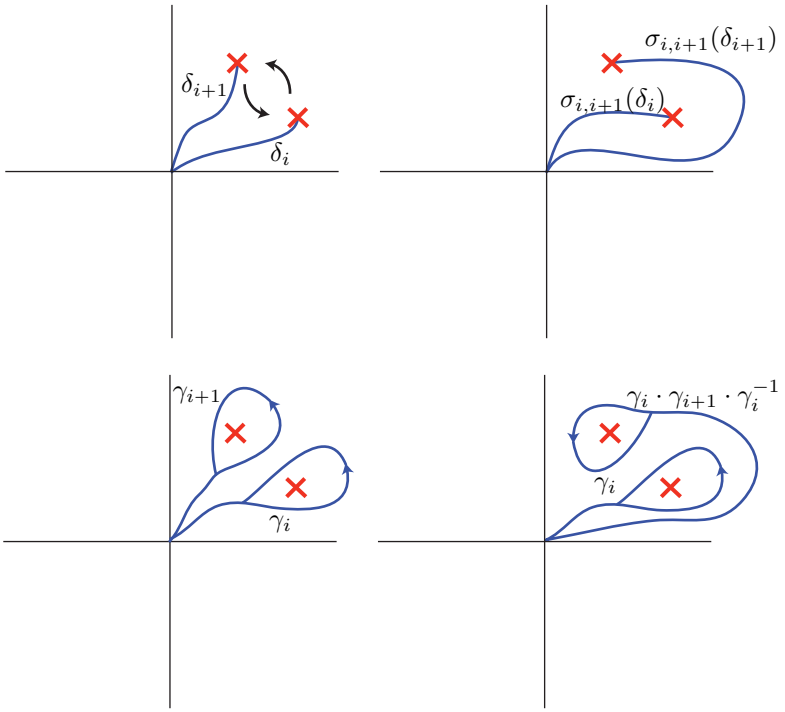

Figure 1.14: (Left) two vanishing paths before and after the operation of applying $\sigma_{i,i+1}$. (Right) the operation on the corresponding generators of the fundamental group.

isotopy). One then checks that the corresponding pair generators $([\gamma_i], [\gamma_{i+1}])$ in $\pi_1(\mathbb{C}P^1 \setminus \{t_1, ..., t_r\}, *)$ is transformed by $([\gamma_i], [\gamma_{i+1}]) \mapsto ([\gamma_i] \cdot [\gamma_{i+1}] \cdot [\gamma_i]^{-1}, [\gamma_i])$ as in Figure 1.14 above. Since the monodromy is an (anti) homomorphism, one sees that two choices of vanishing paths on the same Lefschetz fibration that differ by this operation result in r-tuples of mapping classes that differ by (1.3.4).

One might suspect, since the half twists $[\sigma_{i,i+1}]$ generate the mapping class group of $D^2 - \{t_1, ..., t_r\}$ for some disk large enough to include all the critical values, that this is the only redundancy resulting from different choices of vanishing paths. The following theorem (which is not proved here) due to Kas and Matsumoto, shows that, topologically, Lefschetz fibrations of genus $g \geqslant 2$ are *completely* determined by the r-tuple of Dehn twist up to these two operations.

Theorem 1.45 (Kas [19], Matsumoto [20]). *For $g \geqslant 2$, there is a 1-1 correspondence*

$$\left\{ \begin{array}{c} 4-\textit{manifolds w/ Lefschetz} \\ \textit{fibrations of genus } g \end{array} \right\} \Big/ \textit{Diffeo.} \Longleftrightarrow \left\{ \begin{array}{c} r\textit{-tuples in } Mod(S_g) \\ [\tau_{\nu_1}] \circ \ldots \circ [\tau_{\nu_r}] = Id \end{array} \right\} \Big/ \left\{ \begin{array}{c} \textit{Simultaneous conjugation} \\ \textit{Hurwitz equivalence} \end{array} \right\}$$

On the left, two Lefschetz fibrations $f : X \to S^2$ and $f' : X' \to S^2$ are diffeomorphic if there exist diffeomorphisms $\Phi : X \to X'$ and $\varphi : S^2 \to S^2$ so that $\varphi \circ f = f' \circ \Phi$. In particular, the total spaces are diffeomorphic. A similar correspondence to 1.45 holds for Lefschetz pencils with $Mod(S_g^k)$, the mapping class group of the k-times punctured surface of genus g, in place of $Mod(S_g)$ where k is the number of base points.

This is the characterizations of Lefschetz fibrations by monodromy that was advertised at the beginning of the chapter. It says, essentially, that one can classify the total spaces of Lefschetz fibrations up to

diffeomorphism by knowing only the monodromy information. In principle, this reduces the study of the topology of 4-manifolds possessing Lefschetz fibrations to the study of relations in the mapping class group $Mod(S_g)$.

Remark 1.46. The forward direction of Theorem 1.45 is given by choosing a collection of vanishing paths and obtaining the expression (1.3.2). The reverse direction is given by the handle-body construction described above. One should note also that this handle-body construction can give Lefschetz fibrations that do not obviously arise from pencils on algebraic varieties. By the genus formula, the genus of a Lefschetz fibration resulting from a degree 1 pencil on a (degree d) hypersurface $X \subseteq \mathbb{C}P^3$ will necessarily have genus $g = \frac{(d-1)(d-2)}{2} = 1, 3, \ldots$. It is not *a priori* obvious whether a Lefschetz fibration, say of genus 2, can be obtained from pencils on algebraic surfaces. The handle-body construction, however, gives Lefschetz fibrations with any genus, provided relations of the form $[\tau_{\nu_1}] \circ \ldots \circ [\tau_{\nu_r}] = Id$ exist in $Mod(S_g)$. These include fibrations that do not come from pencils on algebraic varieties. In fact, several authors have given explicit relations in $Mod(S_g)$ that result in genus g Lefschetz fibrations whose total spaces admit no complex structure [21], hence cannot arise from algebraic varieties at all! The above Theorem 1.45 therefore applies to a class of 4-manifolds strictly larger than projective varieties. To some extent, Chapters 3 and 4 are devoted to answering the question of which $4-$manifolds admit Lefschetz fibrations.

Remark 1.47. It is not at all obvious that one cannot have a Lefschetz fibration with no critical points but with non-trivial gluing around the equator. In fact, for $g = 0$, such a fibration exists. There is a non-trivial diffeomorphism $\phi : S^2 \to S^2$ given by reflection through one axis. Gluing $D^2 \times S^2$ to itself with via an S^1 family of ϕ along the boundary results in a non-trivial sphere bundle, often denoted $S^2 \tilde{\times} S^2$. One can check that it is not diffeomorphic to $S^2 \times S^2$ by comparing the cup product structures. In fact, this was the Lefschetz fibration obtained in Example 1.7 from blowing-up a degree 1 pencil on $\mathbb{C}P^2$ at a single base-point. Implicit in Theorem 1.45 is the assertion that any surface bundle of genus $g \geqslant 2$ obtained by gluing two copies $D^2 \times S_g$ along the equator is necessarily the trivial bundle.

Chapter 2

Lefschetz Bifibrations and Vanishing Cycles

Chapter 1 showed that given a Lefschetz fibration $\hat{f} : \hat{X} \to \mathbb{C}P^1$, knowing the vanishing cycles associated to each critical point is, in principle, enough to determine the total space $\hat{X}$. In particular, by the Picard-Lefschetz Theorem (1.35), the vanishing cycles of a Lefschetz fibration determine the monodromy, which in turn, determines $\hat{X}$ up to diffeomorphism by Theorem 1.45. So far, however, this is only an abstract correspondence: given a specific smooth complex variety, it is not at all obvious how to calculate the monodromy.

Consider, for example, the family of **tom Dieck-Petrie Surfaces** $X_{k,\ell} \subseteq \mathbb{C}^3$ defined by

$$X_{k,\ell} = \left\{ \frac{(xz+1)^k - (yz+1)^\ell}{z} = 1 \right\}, \tag{2.0.1}$$

where (k, ℓ) are relatively prime. These are smooth affine surfaces, and so (recall Remark 1.16) admit Lefschetz fibrations over $\mathbb{C}$. Given such a Lefschetz fibration, what is the monodromy? That is, how many vanishing cycles does f have, and what are the vanishing cycles as simple closed curves in the generic fiber? It is not *a priori* evident how to answer these questions for, say, the tom Dieck-Petrie surface $X_{12,7}$. In fact, it is not clear how to answer them even for the fibration of $E(1)$ in Example 1.8, which is perhaps the simplest non-trivial Lefschetz fibration.

A method for calculating vanishing cycles allows one to realize Theorem 1.45 concretely. By the Picard-Lefschetz Theorem, the vanishing cycles determine an explicit r-tuple of Dehn Twists in the mapping class group of the generic fiber. This r-tuple represents the equivalence class on the right side of Theorem 1.45; it determines the diffeomorphism type of $\hat{X}$ among all 4-manifolds that posses Lefschetz fibrations of the same genus, thereby allowing one to say definitively when $\hat{X}$ is diffeomorphic to another variety with a Lefschetz fibration. More generally, the vanishing cycles of a Lefschetz fibration give a handle-body of $\hat{X}$ (as in Section 1.3), which can be compared to handle-bodies of 4-manifolds arising from different constructions.

This chapter describes a general algorithm for explicitly calculating the vanishing cycles of a Lefschetz fibration. Given a Lefschetz fibration f on $\hat{X}$, the end result of the algorithm is a list of simple closed curves in a standard genus g surface that represent the vanishing cycles of the critical points of f. Much of the chapter is devoted to showing in complete detail how this algorithm is realized in the case of the tom Dieck-Petrie (3,2) surface. This chapter therefore provides a concrete, example-driven discussion complementing the general theory described in Chapter 1.

The techniques that appear in the algorithm are also useful beyond simply identifying the diffeomorphism type of $\hat{X}$. In fact, these techniques were originally developed in the context of symplectic geometry by Paul Seidel, Simon Donaldson, Denis Auroux, Vicente Muñoz, Francisco Presas, and others [22, 23]. Lefschetz fibrations can be made compatible with symplectic structures, and the methods used in the algorithm can

provide significant insight into symplectic topology. While a complete discussion of the applications of these techniques to symplectic topology is beyond the scope of this exposition, part of the intent of this chapter is to familiarize the reader with these useful, and slightly more advanced, techniques in the study of Lefschetz fibrations. These techniques are often used in research articles, but are typically excluded from elementary introductions to the subject.

This chapter considers the general case of an affine variety $X \subseteq \mathbb{C}^N$ of (complex) dimension 2 equipped with a Lefschetz fibration $f : X \to \mathbb{C}$ of degree 1. The advantage of working in this case is that one may work in a single global coordinate chart, which greatly simplifies calculation.

Remark 2.1. In fact, the above case is sufficient to understand the case of projective varieties $X \subseteq \mathbb{C}P^n$ of (complex) dimension 2 as well. One can reduce this case to the affine case as follows. Suppose that $f : X \to \mathbb{C}P^1$ is a Lefschetz pencil of degree 1 given by $[P_1; -P_0]$ where P_0, P_1 are homogenous linear polynomials, say of the form $P_i = a_0 z_0 + \ldots + a_N z_N$ in homogenous coordinates $[z_0 \ ; \ \ldots \ ; \ z_N]$ on $\mathbb{C}P^N$. In fact, by a change of coordinates, one may assume that $P_0 = z_N$, and then, take coordinates on the complement of the $\mathbb{C}P^{N-1}$ hyplerplane on which P_0 vanishes to reduce to the case of an affine fibration. Specifically, one restricts to a coordinate chart given by $(x_1, \ldots, x_N) \mapsto [x_1 \ ; \ \ldots \ ; \ x_N \ ; 1]$, in which f is given by $f = [P_1; 1]$. By choosing coordinates $z \mapsto [z; 1]$ on $\mathbb{C}P^1$ as well, one may assume $f : \mathbb{C}^n \to \mathbb{C}$ is given in coordinates by $f(x_1, \ldots, x_N) = a'_1 x_1 + \ldots + a'_N x_N$. In this situation, there are no base points in this coordinate chart, since any base points are necessarily contained in the hyperplane where P_0 vanishes. One can assume (possibly by perturbing the coefficients of f) that $[1; 0] \in \mathbb{C}P^1$ is not a critical value, so that there are no critical points outside the coordinate chart considered. The algorithm obtains vanishing cycles for all the critical points in the affine fiber $F_* \cap \{P_0 \neq 0\}$, which can then be considered in the closed fiber F_* to obtain a description of the vanishing cycles of the fibration $\hat{f} : \hat{X} \to \mathbb{C}P^1$.

Depending on the situation, one may wish to study X itself, or a blow-up of X as in the example of the elliptic surface $E(1)$ regarded as a blow-up of $\mathbb{C}P^2$. Even when one wishes to study X itself, however, it is useful to use the methods of this and the previous chapter to study the blow-up first, and then understand X as the blow-down obtained by collapsing exceptional spheres.

The idea of the algorithm is to consider the fibers of f as branched covers of $\mathbb{C}$ and keep track of the branching behavior near a singular fiber. For an affine fibration $f : X \to \mathbb{C}$ the fibers are surfaces punctured where their projectivization intersects the hyperplane at infinity; the singular fibers also have nodal singularities. The Riemann-Hurwitz formula for a generic branched cover $\rho : \Sigma \mapsto \mathbb{C}$ (i.e. one with only doubly ramified points) gives :

$$\chi(\Sigma) = \deg(\rho)\chi(\mathbb{C}) - (\#\text{ of branch points}) \tag{2.0.2}$$

where χ denotes the Euler characteristic. A singular fiber F' resulting from collapsing a homologically non-trivial vanishing cycle will have one fewer generator of $H_1(F'; \mathbb{Z})$ than the regular fiber F_*, so the Euler characteristics are related by $\chi(F') = \chi(F_*) + 1$. Thus, by the Riemann-Hurwitz formula

$$\{\#\text{ of branch points of singular fiber}\} = \{\#\text{ of branch points of regular fiber}\} - 1. \tag{2.0.3}$$

If one considers a family of fibers F_t with a smoothly varying family of branched covers $\rho_t : F_t \to \mathbb{C}$, the critical values will vary smoothly with t. In particular, choosing a family of fibers above a vanishing path δ_i approaching a singular fiber, (2.0.3) implies that two critical points will come together to become a single critical point in the branched cover of the singular fiber. See Figure 2.1. As will be shown in Section 1.3, the pre-image of a path connecting these two critical points will contain a simple closed curve. As the two branch points come together, this simple closed curve shrinks to a point. This shrinking simple closed curve will be the vanishing cycle.

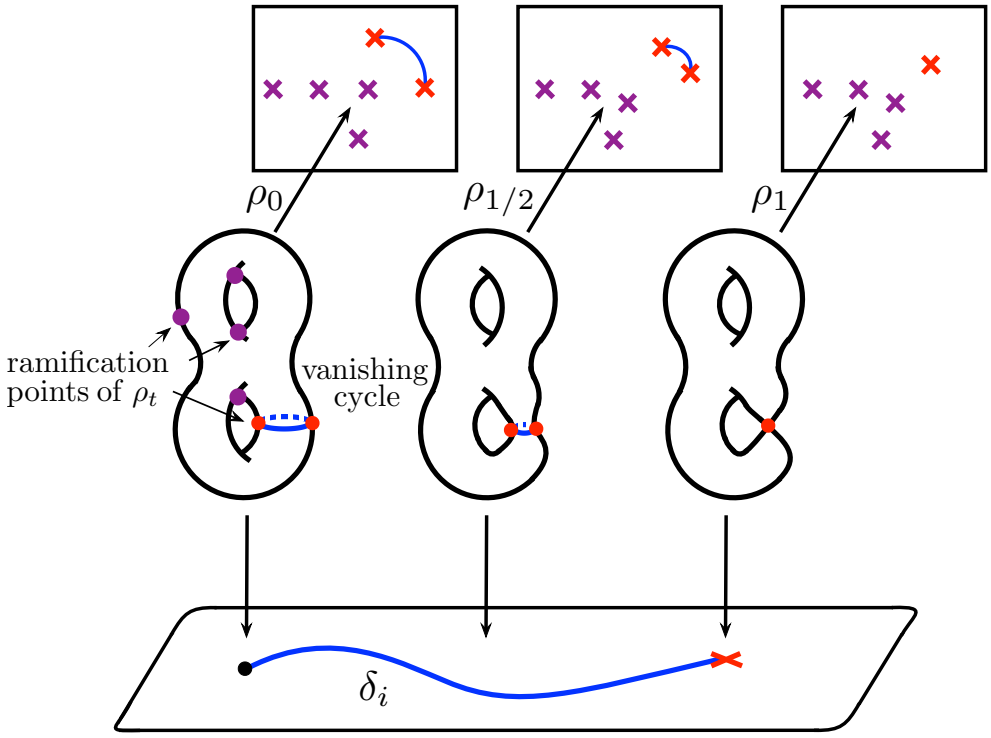

Figure 2.1: A family of fibers F_t above a vanishing path δ_i (blue) equipped with branched covers ρ_t (projection back). For regular fibers, ρ_t has six ramification points and six branch points (crosses). At $t = 1$, two branch points (red crosses) come together to become a single branch point. The pre-image of a line between these two branch points is the vanishing cycle (blue).

Example 2.2. It is instructive to see how the above ideas are realized in the standard coordinate model at a critical point. The standard coordinate model on B^4, given by

$$(z_1, z_2) \mapsto z_1^2 + z_2^2,$$

has a single critical point at the origin. Let $\delta : [0, 1] \to \mathbb{C}$ be the vanishing path $\delta(t) = 1 - t$ which, ends at the critical value. The fiber over $\delta(t)$ is $F_t = \{z_1^2 + z_2^2 = 1 - t\}$ for $t \in [0, 1]$. For each $t \in [0, 1]$, the projection $\rho_t(z_1, z_2) = z_1$ defines a branched cover $\rho_t : F_t \to \mathbb{C}$ whose ramification points satisfy $z_2 = 0$, so are given by $z_1 = \pm\sqrt{1 - t}$. Thus for each $t > 0$, ρ_t has two branch points, namely $t = \pm\sqrt{1 - t} \in \mathbb{C}$. As $t \to 0$, the two branch points merge into a single branch point $(0, 0) \in B^4$. For each fixed t_0, the pre-image under ρ_t of the line segment $[-\sqrt{1 - t_0}, \sqrt{1 - t_0}] \subseteq \mathbb{C}$ is the vanishing cycle of the critical point $(0, 0)$ considered as a subset of the fiber F_t. That is to say, the pre-image of a line connecting the two critical values of ρ_0 that come together at $t = 1$ is the vanishing cycle in the fiber F_0.

Note on terminology: Throughout this section, the algorithm will keep track of the data of both a Lefschetz fibration $f : X \to \mathbb{C}$ and a family of branched covers $\rho : F_t \to \mathbb{C}$. Recall (by Example 1.9) that a generic branched cover (only doubly ramified points) is a specific case of a Lefschetz fibration. In the language of Lefschetz fibrations, the ramification points are the critical points, and the branch points in $\mathbb{C}$ are the critical values. Throughout this chapter, the terminology of branched covers and Lefschetz fibrations will be used interchangeably, the former being useful to avoid confusion, while the latter at times being useful to highlight similarities.

2.1 Matching Cycles

The preceding ideas are now made precise. First, the idea that the pre-image of a path joining two critical points is a simple closed curve is formalized. This is in fact not specific to surfaces, so for a moment let $\dim_{\mathbb{R}}(X) = n$ be arbitrary. Suppose that $f : X \to \mathbb{C}$ is a Lefschetz fibration with critical values $t_1, ..., t_r$. Choose a basepoint $* \in \mathbb{C}$ that is a regular value, and let $\delta_1, ..., \delta_r$ be a collection of vanishing paths.

Definition 2.3. *A path $\mu : [-1, 1] \to \mathbb{C}$ such that the restrictions $\mu|_{[0,1]}$ and $\mu|_{[-1,0]}$ are each vanishing paths is called a* **matching path**. *That is, if $\mu|_{[0,1]} = \delta_i$, and $\mu|_{[-1,0]} = \delta_j$ for some vanishing paths δ_i, δ_j (with δ_j traced in reverse).*

Recall that for each t near t_i, there is a vanishing cycle ν_i in $f^{-1}(t)$. By choosing trivialization of the bundle above δ_i, one may transport this vanishing cycle to the fiber above $\delta_i(t)$ for any other t. Recall the union of these, the Lefschetz thimble, is an embedded ball B^n, now arranged to have boundary $\nu_i \simeq S^{n-1}$ in the fiber F_*. A matching path results in two thimbles diffeomorphic to B^n with boundary ν_i, ν_j in F_*. If $\nu_i = \nu_j$ as subsets of F_*, these two thimbles can be glued together to obtain an embedded sphere $\Sigma_\mu \subseteq X$. In high dimensions, one must carefully consider framings to avoid exotic spheres, though this issue is not addressed here. It would be quite a strange coincidence if the vanishing cycles agreed exactly as sets. Instead, if they are simply isotopic, one can alter the choice of trivialization of the bundle away from the critical points to arrange that this isotopy is realized along the path μ so that the vanishing cycles ν_i, ν_j *do* agree as sets in F_*. Choosing different trivializations to transport the vanishing cycles ν_i to the fiber F_* yields an isotopic sphere, thus Σ_μ is well-defined up to isotopy.

Definition 2.4. *When it exists, the isotopy class $[\Sigma_\mu]$ of embedded spheres is called the* **matching cycle** *of the matching path μ.*

Of course, if the two vanishing cycles ν_i, ν_j are not isotopic, then no matching cycle exists (see Figure 2.2). In the case of a branched cover, $\rho : F \to \mathbb{C}$, the vanishing cycle is the 0-sphere that collapses at the critical points, i.e. it is two points in different sheets of the cover meeting at a ramification point. A matching cycle yields an isotopy class of simple closed curves. For instance, in Example 2.2, the path $[-1, 1] \subseteq \mathbb{C}$ in the image of the branched cover $\rho_1 : F_1 \to \mathbb{C}$ is a matching cycle. In that example, it is obvious that the vanishing cycles agree pointwise because they are both the entire fiber.

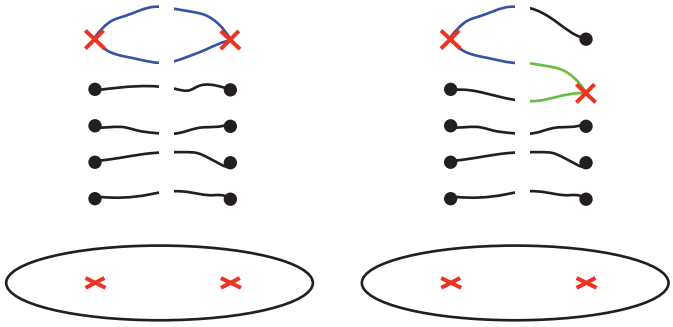

Figure 2.2: Lefschetz thimbles in a branched cover. On the left, the vanishing cycles (blue) agree and there is a well-defined matching cycle. On the right, no matching cycle exists.

Now the algorithm to calculate vanishing cycles is outlined. Each step will take advantage of the idea of matching cycles, using it to express the vanishing cycles of the fibration $f : X \to \mathbb{C}$ as matching cycles. The algorithm consists of three steps.

(1) Express each vanishing cycle $\nu_1, ..., \nu_r \in F_*$ as a matching cycle of some matching path in a branched cover $\rho : F_* \to \mathbb{C}$.

(2) Find a collection of matching paths $a_1, ..., a_k \in \mathbb{C}$ whose matching cycles form a basis of $H_1(F_*; \mathbb{Z})$.

(3) Use half-twists to express the matching cycles of $\nu_1, ..., \nu_r$ in terms of the collection $a_1, ..., a_\ell$. Lifting these to Dehn twists in F_* (recall Lemma 1.34) then gives an expression for each ν_i in terms Dehn twists of the basis elements in $H_1(F_*; \mathbb{Z})$.

The next three sections of this chapter are devoted, one each, to describing these three steps in detail. At the end of the description of each step, the process is carried out in the case of the (3,2) tom Dieck-Petrie surface to elucidate how the algorithm works in practice.

2.2 Lefschetz Bifibrations

The idea of families of branched covers is made precise through the notion of Lefschetz bifibrations, which is due to Paul Seidel [23]. Essentially, a Lefschetz bifibration is the data of a Lefschetz fibration and a Lefschetz fibration of each fiber. These will later allow vanishing cycles to be expressed as matching cycles of certain paths.

Definition 2.5. *A* **Lefschetz Bifibration** *on a smooth affine variety $X \subseteq \mathbb{C}^N$ is a pair of maps ρ, π satisfying the following four conditions:*

$$\begin{array}{ccccc} X & \xrightarrow{\rho} & \mathbb{C} \times \mathbb{C} & \xrightarrow{\pi} & \mathbb{C} \\ & \searrow & & \nearrow & \\ & & f & & \end{array}$$

(i) π has no critical points and the composition $f := \pi \circ \rho : X \to \mathbb{C}$ is a Lefschetz fibration on X.

(ii) Denote by $F_t := f^{-1}(t)$ and $C_t := \pi^{-1}(t)$ the fibers over a point $t \in \mathbb{C}$. The restriction

$$\rho|_t : F_t \to C_t$$

is required to be a Lefschetz fibration. On singular fibers F'_x containing a critical point x, this means a holomorphic map with isolated, non-degenerate critical points with values distinct from $\rho(x)$.

(iii) The derivative $D\rho \in Hom_{\mathbb{C}}(TX, \rho^* T\mathbb{C}^2)$ is transverse to both the zero section and the rank 1 locus. Hence, by counting dimensions, $D\rho$ vanishes nowhere and the rank 1 locus is a complex curve in X, which is denoted $crit(\rho)$.

(iv) At critical points x of f the Hessian $D^2 f$ restricted to $\ker(D\rho) = T_x(crit(\rho))$ is non-degenerate.

To parse this definition, it is helpful to consider the case that $\dim_{\mathbb{C}}(X) = 2$ and π is projection onto the first factor. In this case $\rho = (f, \rho_t)$, where f is the fibration and ρ_t is a branched cover when restricted to the fiber F_t of f. This captures the promised idea of a Lefschetz fibration with a branched cover on every fiber. Points *(iii)* and *(iv)* of Definition 2.5 have two important consequences, which are expounded upon below.

Claim 2.5.1. *The set of critical points of ρ_t is exactly $crit(\rho) \cap F_t$ for each t.*

Claim 2.5.2. *The restriction $f| : crit(\rho) \to \mathbb{C}$ is a branched cover with only doubly ramified points, and these occur exactly at the critical points of $f : X \to \mathbb{C}$.*

(2.5.1) To see that $\text{crit}(\rho) \cap F_t$ contains the critical points of ρ_t, note that at a critical point of ρ_t, the map ρ will necessarily have rank 1. The critical points of ρ_t therefore lie in $\text{crit}(\rho)$, and by definition also lie in F_t. The converse statement follows from Lemma 2.7 below. □

Thus for each t, $\text{crit}(\rho)$ intersects F_t in several critical points of ρ_t As $t \in \mathbb{C}$ varies, the critical points of the branched covers ρ_t form "sheets" intersecting each fiber in the several critical points of ρ_t (see Figure 2.3). These sheets will form the branched cover in Claim 2.5.2.

(2.5.2) First, away from critical points of f, $f| : \text{crit}(\rho) \to \mathbb{C}$ is an even covering. To show this, it suffices to show that $\text{crit}(\rho)$ is transverse to the fibers. Since f must have rank 1 away from its critical points and $\ker(Df) = TF_t$, Df must be an isomorphism restricted to any plane transverse to TF_t. Given that $\text{crit}(\rho)$ is transverse to the fibers, an application of the inverse function theorem shows that $f : \text{crit}(\rho) \to \mathbb{C}$ is local diffeomorphism and therefore an even covering.

The statement that $\ker(\rho) = T_x(\text{crit}(\rho))$ is transverse to the fibers is a condition on second derivative $D^2\rho$. In fact, one can check that the condition on the second derivative is exactly the condition that $\rho_t : F_t \to \mathbb{C}_t$ have non-degenerate critical points (see [23], Lemma 15.7), which was point (ii) of the definition.

Notice now that a critical point x of f necessarily lies in $\text{crit}(\rho)$ because at x one has $Im(D\rho) \subseteq \ker(D\pi)$, hence the image of $D\rho$ must be rank 1. Now to ensure $f| : \text{crit}(\rho) \to \mathbb{C}$ is a branched cover with only doubly ramified points it suffices to show that at x, there are coordinates in which $f| : \text{crit}(\rho) \to \mathbb{C}$ is given by $z \mapsto z^2$. For this, it is enough (by the holomorphic Morse Lemma, 1.21) to show that x is a non-degenerate critical point of $f|$, but this is exactly point (iv) of the definition. □

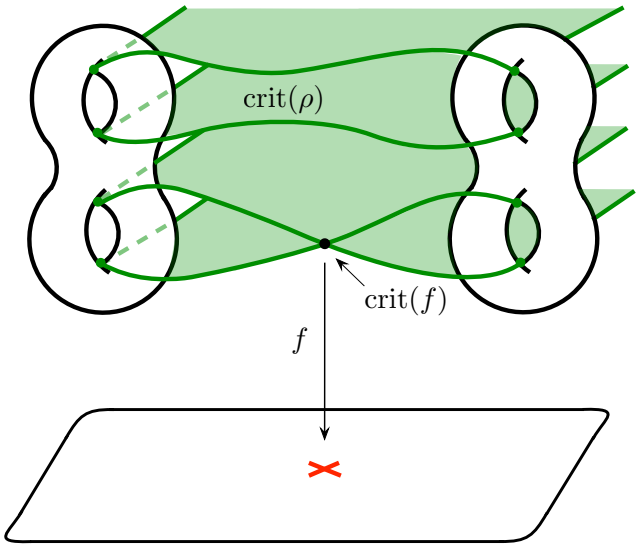

Figure 2.3: A Lefschetz bifibration over a region in $\mathbb{C}$ with the complex curve $\text{crit}(\rho)$ shown (green). The restriction of f to $\text{crit}(\rho)$ is a branched cover, with ramification points exactly at the critical points of f.

Example 2.6. The most important example to keep in mind, and the one the algorithm will use is the case of $\rho : X \to \mathbb{C}^2$ being a pair of Lefschetz fibrations. Let $f, g : \mathbb{C}^3 \to \mathbb{C}$ be linear projections, and let $\rho = (f, g)$ and $\pi(x, y) = x$ be the projection to the first coordinate. For generic choices of f, g, one can use standard techniques from algebraic geometry to show that conditions $(i) - (iv)$ of Definition 2.5, which all hold generically, hold simultaneously generically as well. In particular, this shows that Lefschetz bifibrations exist and are in abundance.

Around a critical point of f, the situation is locally modeled by Example 2.2.

Lemma 2.7. *Let $X \xrightarrow{\rho} \mathbb{C}^2 \xrightarrow{\pi} \mathbb{C}$ be a bifibration. If $x \in X$ is a critical point of $f = \pi \circ \rho$, then there exist local coordinates $(z_1, ..., z_n)$ on X in which the fibration takes the form*

$$(z_1\ ,\ \dots\ ,\ z_n) \xrightarrow{\rho} (z_1^2 + \ldots + z_n^2\ ,\ z_1) \xrightarrow{\pi} z_1^2 + \ldots + z_n^2$$

Proof. (Sketch) since π is a submersion by assumption, one can always find local coordinates on $\mathbb{C}^2$, and $\mathbb{C}$ in which $\pi(w_1, w_2) = w_1$ and $\rho(x) = (0, 0)$. Let $\rho(z_1, ..., z_n) = (h_1, h_2)$ in these coordinates. The remainder of the proof is a parameterized version of the holomorphic Morse Lemma (1.21). Since $D\rho$ has rank 1 by assumption, one has $Dh_2 \neq 0$ at x. Thus the level set $h_2^{-1}(w_2)$ is smooth for $w_2 \in \mathbb{C}^2$ sufficiently close to 0. The lemma follows by an argument applying the holomorphic Morse Lemma to each level set of h_2. See [23], Lemma 15.9. □

As promised earlier, it is straightforward to show by computing in these local coordinates that a point is in the rank 1 locus of ρ if and only if it is a critical point of ρ_t. This finishes the second direction of Claim 2.5.2.

2.3 Vanishing Cycles as Matching Cycles

Lemma 2.7 enables a precise description of how two branch points merge. Let s_i be the critical values of f (changing notation from the earlier t_i to avoid confusion with the parameter t), and $\delta_i : [0, 1] \to \mathbb{C}$ be vanishing paths. Let F_t for $t \in [0, 1]$ be the fibers above δ_i so that $F_0 = F_*$ is the base fiber and F_1 is the singular fiber. The curve $\mathrm{crit}(\rho) \subseteq X$ intersects this family along real curves which are the intersection with each sheet of the branched cover $f| : \mathrm{crit}(\rho) \to \mathbb{C}$. By Claim 2.5.2, exactly two of these sheets have a branching point in the singular fiber F_1. Since for each t, the intersection $F_t \cap \mathrm{crit}(\rho)$ is the critical points of $\rho_t : F_t \to C_t$, the branched cover $\rho_1 : F_1 \to C_1$ has one less critical point than the branched covers for $t < 1$, in agreement with the Riemann-Hurwitz formula.

One can associate a matching path to the vanishing path δ_i as follows. Intuitively, this is just the path that joins the two critical values that merge at $t = 1$. See Figure 2.4 on the next page. To define it precisely, however, requires ensuring that it is unambiguous how the path should be drawn so that it doesn't loop around other critical values.

To formulate this precisely, let $c_1(t), c_2(t)$ be the intersection of these two sheets ramified at $t = 1$ with the fiber F_t. Since the two sheets merge at $t = 1$, one has $c_1(1) = c_2(1) \in F_1$. There exists a neighborhood $U \subseteq X$ of x so that once $c_1(t), c_2(t)$ enter it they do not exit it again. For t sufficiently close to 1, say bigger than $1-\eta$, there exists another neighborhood $V \subseteq C_t$ containing the image $\rho_t(U \cap F_t)$ that contains no other critical values. For a fixed $t_0 > 1 - \eta$ there is (up to isotopy) a unique shortest path μ_i joining $\rho(c_1(t_0))$ to $\rho(c_2(t_0))$ in V.

Definition 2.8. *μ_i as above is called the* **matching path associated to the vanishing path** *δ_i.*

The following proposition formalizes the main idea of the algorithm.

Proposition 2.9. *For each vanishing path δ_i, the matching path μ_i associated to δ_i defined above has a matching cycle. This matching cycle is the vanishing cycle of the critical point above t_i.*

Proof. This is essentially immediate from the local model. Choose coordinates around the critical point as in Lemma 2.7 so that ρ, π are given by

$$(z_1\ ,\ z_2) \xrightarrow{\rho} (z_1^2 + z_2^2\ ,\ z_1) \xrightarrow{\pi} z_1^2 + z_2^2.$$

The situation is now exactly that of Example 2.2. Let $\delta_i(t) = 1-t \in \mathbb{R} \subseteq \mathbb{C}$ be the vanishing path. The fibers intersect this coordinate neighborhood in the surfaces $F_t = \{z_1^2 + z_2^2 = 1-t\}$. The map $\rho_t : F_t \to C_t = \mathbb{C} \times \{t\}$

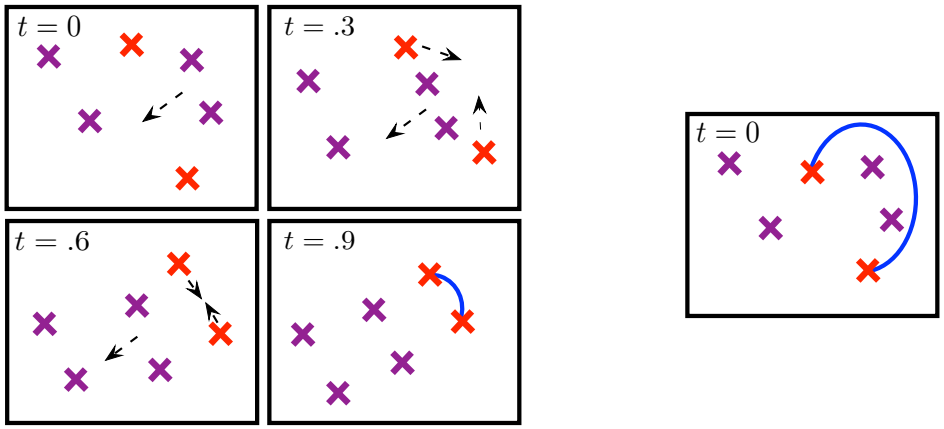

Figure 2.4: (Left) a depiction of the images of the critical values of ρ_t for several values of $t \in [0,1]$. The dashed arrows (black) indicate the motion of the critical values for increasing t. Near $t = 1$ it becomes apparent that the two critical values indicated in red merge. The matching path μ (blue) joining them is unique for t close to 1. (Right) the matching path μ traced back to $t = 0$ by reversing the motion of the critical values.

is projection to the z_1 coordinate. For t close to the intersection $c_1(t), c_2(t) = \mathrm{crit}(\rho) \cap F_t$ are the critical points of ρ_t which solve $z_2 = 0$ and so are given by $\pm\sqrt{1-t}$. For fixed t_0, the path $\mu_i(s) = \pm\sqrt{1-s}$ for $s \in [0, t_0]$ is a choice of matching path associated to $\delta_i(t) = 1 - t$.

Both claims are now quite clear. Locally, there are only two sheets, so the path μ_i *must* be a matching path with a well-defined matching cycle. Moreover, the pre-image of μ_i is the set

$$\{(z_1, z_2) \mid z_1, z_2 \in \mathbb{R}\ ,\ z_1^2 + z_2^2 = 1 - t\} \subseteq F_t$$

which is, by definition, the vanishing cycle ν_i. □

Once a matching path μ_i corresponding to a vanishing path δ_i is obtained, it can be transported back to the base fiber F_*. This is done as follows. By a choice of trivialization, one obtains a representative of the vanishing cycle in F_t for each t as before. It may be assumed that the representative of the vanishing cycle is disjoint from all critical points besides $c_1(t), c_2(t)$ for each t, since if this is not the case an isotopic representative can be chosen. By projecting the vanishing cycle via ρ_t, one obtains a path $\mu_{i,t}$ in C_t for each t that is disjoint from all the critical values besides $\rho(c_1(t)), \rho(c_2(t))$.

In practice, this amounts to saying that once $\mu_{i,t}$ is known for t close to one, one may trace it back to a matching path in the cover $\rho_0 : F_* \to C_0$ by following the image (up to isotopy) in C_t. This is relatively easy when $C_t = \{t\} \times \mathbb{C}$, as Figure 2.4 shows, and just amounts to reversing the motion of the critical values back to $t = 0$. Repeating this for each $i = 1, .., r$ results in a matching path in $\rho_0 : F_* \to C_0$ for each vanishing cycle of f, which completes Step **(1)** of the algorithm.

In practice, Step **(1)** is carried out as follows. One can consider a Lefschetz bifibration given by a pair of linear projections, as in Example 2.6. Let $X \subseteq \mathbb{C}^3$ be an affine variety cut out by the equation $G(x, y, z) = 0$. Choose a generic linear projection f as the first fibration. This will be the composition $f : X \to \mathbb{C}^2 \to \mathbb{C}$ in the definition of bifibration. The critical points of f occur where $T_x X$ is parallel to the kernel of f, thus they solve the system of equations

$$\begin{cases} G(x, y, z) = 0 \\ dG = C \cdot df \end{cases} \tag{2.3.1}$$

for some constant $C \in \mathbb{C}$. To ensure f is indeed a Lefschetz fibration, one checks the non-degeneracy of the Hessian at each critical point.

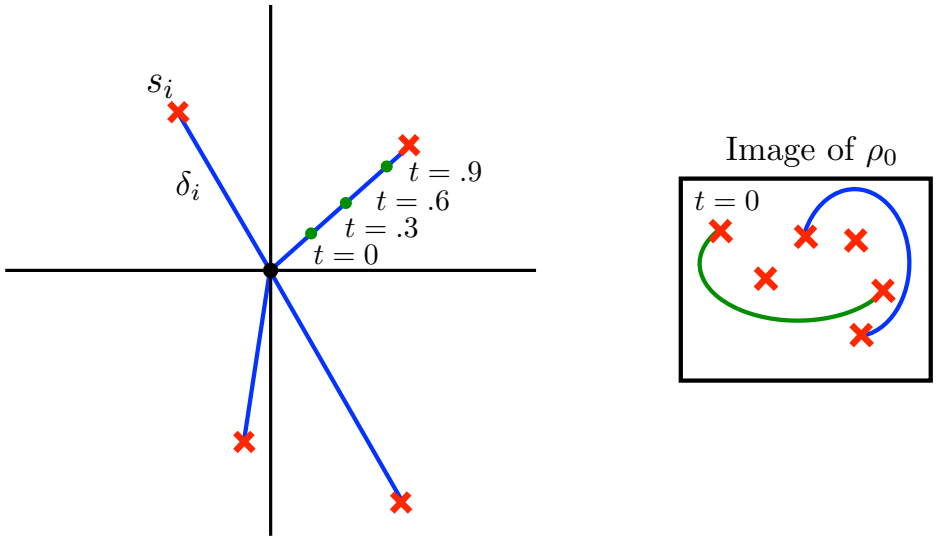

Figure 2.5: (Left) The image of f with the critical values s_i and vanishing paths δ_i indicated. Along each vanishing path, a movie as in Figure 2.4 plays for $t \in [0,1]$ giving a matching path. (Right) tracing these matching paths back to $t = 0$ gives a matching path for each vanishing path whose pre-image is the vanishing cycle (two shown).

Once the critical points are determined, one draws the critical values $s_1, ..., s_r$ of f in $\mathbb{C}$ and chooses a collection of vanishing paths (see Figure 2.5). Generically, no two critical values will lie on the same ray and 0 will not be a critical value, hence the vanishing paths $\delta_i(t) = ts_i$ for $t \in [0,1]$ usually suffice. To find the vanishing cycle of each, one chooses a second generic projection $\rho : \mathbb{C}^3 \to \mathbb{C}$. Restricted to the fibers F_s the second projection is a branched cover. If $f = ax + by + cz$ is the first fibration, the coordinate z in the level sets f can be written as $z = \frac{ts_i - ax - by}{c}$. This allows one to consider everything as functions of x, y (if one has chosen a fibration f with the coefficient $c = 0$, one of the other variables can be swapped for z). Let $H_t(x,y) = G(x, y, \frac{ts_i - ax - by}{c})$ and $\rho'_t(x,y) = \rho(x, y, \frac{ts_i - ax - by}{c})$. The critical points in the fiber F_t occur where TF_t is parallel to $\ker(\rho)$ within the level set $f^{-1}(ts_i)$. Thus for each t, they are the points $(x, y, \frac{ts_i - ax - by}{c})$ where (x,y) solve the simultaneous equations

$$\begin{cases} H_t(x,y) = 0 \\ dH_t = C'_t \cdot d\rho'_t \end{cases} \tag{2.3.2}$$

for some constant $C'_t \in \mathbb{C}$ possibly depending on t. One must again check non-degeneracy. Then, given that the critical points are indeed non-degenerate, one draws the critical values $r_1, ..., r_m$ for $t = 0$ in $\mathbb{C}$. As t varies, each traces out a path $r_i(t)$ in $\mathbb{C}$. At $t = 1$, exactly two of the paths $r_i(t), r_j(t)$ will share an endpoint. The matching path is the path (unique up to isotopy) joining $r_i(t), r_j(t)$ for t close to 1 traced back to $t = 0$.

Example 2.10. (A_2 Milnor Fiber) Consider the A_2 Milnor Fiber $\{x^2 + y^2 + z^2 - 1 = 0\} \subseteq \mathbb{C}^3$. Let $f : \mathbb{C}^3 \to \mathbb{C}$ be projection onto the z coordinate. By (2.3.1) the critical points are the solutions of

$$\begin{cases} x^2 + y^2 + z^2 - 1 = 0 \\ 2x\ dx + 2y\ dy + 2z\ dz = C\ dz, \end{cases}$$

which is readily solved to find two critical points $(0, 0, \pm 1)$ with critical values $s_1 = 1, s_2 = -1$ in $\mathbb{C}$. See Figure 2.6(a). One must check the non-degeneracy of the Hessian at each critical point to ensure this is indeed a Lefschetz fibration, but this calculation is omitted here. Since $0 \in \mathbb{C}$ is not a critical value, it can be chosen as the basepoint $*$. The base fiber is $F_* = \{x^2 + y^2 - 1 = 0, z = 0\} \subseteq \mathbb{C}^3$. Choosing two vanishing

paths $\delta_1(t) = t$ and $\delta_2(t) = -t$ results in vanishing cycles ν_1, ν_2 (see Figure 2.6(a)). Now, one wishes to find the matching cycle associated to each δ_i.

Vanishing cycle ν_1: Let $\rho(x, y, z) = y$ be the second fibration. Consider first the vanishing cycle of the vanishing path $\delta_1(t) = t$. Along δ_1, the fibers are $F_t = \{x^2 + y^2 = 1 - t^2\}$. The critical points are given via (2.3.2) as the solutions of

$$\begin{cases} x^2 + y^2 = 1 - t^2 \\ 2x\ dx + 2y\ dy = C dy, \end{cases}$$

Which is readily solved to yield two critical points $(0, \pm\sqrt{1-t^2}, 0)$. Here, one should again check that these critical points are non-degenerate so that ρ has only double-branching, but this is omitted here. Starting with $t = 0$, where the critical values are ± 1, one can plot the position of the critical values r_1, r_2 of $\rho_t : F_t \to \mathbb{C}$. One finds the two critical values approach each other along the real axis as t increases, meeting at the origin at $t = 1$ (Figure 2.6, (b),(c),(e)). Note it is a coincidence that for $t = 0$ the critical values of ρ_0 happen to be the same as those of f, and this will not be the case in general. The horizontal line $\mu_1(s) = s$ for $s \in [-1, 1]$ between the critical values of ρ_0 is therefore a matching path (Figure 2.6 (f)). This shows that the vanishing cycle of the critical value $s_1 = 1$ of f is represented in F_* by the lift of $[-1, 1] \subseteq \mathbb{C}$. From Section 1.2, it is known that $F_* \simeq T^*S^1$ is the cylinder, and the lift of this path is the zero-section.

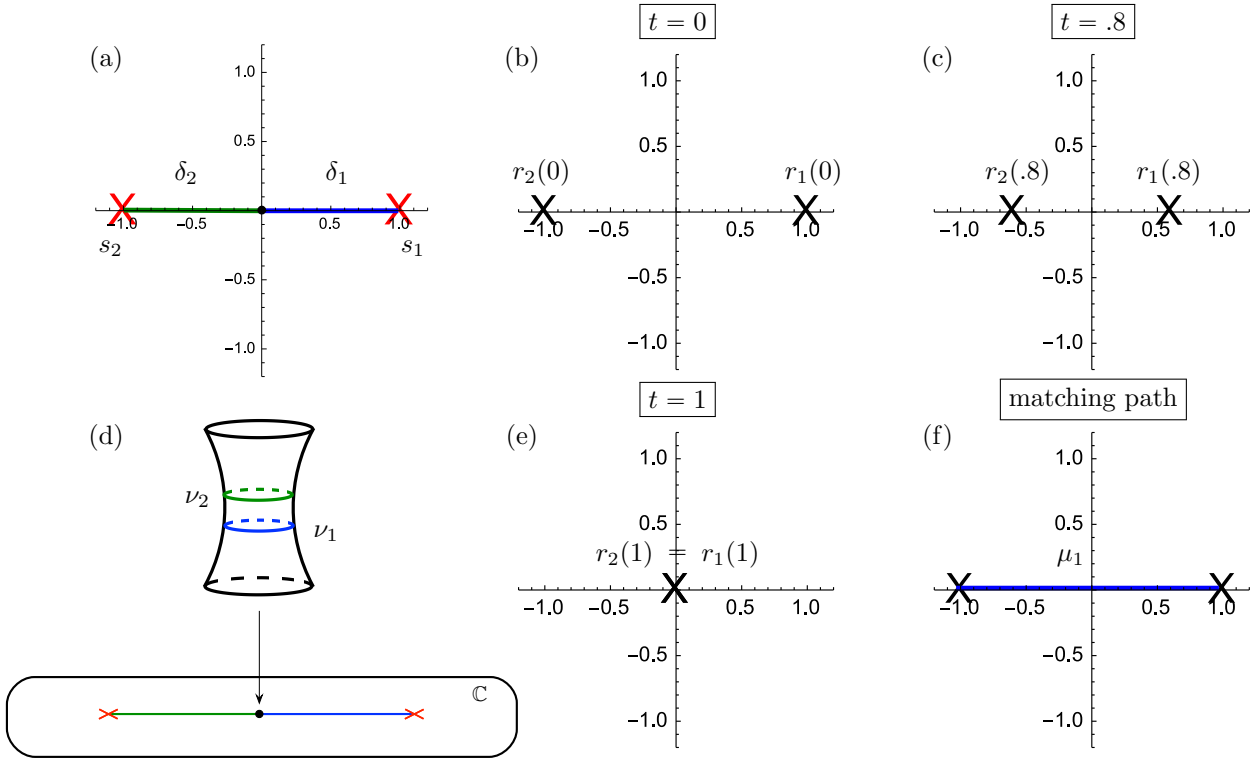

Figure 2.6: (a) the image of fibration f with its critical values s_i and vanishing paths δ_i indicated. (b), (c), (e) the image of ρ_t for three different times with critical points $r_1(t), r_2(t)$ indicated. (f) the resulting matching cycle μ_1. (d) the vanishing cycles ν_1, ν_2 in the base fiber $F_* \simeq T^*S^1$.

Vanishing cycle ν_2: The process is now repeated for the second critical value $s_2 = -1$ of f, with its respective vanishing path $\delta_2(t) = -t$. One sees however, that the form of (2.3.2) is invariant under $t \mapsto -t$. Thus the behavior of the image of ρ_t is identical along the path $\delta_2(t)$ and thus ν_2 is the same isotopy class as ν_1.

To summarize, the A_2 Milnor Fiber with the Lefschetz fibration $f(x, y, z) = z$ has two critical points and a generic fiber $F_* \simeq T^*S^1$. The two vanishing cycles ν_1, ν_2 are both the isotopy class of the zero-section in T^*S^1. See Figure 2.6 (d).

Example 2.11. ($(3, 2)$ tom Dieck-Petrie Surface) The previous example was computationally simple. This example is more complicated and (2.3.2) for $s \in [0, 1]$ can only reasonably be solved numerically. Recall from the introduction to this chapter the (3,2) tom Dieck-Petrie surface given by

$$X_{3,2} = \left\{ \frac{(xz+1)^3 - (yz+1)^2}{z} - 1 = 0 \right\}$$

This is an exotic affine variety (notice the constant term in the numerator cancels so there is no $\frac{1}{z}$ term). It is of interest from the perspective of symplectic and algebraic geometry because it is a (smoothly) contractible surface, but is not biholomorphic to $\mathbb{C}^2$. For an excellent exposition of this and similar surfaces see [24]. Here, it is interesting only to demonstrate the power of these tools to find vanishing cycles in a complicated example.

Consider the fibration $f = 20x + z$. Solving (2.3.1) numerically shows this fibration has 6 critical points, plotted in Figure 2.7 below with their vanishing paths for the basepoint $* = 0$.

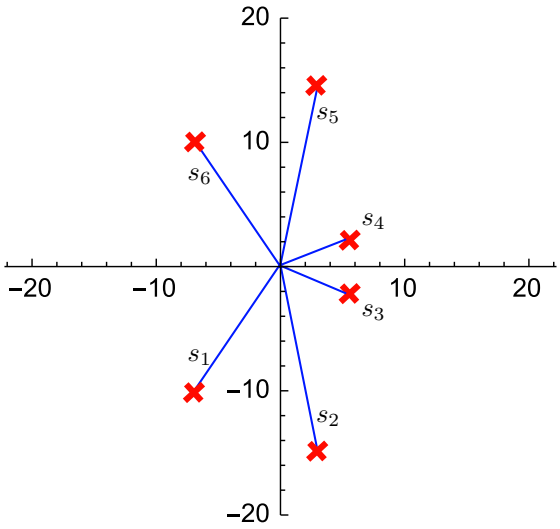

Figure 2.7: The critical values and vanishing paths of the fibration $f = 20x + z$.

One can check that these critical points are non-degenerate. Here, an ordering of vanishing cycles beginning at $\theta = \pi$ is chosen as it will make the pattern of matching cycles more clear. The fiber over the basepoint 0 is

$$F_* = \left\{ \frac{-(1-20x^2)^3 + (1-20xy)^2}{20x} - 1 = 0 \right\}.$$

Choosing $\rho(x, y) = -x + 0.01y$ are the second fibration yields a branched cover of the base fiber, which one can check is non-degenerate. Its image has ten critical values $r_1, ..., r_{10}$, eight of which are shown in the first panel of Figure 2.8 (the two remaining critical values are far from the origin).

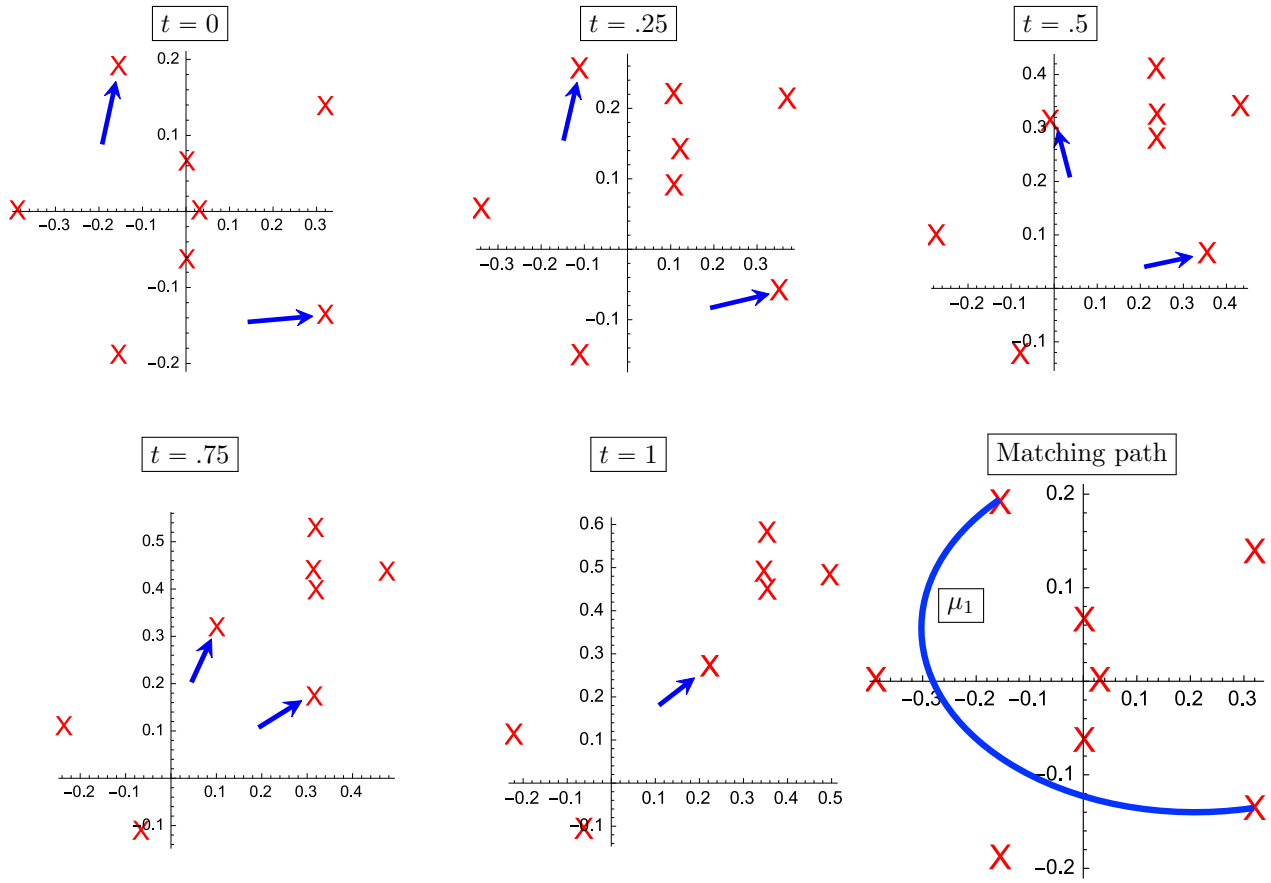

Figure 2.8: The images of the critical values of ρ_t found numerically and plotted for various values of t and the resulting matching path plotted in the image of ρ_0.

Vanishing cycle ν_1. For the vanishing path ts_1, consider the map ρ restricted to the fiber F_t for $t \in [0,1]$. The critical values $r_1, ..., r_8$ of ρ for several values of t are shown below. The two critical values indicated by blue arrows come together at $t = 1$, and tracing a path joining them back to $t = 0$ yields the matching path shown in the sixth panel of Figure 2.8.

Repeating this for the critical values $s_1, ..., s_6$, one finds six matching paths in the image of $\rho_0 : F_* \to \mathbb{C}$ representing the six vanishing cycles $\nu_1, ..., \nu_6$. The matching paths of ν_1, ν_2, ν_3 are shown in Figure 2.9, and matching paths of ν_6, ν_5, ν_4 are their reflections across the real axis respectively.

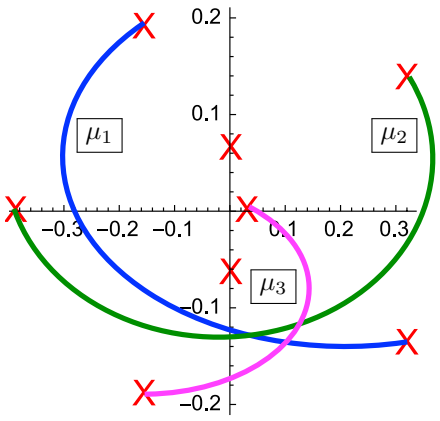

Figure 2.9: The first three matching paths μ_1, μ_2, μ_3. The latter three μ_6, μ_5, μ_4 are the reflections across the real axis respectively.

2.4 Bases of Matching Cycles

This section proceeds to the second of the three steps of the algorithm. To review, the first step of the algorithm has provided a method for expressing the vanishing cycles of a Lefschetz fibration as matching cycles in the branched cover $\rho_0 : F_* \to \mathbb{C}$. The remaining two steps give these matching cycles a concrete realization by choosing an association of F_* with a standard surface of the correct genus, and expressing the matching cycles in terms of specified curves there. Step **(2)** of the algorithm obtains a collection of simple closed curves in F_* representing a basis of $H_1(F_*; \mathbb{Z})$.

This section deals exclusively with the branched cover $\rho_0 : F_* \to \mathbb{C}$ of the base fiber. Here, using the language of Lefschetz fibrations, vanishing cycles of the critical (ramification) points are embedded copies of S^0, and matching cycles are simple closed curves in F_*.

Definition 2.12. *A* **basis of matching paths** *is a collection of matching paths $\mu_1, ..., \mu_m \subseteq \mathbb{C}$ whose matching cycles $[\Sigma_1], \ldots, [\Sigma_m]$ form a basis of $H_1(F_*; \mathbb{Z})$.*

The goal is to find a basis given in this way. Let $r_1, ..., r_m$ be the critical values of ρ_0, and let $\varepsilon_1, ..., \varepsilon_m$ be vanishing paths for them. Generically, $0 \in \mathbb{C}$ will a critical value so the vanishing paths $\varepsilon_i(q) = qr_i$ for $q \in [0, 1]$ usually suffice.

The fiber $\rho^{-1}(0)$ consists of p points where $p = \deg(\rho)$. Traveling along each vanishing path, an S^0 vanishing cycle collapses, i.e. two sheets of the branched cover come together so that there are $p - 1$ points in critical fibers. The next task is to systematically determine which two sheets are ramified at each r_i.

The fiber above $qr_i \in \mathbb{C}$ is a finite number of points, which will be denoted $w_k(q) = (x_k(q), y_k(q)) \in \mathbb{C}^2$ for $k = 1, \ldots, p$. They solve the system of equations:

$$\begin{cases} H_0(x, y) = 0 \\ \rho_0'(x, y) = qr_i \end{cases} \tag{2.4.1}$$

where $H_0(x, y)$ is the equation defining the fiber as in (2.3.2). Here, it is sufficient to consider the fiber as a subset of $\mathbb{C}^2$ since the projection of the plane $f = ax + by + cz$ in which the fiber lies is a diffeomorphism.

The true fiber is still given by $(x, y, \frac{st_i - ax - by}{c})$ where $H(x, y) = 0$, but dragging the third component along plays no role in this step. Solving the above system (usually numerically) for $q \in [0, 1]$ and each $i = 1, ..., m$ yields, a pair (w_{k_1}, w_{k_2}) in the fiber which come together at $q = 1$. This pair is the S^0 vanishing cycle of each r_i.

To keep track of which pairs (w_{k_1}, w_{k_2}) come together at $q = 1$ for each i, it is useful to project $\mathbb{C}^2 \to \mathbb{C}$. Choose a generic projection $\pi(x, y) = \alpha x + \beta y$, and draw the values $\tilde{w}_k(0) := \pi(w_k(0))$ in the plane. Generically, the points w_k will have distinct images under π. The situation is now the same as in Section 2.3, Figure 2.4: for $q \in [0, 1]$ the values $\tilde{w}_k(q)$ move around the plane and at $q = 1$ two come together.

Next, one must label each r_i with its vanishing cycle. To do this systematically, introduce segments between the points $\tilde{w}_i(0)$ forming a connected graph with vertices $\tilde{w}_i$ and exactly one edge meeting each vertex, as in Figure 2.10. Label these segments $\alpha_1, ..., \alpha_{p-1}$. For each $i = 1, ..., m$ draw additional segments β_i joining the values of the two points that are the S^0 vanishing cycle of r_i, which one knows after solving (2.4.1) for each i. Here, (in contrast to step **(1)** of the algorithm) it is not important where the two points among the $\tilde{w}_k$ come together in relation to the others, and any β_i joining the two will suffice). Next, as described below, one expresses each β_i in terms of the the collection $\alpha_1, ..., \alpha_{p-1}$ using 0-dimensional Dehn twists.

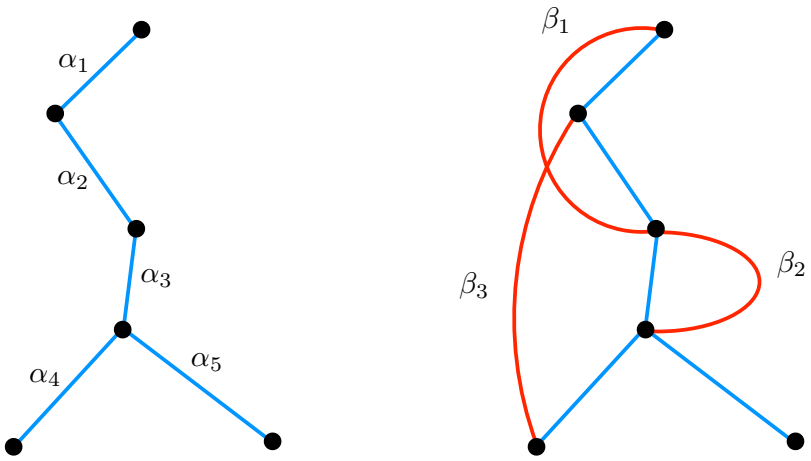

Figure 2.10: (Left) the points $\tilde{w}_i(0)$ projected to $\mathbb{C}$ (black) and line segments $\alpha_1, ..., \alpha_5$ joining them. (Right) the vanishing cycles of r_1, r_2, r_3 by paths $\beta_1, \beta_2, \beta_3$ (red).

Definition 2.13. *For a discrete fiber $\{c_1, ..., c_p\}$ of a branched cover, a* **0-dimensional Dehn Twist** *on a pair of points (c_j, c_ℓ) is the transposition $\{c_1, ..., c_j, ..., c_\ell ..., c_p\} \mapsto \{c_1, ..., c_\ell, ..., c_j ..., c_p\}$.*

The motivation for this terminology comes from the Picard-Lefschetz Theorem 1.35. Recall the theorem says that the monodromy around a critical value is a Dehn Twist about the vanishing cycle. When considering a generic branched cover as Lefschetz fibration, there is a monodromy around each branching point. Since a generic branched cover has only double branching points, the branched cover is locally modeled on $z \mapsto z^2$ in which case the monodromy can be shown to be a transposition. Consequently, using this local model, the monodromy around a critical value r_i of a branched cover is a a transposition of the two points in the sheets that are ramified above r_i. Definition 2.13 ensures the language of the Picard-Lefschetz Theorem applies in this case as well.

In a slight abuse of terminology, one refers to a Dehn twist on a pair (c_j, c_ℓ) as a Dehn twist about the path α joining them, denoted $\tau_\alpha : \{c_1, ..., c_p\} \to \{c_1, ..., c_p\}$. This is that the combinatorics identical to the case of Step **(3)** where the same situation will arise in one more dimension. Note this 0-dimensional case $\tau_\alpha = \tau_\alpha^{-1}$. It is a simple combinatorial problem to express each pair of endpoints of the β_i in terms of transpositions around the chosen $\alpha_1, ..., \alpha_{p-1}$.

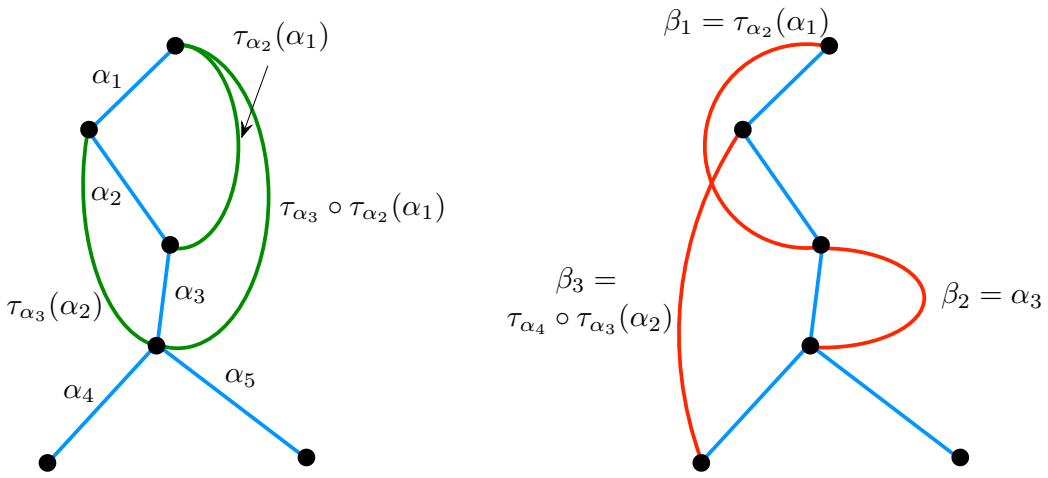

Figure 2.11: (Left) several paths in the configuration from Figure 2.10 that result from Dehn twists around the segments $\alpha_1, ..., \alpha_5$. (Right) expressing the paths $\beta_1, ..., \beta_3$ in terms of $\alpha_1, ..., \alpha_5$ and Dehn twists.

This gives a complete representation of the branching behavior at the critical values r_i of ρ. This can now be used to find matching paths representing homology classes for $H_1(F_*; \mathbb{Z})$.

Finding Matching Paths: Return to the image of the branched cover $\rho : F_* \to \mathbb{C}$. Label each of the critical points $r_1, ..., r_m$ with β_i expressed in terms of $\alpha_1, ..., \alpha_{p-1}$ and Dehn twists around them, as in Figure 2.12.

Two vanishing cycles can be glued to form a matching cycle if and only if they agree as sets in the fiber $\rho^{-1}(0)$. Thus any pair of vanishing paths whose endpoints are labelled with the same expression in terms of α_i form a matching path. One must be careful here, as there is some redundancy in expressing the β_i in terms of α_i. For example, for any adjacent pair α_i, α_{i+1}, one has $\tau_{\alpha_i}(\alpha_{i+1}) = \tau_{\alpha_{i+1}}(\alpha_i)$. Drawing matching paths joining pairs among the r_i labelled with the same vanishing cycle results in matching cycles that are simple closed curves in F_*. Homotopic matching paths result in isotopic matching cycles.

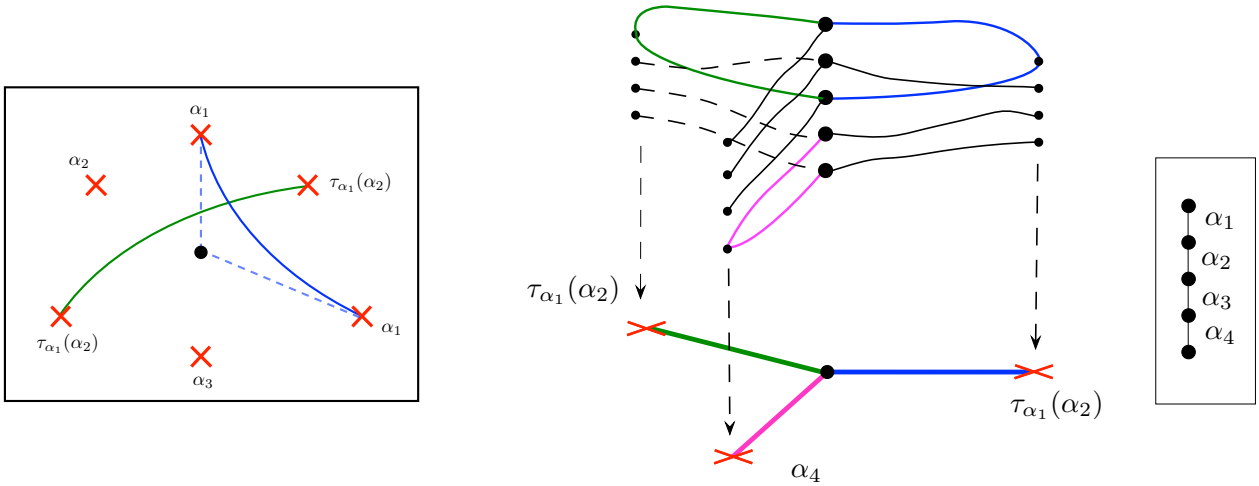

Figure 2.12: The image of ρ_0 with critical values r_i labelled with their vanishing cycles. Matching cycles (blue, green) exist between critical values with the same vanishing cycle. (Right) a similar situation with the branching above the critical points depicted. The base fiber with the segments α_i labelled is boxed.

Using Monodromy to find Matching Paths: It may be the case that there are only several, or even no vanishing cycles that match in the base when using the radial vanishing paths. Choosing different vanishing paths that are not homotopic in $\mathbb{C} - \{r_1, .., r_m\}$ results in different vanishing paths with different vanishing cycles, in which case new matching pairs may appear. In particular, replacing a path by itself plus an additional loop containing a critical point changes the vanishing cycle by the monodromy around that critical point, i.e. a Dehn Twist about the vanishing cycle. This can be used to find additional matching paths, as is demonstrated in Figure 2.13

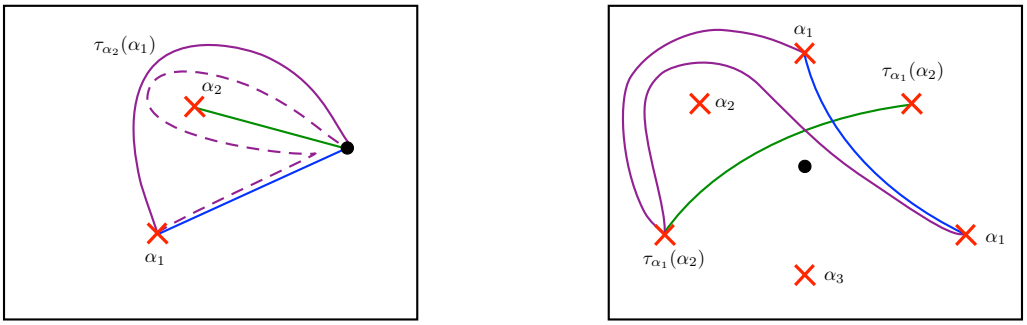

Figure 2.13: (Left) looping a vanishing path with vanishing cycle α_1 around a critical value with vanishing cycle α_2 to obtain a new vanishing path (purple) with vanishing cycle $\tau_{\alpha_2}(\alpha_1)$. (Right) This technique applied to the branched cover from Figure 2.12 to give two additional matching paths.

Bases of Matching Paths: The above methods provide an abundance of matching paths. Next one wants to choose a specific collection of matching paths whose matching cycles represent a basis of $H_1(F^*; \mathbb{Z})$.

First, it is necessary to know the rank of $H_1(F^*; \mathbb{Z})$. If the projectivization of F_* is a smooth curve, the genus formula applies and one find $H_1(F^*; \mathbb{Z})$ has rank twice the genus. When the projectivization of F_* is not smooth, i.e. the intersections with the hyperplane at infinity is singular, the situation must be analyzed more carefully.

Once the rank of $H_1(F^*; \mathbb{Z})$ is known, say it is k, one must find a basis of k matching paths. This usually involves ad hoc arguments or guessing and checking. To check if a proposed collection of k matching paths is indeed a basis, the following strategy is useful. For any connected and simply-connected graph whose vertices include the critical values, the surface F_* deformation retracts onto the pre-image of the graph, since the pre-image includes all the ramification points. Thus the lift of the graph is a 1-skeleton for the surface, and one can check whether the proposed collection of matching cycles are a basis of $H_1(F^*; \mathbb{Z})$ by computing the simplicial homology of the 1-skeleton explicitly (see Figure 2.14 below).

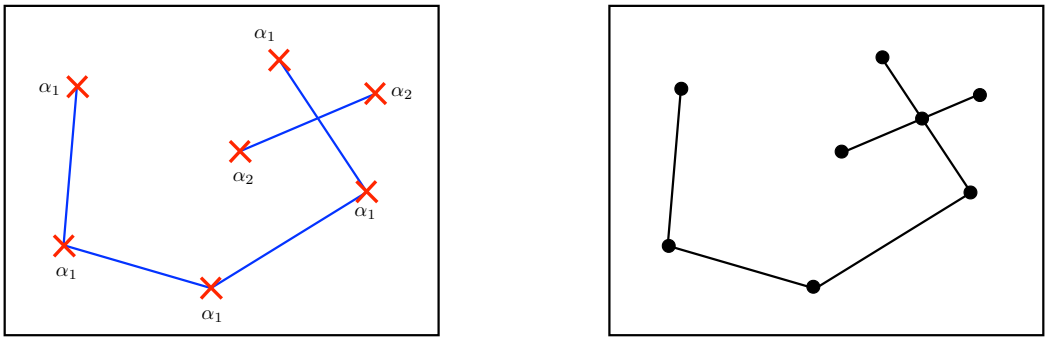

Figure 2.14: (Left) a proposed basis of matching paths. (Right) a simply-connected graph including the proposed basis whose pre-image gives a 1-skeleton for the surface.

Intersection Patterns: It is convenient to not only find a basis for $H_1(F_*;\mathbb{Z})$, but to find one it is nice to work with. In particular, it is convenient to choose a basis with a recognizable intersection pattern. In most cases, a linear intersection pattern (see Figure 2.15) of the homology classes is convenient.

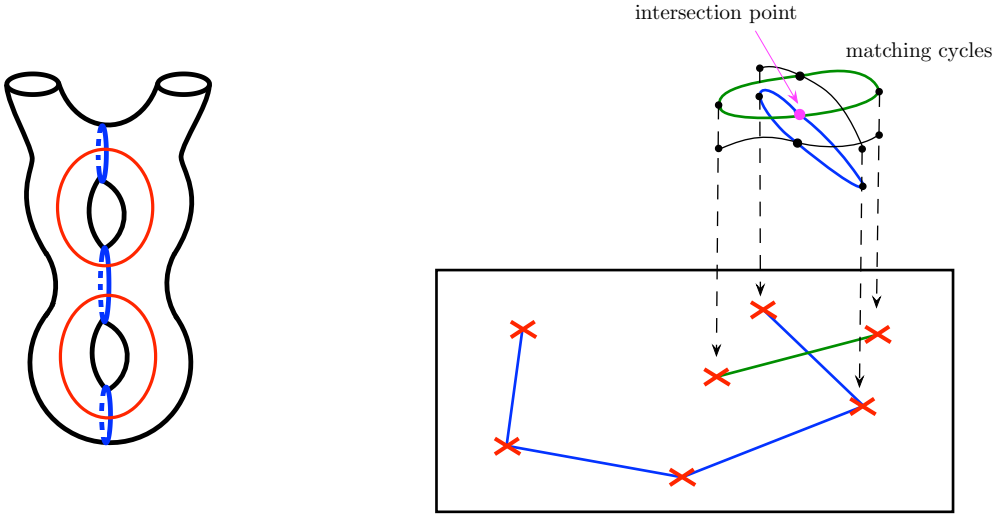

Figure 2.15: (Left) a linear intersection pattern in a surface of genus 2 with 2 punctures. (Right) checking the intersection of two matching paths by looking at the branching above them.

In practice, given two homology classes $[a_1], [a_2]$ that are the matching cycles of matching paths μ_1, μ_2 respectively, one can calculate their intersection directly. If the two paths share an endpoint, a single transverse intersection necessarily occurs there. If two matching paths cross somewhere that is not a branch point, one must check if the matching cycles lie in distinct sheets of the branched cover or not (see Figure 2.15).

Once a basis $[\Sigma_1], ..., [\Sigma_k]$ of matching cycles with a nice or identifiable intersection pattern is obtained, there exists a diffeomorphism with the standard surface S_g^p of genus g with p punctures that takes this basis to a basis with the same intersection pattern in S_g^p [12]. Letting $\phi : F_* \to S_g^k$ be such a diffeomorphism gives an identification of the base fiber with a standard surface. Of course, one could have chosen a diffeomorphism $F_* \simeq S_g^k$ right after obtaining expressions for the vanishing cycles of $f : X \to \mathbb{C}$ in Step **(1)**, but under an arbitrary diffeomorphism, the images of the matching cycles in the standard surface S_g^k could be anything!

Example 2.11 Revisited: Recall the (3,2) tom Dieck-Petrie surface

$$X_{3,2} = \left\{ \frac{(xz+1)^3 - (yz+1)^2}{z} - 1 = 0 \right\}$$

from Example 2.11. In that example, the matching cycles associated to the six vanishing cycles were calculated using a Lefschetz bifibration. The branched cover $\rho : F_* \to \mathbb{C}$ of the base fiber had critical values as shown below in Figure 2.16.

Continuing this example, one can use the above techniques to find a collection of matching paths whose matching cycles form a basis of $H_1(F_*;\mathbb{Z})$. Choosing a base point $0.1i$ for the branched cover is more convenient in this case. The fiber above it consists of 5 points as shown on the left in Figure 2.16. These can be connected by four segments $\alpha_1, ..., \alpha_4$ as shown. The straight line vanishing paths to the critical values r_j are then $qr_j + (1-q)i$ for $q \in [0,1]$. Solving (2.4.1) numerically for these paths yields the vanishing cycles (of the branched cover) for the r_j as labelled in Figure 2.16.

One can check this curve does not have a smooth projectivization, and instead has a singularity at its single intersection with the hyperplane at infinity. A little algebraic geometry can be used to show the affine curve F_* is a genus 2 surface with 3 punctures, so that $H_1(F_*;\mathbb{Z}) = \mathbb{Z}^6$.

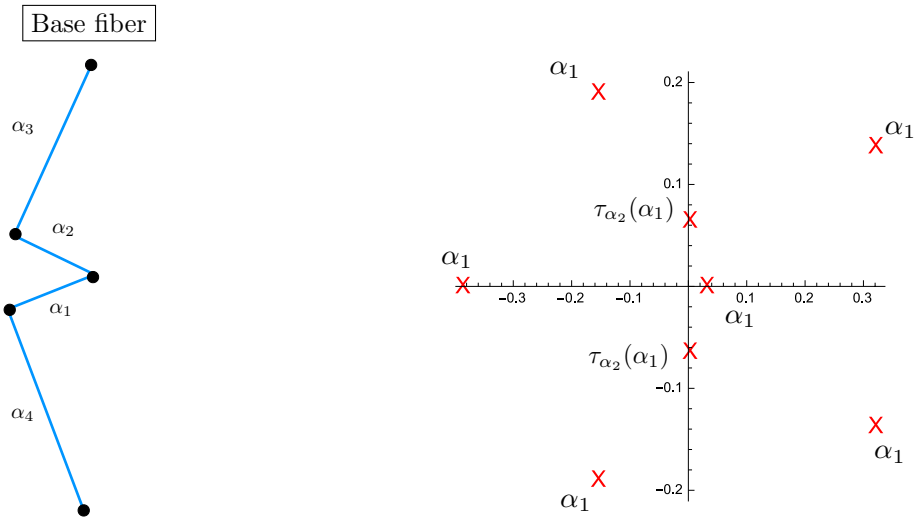

Figure 2.16: (Left) the base fiber $\rho^{-1}(-.01i)$ with segments $\alpha_1, ..., \alpha_4$ labelled. (Right) the image of ρ_0 with the vanishing cycles labelled.

Finding a Basis : It is now possible to find six matching cycles that form a basis of F_* with a convenient intersection pattern. These are shown in Figure 2.17(a). Four matching paths b_1, b_2, c, d (blue) are relatively easy to see, being those that pair all the critical values with vanishing cycle α_1.

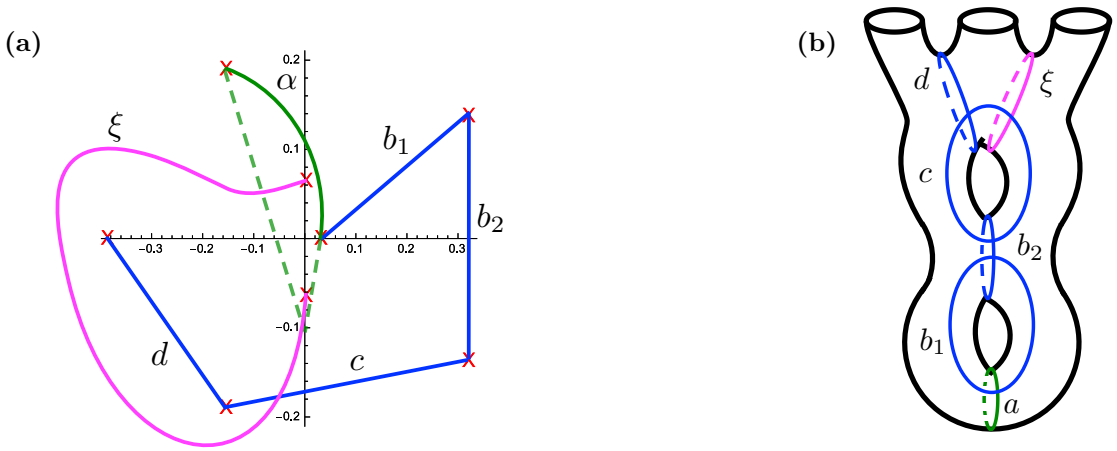

Figure 2.17: (Left) a basis of matching paths in the image of ρ_0. (Right) the image of the basis under a diffeomorphism to the standard surface S^3_2 preserving the intersection pattern.

The fifth matching path a (green), passing over the top, is a matching path because it differs from the concatenation of the two straight line paths (dashed green) by the monodromy around the two middle critical values which is $\tau^2_{\tau_{\alpha_1}(\alpha_2)} = Id$. The sixth path ξ (magenta) is slightly harder to see but the fact that it is a matching path follows similarly from considering monodromy. By contracting onto a 1-skeleton and checking

the intersection above the crossing of ξ, c, one can check this basis has the intersection pattern is as shown in Figure 2.17(b) with both ξ, d intersecting c once, and the remaining classes having a linear intersection pattern. Thus there is a diffeomorphism with the standard surface S_2^3 taking the 6 identified matching cycles to a basis of $H_1(S_2^3;\mathbb{Z})$ with the same intersection pattern, as shown in Figure 2.17(b).

2.5 Expressions for Vanishing Cycles

The final step of the algorithm, Step **(3)**, is to express the matching paths for the vanishing cycles of f from Step **(1)** in terms of the basis found in Step **(2)**. The method for doing this consists of two combinatorial moves: half Dehn twists (familiar from section 1.2) and the Valentine move. These are described in general below, after which they are demonstrated again in the example of the tom Dieck-Petrie surface $X_{3,2}$.

Half Dehn Twists: Recall from Section 1.2 the action of half Dehn twists on the image of a branched cover. An expression for a matching cycle of a matching path μ_i can be found by writing it as the result of a sequence of half-twists around known matching paths.

Proposition 2.14. *Let $\rho : F \to \mathbb{C}$ is a branched cover with critical values $r_1, ..., r_m$. Suppose μ_0 is a matching path with matching cycle α. Let r_i, r_j be two critical values joining by a matching path γ with matching cycle c. If $\mu_1 = \sigma_{i,j}(\mu_0)$ is the matching path obtained by from μ_0 by a half-twist around the two critical values $r_i, r_j \in \mathbb{C}$. Then the matching cycle of μ_1 is related to that of μ_0 by*

$$[\Sigma_{\mu_1}] = [\tau_c](\alpha).$$

Proof. This proposition is immediate from Lemma 1.34: a matching cycle projects to a matching path between to critical points, hence a Dehn twist around the matching cycle is the unique lift of the half twist exchanging the endpoint of γ in $Mod(F)$ □

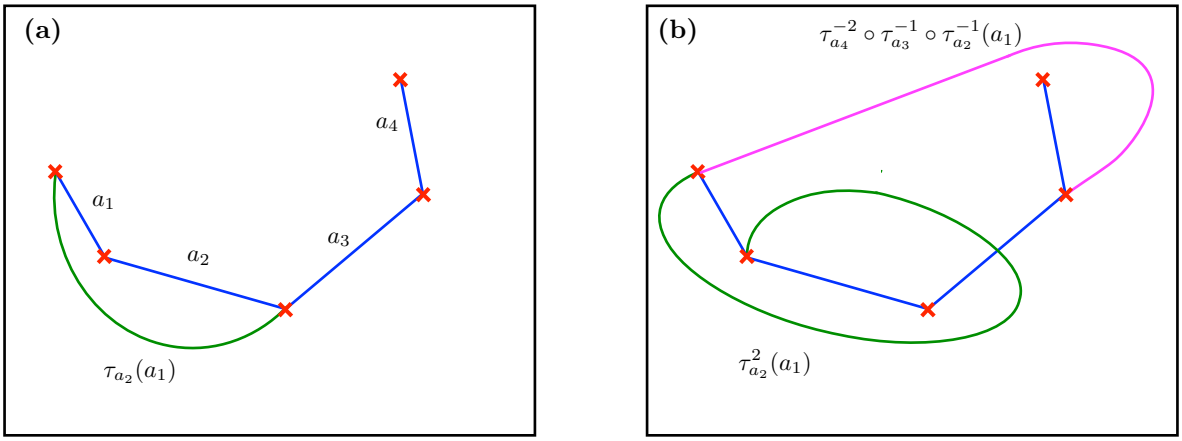

Figure 2.18: (Left) a simple example of a path (green) expressed using Dehn twists about the basis elements $a_1, ..., a_4$ (blue). (Right) two more complicated examples.

This is applied as follows. One draws both the matching paths $a_1, ..., a_k$ from Step **(2)** whose matching cycles $\alpha_1, ..., \alpha_k$ represent a basis of $H_1(F_*;\mathbb{Z})$. One also draws the matching paths $\mu_1, \ldots, \mu_r$ of the vanishing cycles from Step **(1)**. One can then express the matching paths μ_i as combinations of half twists around the endpoints of a_j. Combinatorially, this process is the same as the process by which the paths β_i were expressed in terms of the segments α_j in Section 2.4. Here, however, slightly more care must be taken as

the placement of the paths with relation to the others matters. Additionally, one no longer has $\tau_\alpha^2 = Id$. A few examples are shown in Figure 2.18.

If the matching path μ_i of a vanishing cycle can be written as a sequence of twists $\sigma_{a_{j_n}} \circ \ldots \circ \sigma_{a_{j_1}}$ acting on some basis path a_{j_0} (where by an abuse of notation, the half-twist flipping the endpoints of a_j is denoted by σ_{a_j}), then successive applications of Proposition 2.14 show the vanishing cycle of μ_i is

$$[\tau_{\alpha_n}] \circ \ldots \circ [\tau_{\alpha_1}](\alpha_{j_0}).$$

Valentine Move: This second move has a slightly different flavor than the previous one. In certain cases, there are vanishing paths with different endpoints that define thimbles that are isotopic in the total space. There are case when it is possible to exchange one half of a matching path for a different vanishing path without changing the isotopy class of the matching cycle.

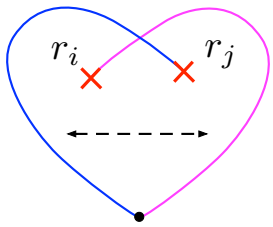

Figure 2.19: The Valentine move exchanges vanishing paths (blue, purple) without changing the vanishing cycle. This moves gets its name from the distinctive heart-shaped pattern formed by the two vanishing cycles.

Proposition 2.15. *Suppose that two critical points r_i, r_j have vanishing cycles which have a single transverse intersection. Then the thimbles defined by the two vanishing paths depicted in Figure 2.19 are isotopic, hence when joined with any other vanishing path to form a matching path, the two resulting matching cycles are the same (i.e. isotopic as embedded spheres).*

Proof. A proof can be found in [25] and the citations therein (e.g [26]). □

Example 2.11 Revisited (the last time): Here, the above two moves are applied to Example 2.11 to express the vanishing cycles found therein in terms of the basis found in Example 2.11 Revisited. Recall the first vanishing cycle ν_1 was the matching cycle of the matching path in Figure 2.9. It is convenient, for expressing the vanishing cycles, to momentarily introduce another homology class $\overline{\alpha}$ as indicated in Figure 2.20. Then two Dehn twists express ν_1 in terms of the basis a, b_1, b_2, c, d, ξ and $\overline{\alpha}$ as shown in Figure 2.20.

Repeating a similar process to express the other vanishing cycles $\nu_2, ..., \nu_6$ one finds they are (the isotopy classes of)

$$\begin{aligned} \nu_1 &= \tau_c^{-1} \circ \tau_d^{-1}(\overline{\alpha}) & \qquad \nu_4 &= a \\ \nu_2 &= \tau_{b_2}^{-1} \circ \tau_d(c) & \qquad \nu_5 &= \tau_{b_2} \circ \tau_{b_1}^{-1} \circ \tau_a(\overline{\alpha}) \\ \nu_3 &= \tau_{b_1}^{-1} \circ \tau_{b_2}^{-1}(c) & \qquad \nu_6 &= \tau_d^{-1}\tau_{b_1}^{-1}\tau_a(\overline{\alpha}). \end{aligned}$$

Thus it remains only to express the class $\overline{\alpha}$ in terms of the basis. This can be done by the sequence of half Dehn twists and valentine moves shown in Figure 2.21.

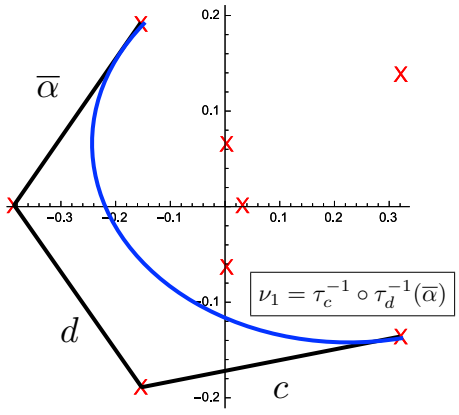

Figure 2.20: The matching path μ_1 written as two Dehn twists applied to $\overline{\alpha}$.

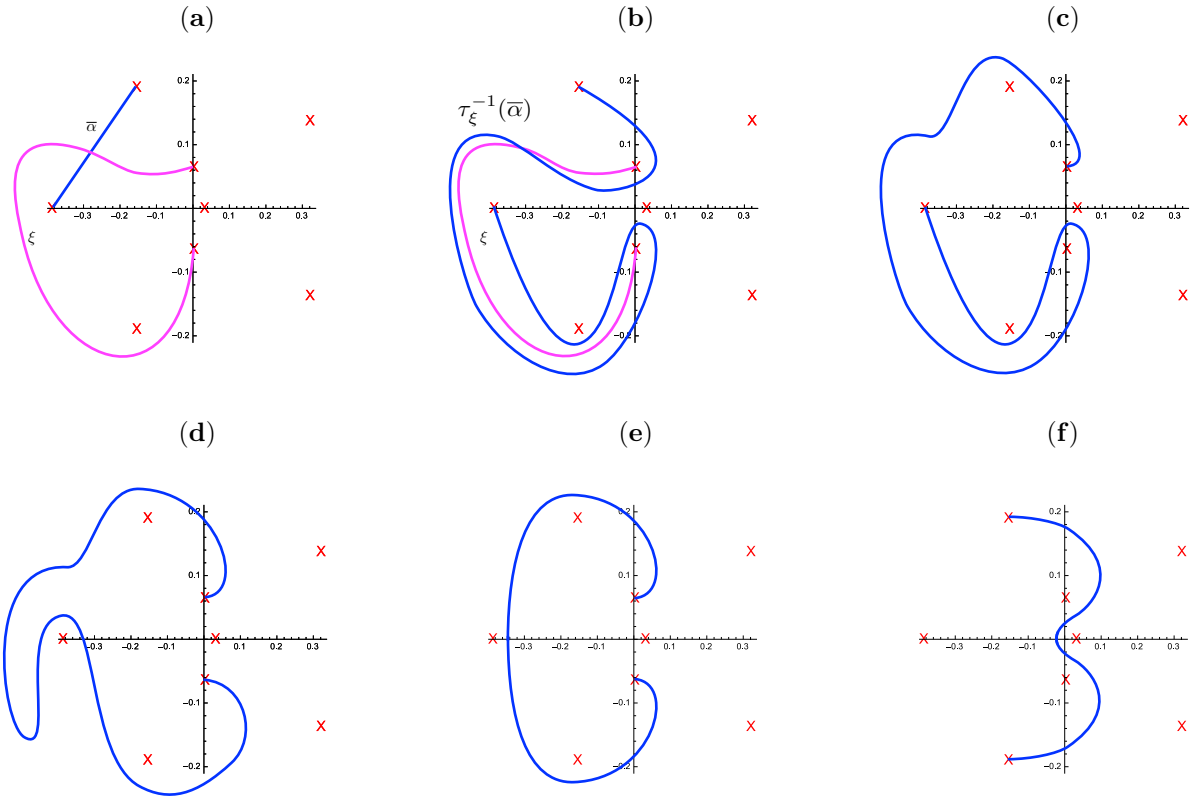

Figure 2.21: Expressing $\overline{\alpha}$ in terms of the other basis elements by the following operations. (b) An inverse half Dehn twist around ξ. (c) a valentine move on the top two critical values (valid because the two vanishing cycles have a single intersection). (d) a valentine move on the two bottom critical values. (e) an isotopy of the path. (f) two valentine moves on both the top and bottom pairs of critical values.

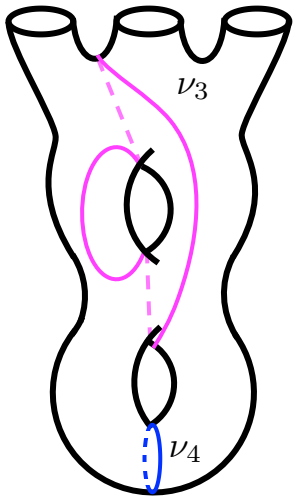

Figure 2.22: Two of the vanishing cycles ν_3 (magenta), and ν_4 (blue) drawn in the standard surface S_2^3.

The matching cycle of the matching path in the final panel of Figure 2.21 is $\tau_c \circ \tau_{b_2} \circ \tau_{b_1}(a)$. Thus one obtains the relation:

$$\tau_\xi^{-1}\overline{\alpha} = \tau_c \circ \tau_{b_2} \circ \tau_{b_1}(a) \quad \Rightarrow \quad \overline{\alpha} = \tau_\xi \circ \tau_c \circ \tau_{b_2} \circ \tau_{b_1}(a).$$

Hence the expressions for the vanishing cycles become :

$$\begin{aligned}
\nu_1 &= \tau_c^{-1} \circ \tau_d^{-1} \circ \tau_\xi \circ \tau_c \circ \tau_{b_2} \circ \tau_{b_1}(a) & \qquad \nu_4 &= a \\
\nu_2 &= \tau_{b_2}^{-1} \circ \tau_d(c) & \qquad \nu_5 &= \tau_{b_2} \circ \tau_{b_1}^{-1} \circ \tau_a \circ \tau_\xi \circ \tau_c \circ \tau_{b_2} \circ \tau_{b_1}(a) \\
\nu_3 &= \tau_{b_1}^{-1} \circ \tau_{b_2}^{-1}(c) & \qquad \nu_6 &= \tau_d^{-1}\tau_{b_1}^{-1}\tau_a \circ \tau_\xi \circ \tau_c \circ \tau_{b_2} \circ \tau_{b_1}(a)
\end{aligned}$$

By the above, the vanishing cycles of the fibration $f : X_{3,2} \to \mathbb{C}$ have been expressed as isotopy classes of simple closed curves in the standard surface S_2^3. This was the promised outcome of the algorithm.

Chapter 3

Symplectic Lefschetz Pencils

The two previous chapter have studied exclusively smooth complex varieties. The results of Chapter 1 showed that a Lefschetz fibration can provide significant insight into the topology of a variety. Among these results, Theorem 1.45 was particularly powerful, giving the following correspondence.

$$\left\{ \begin{array}{c} 4-\text{manifolds w/ Lefschetz} \\ \text{fibrations of genus } g \end{array} \right\} \Big/ \text{Diffeo.} \Longleftrightarrow \left\{ \begin{array}{c} \text{r-tuples in } Mod(S_g) \\ [\tau_{\nu_1}] \circ \ldots \circ [\tau_{\nu_r}] = Id \end{array} \right\} \Big/ \left\{ \begin{array}{c} \text{Simultaneous conjugation} \\ \text{Hurwitz equivalence} \end{array} \right\} \tag{3.0.1}$$

In principle, this theorem reduced the study of the topology of total spaces of Lefschetz fibrations to the study of the mapping class group $Mod(S_g)$, which is in general better understood than arbitrary 4-manifolds. Chapter 2 gave a computational algorithm allowing this correspondence to be realized concretely: given a complex algebraic variety, the algorithm computes an r-tuple of Dehn twists representing the equivalence class to which it corresponds. Together, these tools are an enormous asset in studying the topology of complex varieties. Complex algebraic varieties, however, comprise only a fraction of all possible 4-manifolds. As was remarked in 1.46, the collection of 4-manifolds which possess Lefschetz fibrations has been shown to be larger than only the complex algebraic varieites. The question now becomes: how large is it? That is to say, which of all 4-manifolds admit the structure of a Lefschetz fibration or pencil. This and the following chapter will provide a nearly complete answer to this question.

In 1995, Simon Donaldson expanded the class of 4-manifolds known to admit Lefschetz pencils to include all compact symplectic manifolds. A symplectic manifold is a pair (X, ω) of a smooth manifold X and a closed, non-degenerate 2-form ω. These manifolds are of immense importance in topology, geometry and mathematical physics. Much could be said at this point on the motivation and techniques for studying symplectic manifolds, but such a discussion is beyond the scope of this exposition. The reader not familiar with symplectic geometry is referred to [27, 28, 29] for several extensive introductions.

Donaldson proved:

Theorem 3.1. (Donaldson, [30, 31]) *Suppose (X, ω) is a compact symplectic manifold of dimension $2n$ and that $[\omega/2\pi] \in H^2(X; \mathbb{R})$ is the reduction to real coefficients of an integral class. Then X admits a topological Lefschetz pencil $f : X \setminus B \to \mathbb{C}P^1$ such that the fibers of f are symplectic submanifolds of X.*

Here, a topological Lefschetz pencil is as in Definition 1.15. For singular fibers, "symplectic submanifold" is taken to mean that the (non-closed) submanifold obtained by removing the critical point(s) is a symplectic submanifold.

Definition 3.2. *Topological Lefschetz pencils that are compatible with a symplectic structure in the above sense are called* **symplectic Lefschetz pencils**.

This theorem applies to a strictly larger class of manifolds than has been dealt with thus far. Every

(smooth) complex variety is a symplectic manifold, but there are compact symplectic manifolds that are not complex varieties [32]. Theorem 3.1 is interesting from two distinct perspectives:

Topologically: This theorem expands the class of 4-manifolds which can be characterized topologically via Theorem 1.45.

Geometrically: The compatibility of the Lefschetz pencil structure with the symplectic structure has the potential to reduce questions about symplectic geometry to questions about the monodromy of Lefschetz pencils.

The following chapter is devoted mainly to explaining the proof of Theorem 3.1. In the final two sections, a discussion about the extent to which the second of the above points can be realized is given. Because Donaldson's original exposition of the theorem [30, 31] is concise, elegant, and largely self-contained, the exposition here is intended to complement, rather than replace, the exposition therein by providing background and intuition for Donaldson's arguments.

3.1 Outline of the Proof

In this section, the main ideas of the proof of Theorem 3.1 are summarized. The subsequent sections provide details.

Recall that a Lefschetz pencil f on a complex variety could be constructed by taking homogenous polynomials P_0, P_1 and defining $f = [P_1, -P_0]$. In this case, the base locus was the mutual vanishing locus of P_0, P_1 and the fiber above $[t_0; t_1] \in \mathbb{C}P^1$ was defined by $t_0P_1 + t_1P_0 = 0$. This is the perspective that is generalized by Donaldson's theorem. More generally, instead of considering two homogenous polynomials, one can consider a pair s_0, s_1 of smooth sections of complex line bundle $\mathcal{L} \to X$. Away from the mutual vanishing set $B = \{x \in X \mid s_0(x) = s_1(x) = 0\}$ there is a map $f : X \setminus B \to \mathbb{C}P^1$ defined by choosing a trivialization $U \times \mathbb{C} \to \mathcal{L}$ at x and taking

$$f(x) := [s_0; s_1]. \tag{3.1.1}$$

The projective coordinates ensure that this map does not depend on the choice of trivialization: given two distinct trivializations of $\mathcal{L}$ at x, there is a transition map $\varphi : U \to \mathbb{C}^\times$ between them, hence the values $s_0(x), s_1(x)$ obtained via one trivialization both differ from those obtained via the second trivialization by multiplication by $\varphi(x)$. Consequently, the projectivized pair $[s_0; s_1]$ does not depend on the choice of trivialization, so f is well-defined.

The strategy of the proof of Theorem 3.1 is to construct a map f in this way. The resulting pencil will be similar in spirit to those obtained in the case of complex varieties from a pair of homogenous polynomials P_0, P_1. The mutual vanishing locus of s_0, and s_1 (still called the base) will be a (real) codimension 4 submanifold, and the fibers of f will be where s_0, s_1 have a fixed ratio. Locally, choosing a trivialization of $\mathcal{L}$, the fiber over $[t_0; t_1] \in \mathbb{C}P^1$ is the set on which $s_0t_1 - s_1t_0 = 0$, again analogous to the case of varieties.

For f of the form (3.1.1) to be a symplectic Lefschetz pencil, the sections s_0, s_1 must satisfy several conditions. First and not too difficult, their zero-sets must be transverse as codimension 2 submanifolds, which ensures the base locus is a smooth (codimension 4) submanifold. A second and rather trickier condition is required to ensure the fibers are symplectic submanifolds everywhere.

The construction of a map $f = [s_0; s_1]$ such that the fibers are symplectic submanifolds relies on the fact that symplectic geometry is, in some sense, "close" to complex geometry. As will be made precise in Section 3.2, real subspaces of a complex vector space that are "close" to complex subspaces must be symplectic subspaces. Applying this to the tangent bundle of a symplectic manifold (recall that the tangent bundle of a symplectic manifold admits an almost-complex structure $J : TX \to TX$ such that $J^2 = -Id$, [28]) will show that a submanifold whose tangent spaces are close to complex subspaces in TX has symplectic tangent spaces and is therefore, by definition, a symplectic submanifold.

The fibers of f will have tangent spaces close to complex subspaces provided f is sufficiently "close" to being holomorphic. If $\mathcal{L} \to X$ were a holomorphic vector bundle on a complex manifold, and if s_0, s_1 were holomorphic sections, then f itself would be holomorphic and thus the fibers would have complex tangent

spaces. In general, X need not be a complex manifold, but constructing sections s_0, s_1 that are "close" to being holomorphic will ensure the tangent spaces of the zero-sets are close to complex subspaces. More specifically, as will be shown in Section 3.2, f will have symplectic fibers if

$$|\overline{\partial} f| < |\partial f| \tag{3.1.2}$$

where $\overline{\partial}$ and ∂ are the complex linear and anti-linear parts of the differential df, which are defined precisely in Section 3.3. In general, a function or section satisfying an estimate of the form (3.1.2) is called an **approxiately holomorphic section**. Of course, in the truly holomorphic case $|\overline{\partial} f|$ vanishes completely. Estimates of this form make the notion of being "close" to holomorphic quantitative.

In order for f to satisfy (3.1.2), the two sections s_0, s_1 must satisfy rather stronger estimates, so that $|\overline{\partial} s_i| << |\partial s_i|$ where $\overline{\partial}, \partial$ are now the complex linear and anti-linear parts of the covariant derivative with respect to some connection on $\mathcal{L}$ (defined precisely in Section 3.3). The majority of the proof of Theorem 3.1 is constructing sections satisfying these stronger estimates. The construction is carried out with a fixed line bundle $L \to X$ whose first chern class $c_1(L)$ is related to $[\omega] \in H^2(X; \mathbb{R})$. In general, however, L itself will not necessarily have approximately holomorphic sections. Instead, the construction results in approximately holomorphic sections of $L^{\otimes k}$ for some sufficiently large k. Specifically, two types of estimates are needed on sections s_0, s_1 of $L^{\otimes k}$:

$$|\overline{\partial} s_i| \leqslant \frac{C}{\sqrt{k}} \qquad\qquad |\partial s_i| > \varepsilon \quad \text{along } Z(s_i). \tag{3.1.3}$$

Together these estimates imply $|\overline{\partial} s_i| << |\partial s_i|$ once k is large. Sections satisfying estimates of the first type are said to be **asymptotically holomorphic**, because they approach holomorphicity as $k \to \infty$. Sections satisfying estimates of the second type are said to be ε**-transverse**, as it is a condition similar to transversality, but requires the derivative to be bounded below instead of simply non-zero.

The main difficulty of the proof of Theorem 3.1 is to construct sections s_0, s_1 that are both asymptotically holomorphic and ε-transverse. The proof consists of three main steps:

(I) Construction of asymptotically holomorphic sections.

(II) Construction of ε-transverse sections.

(III) Modification of $f = [s_0; s_1]$ for two sections s_0, s_1 that are both asymptotically holomorphic and ε-transverse. The modification makes f satisfy (3.1.2), and also guarantees the local behavior required to be a Lefschetz pencil.

Specifically, the construction of asymptotically holomorphic sections requires piecing together local approximately holomorphic sections. To construct sections that are also ε-transverse relies on an extension of transversality techniques that includes quantitative information. Throughout the proof, the parameter k plays an essential role. In many cases, the key point is ensuring certain quantities do not depend on k.

Remark 3.3. For the reader familiar with some algebraic geometry, it should be noted that the statement and proof of Theorem 3.1 are closely related to the Kodaira Embedding Theorem [11]. That theorem establishes the existence of embeddings of complex manifolds satisfying certain conditions into $\mathbb{C}P^N$ for large N. The approach of the standard proof is to take a line bundle L on the manifold, and show that for sufficiently large k, the line bundle $L^{\otimes k}$ has many holomorphic sections. A map to $\mathbb{C}P^N$ constructed from such sections yields the embedding. Theorem 3.1 mimics this proof by showing that sufficiently high powers of a line bundle admit sections. Donaldson's theorem can therefore be thought of as a symplectic or almost-complex analogue of the Kodaira Embedding Theorem.

3.2 Symplectic Submanifolds

This section makes precise the fact that sections satisfying (3.1.2) have zero sets that are symplectic submanifolds. This will reduce the problem of constructing Lefschetz pencils with symplectic fibers to the problem of producing sections satisfying the two types of estimates (3.1.3).

The following lemma is a linear algebra fact characterizing symplectic subspaces. It will shortly be extended an analogous statement on vector bundles. Consider $\mathbb{C}^n$ with the standard complex structure J and symplectic form ω. Denote the standard real metric g by $\langle\ ,\ \rangle$ and the standard hermitian metric h by $(\ ,\ ) = \langle\ ,\ \rangle + i\omega$.

Lemma 3.4. *Let $T : \mathbb{C}^n \to \mathbb{C}$ be a* **real** *linear map. Decompose T as $T = A + B$ where A, B are the complex linear and anti-linear parts respectively. If $|B| < |A|$, then $\ker(T) \subseteq \mathbb{C}^n$ is a symplectic subspace of dimension $2n-2$.*

Here the norm is that induced on $(\mathbb{C}^n)^* \otimes \mathbb{C}$ by $\langle\ ,\ \rangle$ and the standard metric on $\mathbb{C}$. More explicitly, after choosing a basis, it is the square root of the sum of the squares of the matrix entries of T.

Proof. The statement about the dimension is straightforward: if the map has rank 1 then $|A| = |B|$ and the estimate cannot hold. To see this, note that if the image is a (real) line $\mathbb{R}e^{i\theta}$ then for any v one has $e^{-i\theta}Av$ conjugate to $e^{-i\theta}Bv$ and so $|A| = |B|$. Clearly if Rank(T)=0 the strict inequality similarly fails. To prove the kernel is a symplectic subspace, consider the "Kähler Angle" of a vector subspace W of (real) codimension 2 defined as follows. The restriction of the metric gives rise to a natural volume form $\Omega_W = e_1 \wedge \ldots \wedge e_{2n-2}$ where $\{e_i\}$ form an orthonormal basis of W. Then for any i, j, one has $\omega(e_i, e_j) = \langle e_i, Je_j\rangle \leqslant |e_i||Je_j| = 1$, and hence $|\omega^{n-1}(e_1 \wedge \ldots \wedge e_{2n-2})| \leqslant (n-1)!$ since it is a sum of exactly $(n-1)!$ terms that are products of ω applied to basis vectors, so are less than 1. Therefore $\frac{1}{(n-1)!}\omega^{n-1}$ is a multiple $t\Omega_W$ for some $t \in [-1, 1]$. The Kähler angle is defined by

$$\cos(\theta_W) := \frac{\frac{1}{(n-1)!}\omega^{n-1}\big|_W}{\Omega_W}.$$

W is a symplectic subspace by definition exactly when $\frac{1}{(n-1)!}\omega^{n-1}$ is a volume form on W oriented positively with respect to Ω_W, so the symplectic subspaces are those for which the right side is strictly positive. The same holds for subspaces of any even dimension $2k$ replacing $n-1$ by k. To complete the lemma, it therefore suffices to show that $|B| < |A|$ implies $\cos(\theta_{\ker T}) > 0$.

Notice that a subspace is symplectic if and only if its orthogonal complement with respect to the metric g is symplectic. This reduces the problem to the case of subspaces of (real) dimension 2 by considering the adjoint of T. Let $a, b : \mathbb{C} \to \mathbb{C}^n$ be the adjoints of A, B respectively. Clearly, the norm of the matrices is unchanged by transposition so $|A| = |a|$ and likewise for B. Taking the adjoint also respects the decomposition into complex linear and anti-linear parts, hence $\ker(T)^\perp = \mathrm{Im}(T^T) = \mathrm{Im}(a + b)$. The image is the space spanned by the images of $1, i$. By slight abuse of notation, denote $a(1), b(1)$ by just a, b. Then

$$T^T(1) = a + b \qquad T^T(i) = Ja - Jb$$

where the second expressions follows since a, b are complex linear and anti-linear respectively. Now simply compute $\cos(\theta_{\ker(T)^\perp})$ writing both volumes in terms of $T(1) \wedge T(i)$.

$$\begin{aligned} \omega(a + b, Ja - Jb) &= \omega(a, Ja) - \omega(b, Jb) + \omega(b, Ja) - \omega(a, Jb) \\ &= |a|^2 - |b|^2 \end{aligned}$$

as $\omega(\ , J\ ) = \langle\ ,\ \rangle$. Likewise, becuase $\Omega_{Im(T^T)} = \sqrt{\det|g|}T(1) \wedge T(i)$ where g is the restricted metric, one has

$$\begin{aligned} \Omega(a + b, Ja - Jb) &= |a + b|^2|Ja - Jb|^2 - \langle a + b, Ja - Jb\rangle^2 \\ &= (|a|^2 + |b|^2)^2 - 4|(a, b)|^2 \end{aligned}$$

where the second equality follows from the expression for the hermitian metric in term of ω and g. In particular $\Omega(a + b, Ja - Jb)$ is positive, so if $|A| > |B|$ then

$$\cos(\theta_{\ker(T)}) = \cos(\theta_{\ker(T)^\perp}) = \frac{\omega\big|_W}{\Omega_W} = \frac{|A|^2 - |B|^2}{\Omega} > 0.$$

□

Now the above lemma is extended to the case of vector bundles. First a little set-up is required, after which the statement for vector bundles is essentially immediate. Let (X, ω) be a compact symplectic manifold. Choose a compatible almost-complex structure $J : TX \to TX$, and consider the metric $g = \omega(-, J-)$. A triple (ω, J, g) related in this way is called a **compatible triple**. Additionally, let $\mathcal{L} \to X$ be a complex line bundle, endowed with a hermitian metric h. The almost-complex structure J makes TX into a complex vector bundle, hence at a point x, it makes sense to consider the complex linear and anti-linear parts of a linear map $T : T_xX \to V$ for a complex vector space V.

In particular, one can apply this to the derivative $\nabla s : T_xX \to \mathcal{L}_x$ along the zero-set of s. Recall that along the zero-set, the derivative of a section is canonically defined without choosing a connection. To see this, note that for $(0, v) \in \mathcal{L}$ the tangent space of the total space of the bundle splits canonically as

$$T_{(x,0)}\mathcal{L} = T_xX \oplus \mathcal{L}_x$$

since the image of T_xX under the zero-section provides a canonical horizontal subspace. Said a different way, a choice of connection ∇ gives a covariant derivative $\nabla s = (d + A)s$ in a local trivialization, where A is a matrix-value 1-form, and along the zero-set $\nabla s = ds$ is independent of A hence does not depend on the choice of connection. This shows the derivative is well-defined along the zero-section. At each point on the zero-set, one therefore has complex linear and anti-linear parts ∂s, and $\overline{\partial} s$ of ∇s.

Theorem 3.5. *Suppose that $s : X \to \mathcal{L}$ is a section such that along the zero-set $Z(s)$ of s*

$$|\overline{\partial} s| < |\partial s|. \tag{3.2.1}$$

$T\,Z(s)$ is a symplectic submanifold. Here, the norm is the one induced on $Hom(T_xX, \mathcal{L}_x) \simeq T_x^*X \otimes \mathcal{L}_x$ by the metrics on X and $\mathcal{L}$

Proof. At each $x \in Z(s)$, consider the composition $\nabla s : T_xX \to T_xX \oplus \mathcal{L}_x \to \mathcal{L}_x$. The condition that $Z(s)$ is a submanifold is a local, and is the condition that at each x, this composition has full rank. In this case, the tangent space of $Z(s)$ is the kernel of ∇s. For each x, choose bases of T_xX and $\mathcal{L}_x$ so that (ω, J, g) and h are standard in these bases. The theorem then follows by applying Lemma 3.4 to ∇s in these bases, as at x, (3.2.1) is exactly the assumption of the lemma. □

Corollary 3.6. *If $\mathcal{L} = \mathbb{C}$ is the trivial bundle (i.e. s is a complex valued function) then (3.2.1) implies that every level-set of s is symplectic submanifold.*

Proof. The fact that this holds for the zero-section of s is a specific case of Theorem 3.5. Since the estimate (3.2.1) depends only on the derivative, the same conclusion follows for s shifted by a constant. □

Theorem 3.5 reduces the proof of Theorem 3.1 to the construction of sections s_0, s_1 satisfying sufficient asymptotically holomorphic and ε-transversality estimates. More specifically, recall step **(III)** from the outline of the proof in Section 3.1. A slightly more rigorous statement is:

Theorem 3.7. *Suppose $s_0^{(k)}, s_1^{(k)}$ are sequences of sections so that $s_i^{(k)}$ is a section of $L^{\otimes k}$ for all k. Suppose additionally that these sequences satisfy suitable asymptotically holomorphic and ε-transversality estimates. Let F be the $\mathbb{C}$-valued function defined on $X \setminus Z(s_0)$ by $F = s_1/s_0$. Then for sufficiently large k, $f = [s_0; s_1]$ can be modified so that it satisfies i) f is a topological Lefschetz pencil, and ii) F is approximately holomorphic except at its critical points.*

The precise meaning of "suitable asymptotically holomorphic and ε-transversality estimates" is given by Definition 3.15 below. Even without the precise definition, however, one concludes:

Claim 3.7.1. *Provided sequences as in the hypothesis of Theorem 3.7 exist, Theorem 3.7 implies Theorem 3.1.*

Proof. Asymptotically holomorphic sections that are also ε-transverse satisfy (3.2.1) for sufficiently large k since $|\overline{\partial} s_i| < \frac{C}{\varepsilon\sqrt{k}}|\partial s|$. If f is modified as in the conclusion of Theorem 3.7, then the fibers, $Z(s_0)$ and the level sets of $F : X \setminus (Z(s_0) \cup \mathrm{crit}(f))$, are all symplectic submanifolds by Theorem 3.5 and Corollary 3.6. f is therefore, by definition, a symplectic Lefschetz pencil. □

3.3 Asymptotically Holomorphic Sections

The next three sections are devoted, one each, to explaining the three steps in the proof of Theorem 3.1. This and the next section formulate more precisely and show the existence of asymptotically holomorphic and ε-transverse sections as in the hypothesis of Theorem 3.7. Section 3.5 addresses the proof of Theorem 3.7, thereby completing Theorem 3.1. In all these sections, all results are due to [30, 31] and [33]. In many cases, the precise details of estimates are omitted and can be found in these references.

Here and throughout the subsequent sections, fix a compact symplectic manifold (X, ω) of dimension 2n with a compatible almost-complex structure J, and a compatible metric g_1. Additionally, fix a complex line bundle $L \to X$ with a hermitian metric h such that the first chern class $c_1(L)$ is the integral lift of $[\omega/2\pi] \in H^2(X; \mathbb{R})$ (such a line bundle always exists, see for instance [34]). L can be endowed with a connection ∇ that has curvature $-i\omega$. For each positive integer k the line bundle $L^{\otimes k}$ (denoted from here on simply by L^k), possesses an induced connection with curvature $-ik\omega$.

Throughout, it is convenient to introduce the family of scaled metrics $g_k = kg_1$ on X so that $(k\omega, J, g_k)$ is a compatible triple for each k. Distances measured in the g_k metric on X are larger by a factor of $k^{1/2}$ than when measured in the g_1 metric. The convention is taken that the C^r norm of a section $s^{(k)}$ of L^k means the C^r norm where the derivatives are taken using the connection induced on $(T^*X)^{\otimes i} \otimes_{\mathbb{R}} L^k$ for $i \leqslant r$ by ∇ and the Levi-Civitas connection of g_k, and where the norms are measured with respect to the metrics induced by g_k and h.

The covariant derivate ∇s of a section can be decomposed into its complex linear and anti-linear parts with respect to J so that $\nabla s = \overline{\partial}_J s + \partial_J s$. The definition of these operators is now given precisely. In the simplest case where ∇ is a connection on a vector bundle $\mathcal{L}$ on $\mathbb{C}^n$ with the standard almost-complex structure J_0, the covariant derivative ∇s of a section s could be split into the complex linear and anti-linear covariant parts in the standard way at each point. That is, in coordinates where $\nabla = d + A$ for some matrix-valued 1-form A, the complex linear and anti-linear derivatives are defined as

$$\partial_{J_0} s = \partial s + A^{1,0} s \qquad \overline{\partial}_{J_0} s = \overline{\partial} s + A^{0,1} s$$

respectively, where $\partial, \overline{\partial}$ are the complex linear and anti-linear parts of $df : T_x\mathbb{C}^n \to \mathbb{C}$ and $A^{1,0}(z), A^{0,1}(z)$ are the complex linear and anti-linear parts of $A(z)$. This can be phrased more invariantly as follows: there is a splitting $T^*\mathbb{C}^n \otimes \mathbb{C} = \Omega^{1,0} \oplus \Omega^{0,1}$ where $\Omega^{1,0}, \Omega^{0,1}$ are the spaces of J_0-linear and anti-linear forms with projections $\pi^{1,0}$ and $\pi^{0,1}$ to them respectively. Then $\partial_{J_0} s = \pi^{1,0} \circ \nabla s$, and $\overline{\partial}_{J_0} s = \pi^{0,1} \circ \nabla s$. In the case of a manifold X with an almost-complex structure J, the construction is analogous, except the projections now vary pointwise: for each $x \in X$ there is a splitting $T_x X \otimes_{\mathbb{R}} \mathbb{C} = \Omega^{1,0}_x \oplus \Omega^{0,1}_x$ with projections $\pi^{1,0}_J, \pi^{0,1}_J$ to the J-linear and anti-linear components. The complex linear and anti-linear parts of ∇ are then defined, in general, as

$$\partial_J(s) = \pi^{1,0}_J \circ \nabla s \qquad \overline{\partial}_J(s) = \pi^{0,1}_J \circ \nabla s. \tag{3.3.1}$$

Definition 3.8. *A sequence of sections s_k of L^k is said to be* **asymptotically holomorphic** *if there exists a constant $C \in \mathbb{R}$ so that*

$$||s_k||_{C^3(X)} \leqslant C \qquad ||\overline{\partial}_J s_k||_{C^2(X)} \leqslant Ck^{-1/2} \tag{3.3.2}$$

holds for all k sufficiently large.

The existence of asymptotically holomorphic sequences is rather trivial: one can just multiply each s_k by a constant c_k until the bounds are satisfied. The point here, however, is to construct sequences that can later be modified to *also* be ε-transverse. Here, asymptotically holomorphic sequences of a specific form that will allow them to be modified to be ε-transverse are constructed. The construction is done first locally then globally, and the modification to be ε-transverse is carried out in Section 3.4.

The Local Construction

Lemma 3.9. *There exists sequences of local asymptotically holomorphic sections of L^k, supported in neighborhoods of size $O(k^{-1/3})$.*

The fundamental tool that will be used to produce these sequence is scaling by factors of k. The local sections at each point will have the simple local model of a Gaussian, i.e. $e^{-|x|^2}$.

First, consider the case of $k = 1$. At each $p \in X$, let $\chi_p : B^{2n} \to X$ be a Darboux coordinate chart so that in these coordinates ω is given by the standard form $\frac{i}{2}\sum_{j=1}^n dz_j d\overline{z}_j$. By a parameterized version of Darboux theorem, these coordinate charts can be taken to vary smoothly with the point p. Moreover, by composing with a complex linear transformation, it can be assumed that the almost-complex structure is the standard one at the origin for each p. The pullback bundle $\chi_p^*(L)$ is trivial, and there is a preferred trivialization given by parallel transporting out from the origin. In this trivialization, the connection matrix is $A = \frac{1}{4}\sum_{j=1}^n z_j d\overline{z}_j - \overline{z}_j dz_j$ (see [30] Page 674).

The local model used to construct asymptotically holomorphic sequences is

$$f(z) = e^{-|z|^2/4}$$

In the *standard* complex structure J_0 in these coordinates, the complex linear and anti-linear covariant derivatives $\partial_{J_0}, \overline{\partial}_{J_0}$ are as above and $f(z)$ is truly holomorphic (locally) since

$$\overline{\partial}_{J_0}(e^{-|z|^2/4}) = \overline{\partial} f + A^{0,1} f = \frac{1}{4}\left(\sum_{j=1}^n z_j d\overline{z}_j - \sum_{j=1}^n z_j d\overline{z}_j\right) e^{-|z|^2/4} = 0. \tag{3.3.3}$$

Here, however, one wishes to construct sections that are holomorphic in the fixed almost complex structure J, rather than the complex structure J_0 given by the local coordinates. Since $J = J_0$ at the origin, the above section will fail to be J-holomorphic by an amount that is $O(|z|)$. Therefore, scaling the section to be more localized at the origin will make it closer to being J-holomorphic in the sense that $\overline{\partial}_J$ will be small and will lead to a local estimate as in Definition 3.8.

Lemma 3.10. *The following estimates hold for f (in the norms induced by the standard metric in coordinates).*

$$|\overline{\partial}_J(f)| \leqslant C|z|^2 e^{-|z|^2/4}$$
$$|\nabla_X \overline{\partial}_J(f)| \leqslant C(|z| + |z|^2 + |z|^3) e^{-|z|^2/4}$$

where ∇_X is the Levi-Civitas connection of g_1 on X.

Proof. Note that the difference of the projections $\pi_J^{0,1} - \pi^{0,1}$ as in the definition of $\overline{\partial}_J$ vanishes at the origin so is $O(|z|)$, and therefore bounded by $C|z|$ for some constant C. The constant C can be taken to be uniform over all $p \in X$, hence:

$$\overline{\partial}_J(f) \quad = \quad \pi^{0,1} \circ \nabla f + (\pi_J^{0,1} - \pi^{0,1}) \circ \nabla f \leqslant 0 + C|z|\left(\sum_{j=1}^n z_j d\overline{z}_j + \overline{z}_j dz_j + A\right) e^{-|z|^2/4} \leqslant C|z|^2 e^{-|z|^2/4}.$$

The derivative estimate follows by differentiating and noting that the Christoffel symbols of ∇_X are uniformly bounded on X. □

Now consider the effect of scaling by k. Scale the metric on both the manifold and in coordinates by k to obtain a new chart $\chi_{p,k}$. Up to isometry, one may consider $\chi_{p,k}$ as a chart $\chi_{p,k} : k^{1/2}B^{2n} \to X$ on the scaled ball with the standard metric. The image in X remains the same, but its diameter is larger by $k^{1/2}$ when measured in g_k . Consider the local section

$$f_k(z) = e^{-|z|^2/4}$$

on this new chart. Although the function has the same form as the original, it is now considered on the scaled ball, so on X the Gaussian is steeper by a factor of k. Since in this new chart $\chi^*_{p,k}(k\omega) = \omega_0$ is the standard form, this chart with the trivial $\mathbb{C}$ bundle provides a connection-preserving trivialization of L^k.

In the new chart $\chi_{p,k}$, the almost complex structure is also scaled, so that $J(z) = J(k^{1/2}\tilde{z})$ where $\tilde{z}$ is the original χ_p coordinate. Thus the projections to the J- and anti-linear parts are also scaled, so $\pi_J^{0,1} - \pi^{0,1}$ is $O(k^{-1/2}|z|)$ in the scaled chart, and the same calculation as Lemma 3.10 yields:

$$|\overline{\partial}_J(f_k)| \leqslant Ck^{-1/2}\ |z|^2 e^{-|z|^2/4} \tag{3.3.4}$$

$$|\nabla_X \partial_J(f_k)| \leqslant Ck^{-1/2}\ (|z| + |z|^2 + |z|^3)e^{-|z|^2/4} \tag{3.3.5}$$

Finally, one wishes to convert these estimates to ones of local sections on X. First, this requires the introduction of a bump function so that the sections are compactly supported on X. Second, this requires converting the estimatess to ones in terms of the distance and metric measured on X (notice the left hand side in the above is still measured in the standard metric in the local coordinates). For the first point, let β_k be a smooth bump function on $k^{1/2}B^{2n}$ such that $\beta_k(z) = 1$ for $z \in \frac{k^{1/6}}{2}B^{2n}$ and β_k is compactly supported in $k^{1/6}B^{2n}$. Then define a new section $\sigma_{k,p}(z)$ to be $\beta_k \cdot f_k(z)$, where f_k is center at $p \in X$. Since β_k can be taken so that $|\nabla\beta_k| = O(k^{-1/6})$, one can check by the product rule that estimates identical to (3.3.4) and (3.3.5) hold for $\sigma_{k,p}$ as well.

For the second point, recall that in the chart χ_p, g_1 is the standard metric at the origin, since ω, J are standard there, hence g_k is also standard at the origin in the chart $\chi_{k,p}$. Thus the difference between the pullback metric and the standard metric in coordinates is $O(|z|)$ and one has $|g_0 - g_1^*| \leqslant C|z|$ in χ_p, and by scaling $|g_0 - g_k^*| \leqslant Ck^{-1/2}|z|$ on $k^{1/2}B^{2n}$ in $\chi_{k,p}$. Then, letting $d_k(p,q)$ be the distance on X induced by the metric g_k one has

$$|d_k(p,q)^2 - |z|^2| \leqslant \int_{\gamma(t)=tz} |g_0 - g_k^*|dt \leqslant Ck^{-1/2}|z| \cdot |z|^2. \tag{3.3.6}$$

Since the support of $\sigma_{k,p}(z)$ is $O(k^{-1/3})$, for k sufficiently large one has $Ck^{-1/2}|z| < 1/4$, and thus both $|z|^2/5 \leqslant d_k^2(p,q)/4$ and $d_k^2(p,q)/5 \leqslant |z|^2/4$.

Using this, one can show that in terms of the invariant quantities on X, (3.3.4) and (3.3.5) yield

$$\begin{aligned} |\sigma_{k,p}(q)| &\leqslant e^{-d_k^2(p,q)/5} \\ |\overline{\partial}_J\sigma_{k,p}(q)| &\leqslant Ck^{-1/2}d_k^2(p,q)e^{-d_k^2(p,q)/5} \\ |\nabla_X\overline{\partial}_J\sigma_{k,p}| &\leqslant Ck^{-1/2}(d_k(p,q) + d_k^2(p,q) + d_k^3(p,q))e^{-d_k(p,q)/5}. \end{aligned}$$

In fact, repeating the entire process taking more derivatives only introduces extra factors of $|z|$ which result in the same estimates with higher powers of $d_k(p,q)$.

Lemma 3.11. *The local sections $\sigma_{k,p}$ satisfy:*

$$||\sigma_{k,p}(q)||_{C^3(X)} \leqslant Ce^{-d_k(p,q)/5} \qquad ||\overline{\partial}_J\sigma_{k,p}(q)||_{C^2(X)} \leqslant Ck^{-1/2}\left(d_k(p,q) + \ldots + d_k^\ell(p,q)\right)e^{-d_k(p,q)/5}$$

for some $\ell \leqslant 5$.

The Global Construction

Now the sections $\sigma_{k,p}$ are added together into globally asymptotically holomorphic sections. These sections are constructed by summing over the local sections $\sigma_{p,k}$. Let $\{\psi_m\}$ be a fixed (finite) collection of charts covering X such that

$$\frac{1}{2}|x - y| \leqslant d_1(\psi(x), \psi(y)) \leqslant 2|x - y|. \tag{3.3.7}$$

For each k, consider the lattice $\Lambda(k) := \frac{1}{2k^{1/2}}\left(\frac{n}{2}\right)^{1/2}(\mathbb{Z}^n \oplus i\mathbb{Z}^n) \subseteq \mathbb{C}^n$. Let $\{p_i\}$ be the collection of the images of the lattice under $\{\psi_m\}$ for all m together so that p_i are roughly a lattice covering X. The balls of radius $\frac{1}{2}k^{-1/2}$ around the lattice points cover $\mathbb{C}^n$ by the choice spacing of $\Lambda(k)$, and by (3.3.7) the balls of d_k radius 1 cover X once k is sufficiently large. Let $N(k)$ be the total number of points p_i in the lattice, which is $O(k^n)$. Define a global section of L^k by

$$s_k(q) := \sum_{i=1}^{N(k)} w_i \ \sigma_{i,k}(q) \tag{3.3.8}$$

where $w_i \in \mathbb{C}$ has $|w_i| \leqslant 1$ and $\sigma_{p_i,k} = \sigma_{i,k}$. The following proposition will be used to show *any* sequence of sections constructed in this way asymptotically holomorphic.

Proposition 3.12. *With p_i and $N(k)$ as above and $q \in X$ fixed, given any $r \geqslant 0$ then for k sufficiently large there is a constant C independent of k such that*

$$\sum_{i=1}^{N(k)} d_k(p_i, q)^r \, e^{-d_k^2(p_i,q)} \leqslant C.$$

Proof. (Sketch) Recalling the definitions of $d_k(p_i, q)$ and $e_k(p_i, q)$, the above sum roughly has the form

$$\sum_{\psi_m} \sum_{i \in \Lambda(k)} |x_i - y|^r e^{|x_i - y|^2/5}$$

for fixed y, but there are finitely many ψ_m and the latter sum is bounded above (independently of k) by $\int |x - y|^r e^{|x-y|^2/5} dx$ which converges for all r. □

Using Proposition 3.12, one has

Proposition 3.13. *A sequence of sections s_k constructed as in (3.3.8) is asymptotically holomorphic.*

Proof. By Lemma 3.11, one has

$$||\overline{\partial}_J(s_k)||_{C^2} \leqslant \sum_{i=1}^{N(k)} |w_i| \, |\overline{\partial}_J(\sigma_{i,k})|_k \leqslant Ck^{-1/2} \sum_{i=1}^{N(k)} \left(d_k(p_i, q) + \ldots + d_k^\ell(p_i, q)\right) \, e^{-d_k^2(p_i,q)} \leqslant Ck^{-1/2}$$

by applying Proposition 3.12 for each $r = 1, \ldots \ell$. The other bound follows identically. □

3.4 Quantitative Transversality

This section discusses ε-transversality of section of L^k. These sections will be constructed by extending standard transversality techniques that will allow the careful choice of the coefficients w_i in $s_k = \sum w_i \sigma_{i,k}$. A main result discussed in this section, due also to Donaldson, is a quantitative version of Sard's theorem that is interesting in its own right.

Definition 3.14. *Let $U \subseteq \mathbb{C}^n$ be open. A map $f : U \to \mathbb{C}^m$ with $m \leqslant n$ is said to be ε-transverse to $w \in \mathbb{C}^m$ over U if at all points $z \in U$ with $|f(z) - w| < \varepsilon$, the derivative Df_z is surjective and satisfies $|Df_z| \geqslant \varepsilon$.*

An equivalent statement holds for sections of bundles with a connection ∇: a section s is said to be ε-transverse to 0 if at all points with $|s| < \varepsilon$, then $|\nabla s| \geqslant \varepsilon$. A crucial observation is that ε-transversality is preserved under C^1-closeness. That is, if s is ε-transverse to 0, and s' is another section (function) with $||s - s'||_{C^1} < \delta$, then s' is $\varepsilon - \delta$-transverse to 0.

The precise restatement of the condition "appropriate asymptotically holomorphic and ε-transversality estimates" that appeared in the statement of Theorem 3.7 can now be given.

Definition 3.15. *Fix an ω-compatible almost-complex structure J. Let $\mathcal{L}_k(J, C, \varepsilon)$ be the set of pairs of sections of L^k satisfying the following conditions.*

(I) *s_0, s_1 are asymptotically holomorphic with respect to J with (3.3.2) holding for the constant C.*

(II) *s_0 is ε-transverse to 0 as a section of L^k.*

(III) *(s_0, s_1) is ε-transverse to 0 as a section of $L^k \oplus L^k$.*

(IV) *The complex linear derivative ∂F of $F = s_1/s_0$ is ε-transverse to 0 over $X \setminus Z(s_0)$.*

Proposition 3.16. *For a fixed ω-compatible almost-complex structure J, and for sufficiently large k, there exist constants C, ε so that $\mathcal{L}_k(J, C, \varepsilon)$ is non-empty.*

To construct sections in $\mathcal{L}_k(J, C, \varepsilon)$, one begins with a section $s_k = \sum_i w_i \sigma_{i,k}$, which by the content of the previous section already satisfies (I), and modifies the coefficients w_i in stages so that at each stage the ε-transversality condition is satisfied on a larger subset of X. Consider the case of condition (II) first. Recall the p_i were the points around which $\sigma_{i,k}$ were centered. These cover X in an approximate lattice, and there are more of them for each k. The key point of the proof is that ε-transversality can be achieved by modifying the coefficients w_i in a finite number of stages that is *independent of* k. The following proposition gives a crucial partition of the p_i used throughout the remainder of the proof.

Lemma 3.17. *Given $D > 0$ there is a number $N(D)$ independent of k so that $\{p_i\}$ can be partitioned into $N(D)$ subsets $I_1, ..., I_{N(D)}$ such that*

$$d_k(p_i, p_j) \geqslant D \qquad p_i, p_j \in I_\alpha$$

for all α. In fact, $N(D)$ can be chosen to satisfy $N(D) \leqslant CD^{2n}$ for some constant C independent of k.

Proof. As in Proposition 3.12, the number of charts ψ_m is fixed independent of k, so it suffices to partition the lattice in the image of each chart ψ_m separately. Within each chart, let $D\Lambda(k)$ be D times the lattice $\Lambda(k)$. Then partition $\Lambda(k)$ by taking equivalence classes in $\Lambda(k)/D\Lambda(k)$, of which there are D^{2n}. Since there are finitely many charts $\{\psi_m\}$ the total number is bounded by CD^{2n} for some C independent of k. □

The tool that will allow a careful choice of w_i is Donaldson's quantitative extension of Sard's Theorem:

Theorem 3.18. (Donaldson, [31]) *Suppose f is a holomorphic map from the unit ball in $\mathbb{C}^n$ to the unit ball in $\mathbb{C}^m$ where $m \leqslant n$, and let $0 < \eta < 1/2$ and $0 < \gamma < 1$. For any $w \in \mathbb{C}^m$, there exists a $p \in \mathbb{N}$ so that the set*

$$U(f, \eta, w, \varepsilon) := \{w' \in B_\eta(w) \mid f \text{ is } \varepsilon\text{-transverse to } w' \text{ over } \frac{1}{2}B^{2n}\}$$

for $\varepsilon = \eta Q_p(\eta)$ where $Q_p(\eta) = \frac{1}{\log(\frac{1}{\eta})^p}$ has a connected component whose measure is at least γ times the measure of $B_\eta(w)$.

The classical Sard's theorem states that the derivative must be non-zero on a set of full measure. This theorem extends the result to say that for small $\varepsilon > 0$ the derivative must be greater than ε on a set of large measure. Of course, if in the statement of the theorem one demands transversality hold over a larger portion γ of the ball, the resulting p will increase, hence ε will decrease. The proof of Proposition 3.16 only relies on the existence of a single point in $B_\eta(w)$ where ε-transversality holds, but the full result is interesting in its own right. A full proof of the theorem is not given here. For a complete proof see [31]. Briefly, the proof uses the fact that holomorphic functions are well-approximated by polynomials, and then exploits the geometry of the zero-sets of complex polynomials.

Now the modification of s_k is carried out in stages, applying Theorem 3.18 at each stage. The process will have $N(D)$ stages in total. At each stage α for $\alpha = 1, ..., N(D)$, the section s_k is modified so that s_k becomes ε-transverse to 0 over I_α. It must also be modified in such a way that the transversality over

$I_1, ..., I_{\alpha-1}$ is not disrupted. Since there are *finitely* many stages (independent of k), at each stage α k, may be increased and $\varepsilon > 0$ may be decreased.

To describe the modification required at each stage α, is convenient to introduces the function $f_{i,k}$ on the balls B_i of d_k radius 1 around p_i so that $s_k = f_{i,k}\sigma_{i,k}$. Thus modifying $f_{i,k}$ to $f_{i,k} - \beta$ is equivalent to modifying the coefficient $w_i \mapsto w_i - \beta$.

By the product rule, one has

$$\nabla s_k = \nabla f_{i,k}\sigma_{i,k} + f_{i,k}\nabla\sigma_{i,k}.$$

Using this, one can show f must satisfy similar bounds to s_k, i.e. $||f||_{C^1(B_i)} \leqslant C, ||\overline{\partial} f||_{C^1(B_i)} = O(k^{-1/2})$. Moreover, using also the fact that $\sigma_{i,k}$ is uniformly bounded below on the balls B_i of unit g_k radius, one can show that s_k is ε-transverse to 0 over B_i if and only if $f_{i,k}$ is $C\varepsilon$-transverse to 0 for some C. It therefore suffices to choose the coefficients w_i so that $f_{i,k}$ is ε-transverse to 0 over B_i for all i at once, since B_i cover X by the discussion preceding Proposition 3.12.

Proceeding by induction, assume that the coefficients have already been modified so that s_k is $\varepsilon_{\alpha-1}$-transverse over $I_{\alpha-1}$ ($I_0 = \varnothing$ can be taken as the base case). Denote by $s_k^{\alpha-1} = \sum_i w_i^{(\alpha-1)}\sigma_{i,k}$ the section obtained after the first $\alpha - 1$ modifications, and let $f_{i,k}^{(\alpha-1)}$ be the corresponding function as defined above. Stage α of the modification is now performed as follows:

(1) There exists a $\delta_\alpha > 0$ such that if $|w_i^{(\alpha)} - w_i^{(\alpha-1)}| < \delta_\alpha$ then

$$||f_{i,k}^{(\alpha)} \ - \ f_{i,k}^{(\alpha-1)}||_{C^1(B_i)} \leqslant \frac{1}{2}\varepsilon_{\alpha-1}.$$

In fact, there is a constant $C > 1$ (independent of $k, \varepsilon_{\alpha-1}$) so that $\delta_\alpha = \frac{\varepsilon_\alpha}{C}$ works. Consequently, if the coefficients $w_i^{(\alpha)}$ are chosen with δ_α of $w_i^{(\alpha-1)}$, the functions $f_{i,k}^{(\alpha)}$ are still $\frac{1}{2}\varepsilon_\alpha$-transverse to 0 over B_i for $i \in I_1 \cup \ldots \cup I_{\alpha-1}$.

(2) By the elliptic theory of the $\overline{\partial}$ operator, $f_{i,k}^{(\alpha-1)}$ can be well approximated by a holomorphic function. In particular, there exists a holomorphic function $h_{i,k}$ so that the elliptic estimate:

$$||f_{i,k}^{(\alpha-1)} - h_{i,k}||_{C^1(rB_i)} \leqslant \tilde{C}||\overline{\partial} f_{i,k}^{(\alpha-1)}||_{C^1(B_i)} \leqslant \tilde{C}k^{-1/2}$$

holds.

(3) Apply Theorem 18 (with $m = 1$) to the holomorphic function $h_{i,k}$ (scaled so that it is a map between unit balls), and conclude there exists a v_i with $|v_i| < \delta_\alpha$ so that $h_{i,k}$ is $\delta_\alpha Q_p(\delta_\alpha)$-transverse to 0 over B_i. Equivalently, $h_{i,k} - v_i$ is $\delta_\alpha Q_p(\delta_\alpha)$-transverse to 0 over B_i.

(4) By **(2)**, once k is sufficiently large that $\tilde{C}k^{-1/2} < \frac{1}{2}\delta_\alpha Q_p(\delta_\alpha)$, then $(f_{i,k}^{(\alpha-1)} - v_i)$ is $\frac{1}{2}\delta_\alpha Q_p(\delta_\alpha)$-transverse to 0 over B_i. By increasing p, it can be assumed that $(f_{i,k}^{(\alpha-1)} - v_i)$ is $2\varepsilon_{\alpha-1}Q_p(\varepsilon_{\alpha-1})$-transverse to 0 over B_i. That is, increase p until $2\varepsilon_{\alpha-1}Q_p(\varepsilon_{\alpha-1})$ with the new p is less than $\frac{1}{2}\delta_\alpha Q_p(\delta_\alpha)$ with the old p.

(5) Now the careful partitioning of $\{p_i\}$ into $I_1, ..., I_{N(d)}$ comes into play. Because $\sigma_{i,k}$ falls off like $e^{-d_k^2(p_i,q)}$ away from p_i, modifying w_i by an amount less than δ_α results in a change in $f_{j,k}$ on the order of $\delta_\alpha e^{-D^2/5}$ for $j \neq i$ because distinct points of I_α are separated by at least D. More precisely, if

$$w_j^{(\alpha)} = \begin{cases} w_j^{(\alpha-1)} & \text{if } j \neq i \\ w_i^{(\alpha-1)} - v_i & \text{if } j \in I_\alpha \end{cases}$$

then for all $i \neq j$ one has

$$||f_{i,k}^{(\alpha)} - (f_{i,k}^{(\alpha-1)} - v_i)||_{C^1(B_j)} \leqslant C\delta_\alpha e^{-(D-2)^2/5} \leqslant C\varepsilon_{\alpha-1}e^{-(D-2)^2/5}.$$

(6) Consequently, provided the right hand side satisfies

$$C\varepsilon_{\alpha-1}e^{-(D-2)^2/5} \leqslant \varepsilon_{\alpha-1}Q_p(\varepsilon_{\alpha-1}) \tag{3.4.1}$$

then $f_{i,k}^{(\alpha)}$ is $\varepsilon_\alpha := \varepsilon_{\alpha-1}Q_p(\varepsilon_{\alpha-1})$-transverse to 0 over B_i for all $i \in I_\alpha$. It therefore suffices to show that for D sufficiently large, (3.4) is satisfied for each $\alpha = 1, ..., N(D)$, which is a question only about the sequence of real numbers ε_α. By choice of δ_α in **(1)**, the section s_k^α is ε_α-transverse to 0 over all B_i for $i \in I_1 \cup \ldots \cup I_{\alpha-1}$ as well, hence over all $I_1 \cup \ldots \cup I_\alpha$. At the end of the induction, one obtains a section s_k that ε-transverse to 0 everyone on X where $\varepsilon := \varepsilon_{N(D)}Q_p(\varepsilon_{N(D)})$ for the largest p used. This completes the construction of sections satisfying (I) and (II) of Definition 3.15.

For conditions (III) and (IV) of Definition 3.15 the argument is essentially identical, except more parameters must be kept track of. For (IV), since ∂F has n components, it must be modified in all components at once. Suppose s_0, s_1 satisfy conditions (I) and (II). Let

$$\sigma_{\pi,i} = \pi\sigma_{i,k}$$

where $\pi = \sum_\ell \pi_\ell z_\ell$ is a linear functional on $\mathbb{C}^n$. Without choosing coordinates π should be thought of as an element of $T^*X \otimes L^k$. Then consider perturbing s_1 by $\sigma_{\pi_i,i}$ for some vector π at each i so that in total

$$F = \sum_i \frac{s_1 + \sigma_{\pi,i}}{s_0}.$$

Here, the vectors $\pi_i \in \mathbb{C}^n$ play the role that $v_i \in \mathbb{C}$ did in the the modification of $s_k = \sum_i w_i\sigma_{i,k}$. One then proceeds by repeating steps **(1)-(6)**, now applying Theorem 3.18 with $m = n$ to find a vector π_i so that the addition of π_i in the definition of F achieves transversality over B_i. One can check, moreover, that this process can be done without disrupting the ε-transversality of s_1 itself. Condition (III) is again similar, but Theorem 3.18 is applied with $m = 2$. This completes the outline of the proof of Proposition 3.16.

3.5 Constructing Pencils

This section brings together the previous sections by giving a proof of Theorem 3.7, thereby completing the proof of Theorem 3.1. Theorem 3.7 can now be stated as:

Theorem 7: *Suppose $s_0^{(k)}, s_1^{(k)}$ are sequences of sections in $L_k(C, J, \varepsilon)$ for some fixed ω-compatible almost complex structure J and fixed constant C, ε. Then for sufficiently large k, $f = [s_0^{(k)}; s_1^{(k)}]$ can be modified so that it satisfies i) f is a topological Lefschetz pencil, and ii) F is approximately holomorphic except at its critical points.*

Since s_0 is asymptotically holomorphic and ε-transvsere, the zero set $Z(s_0)$ is a symplectic submanifold for k sufficiently large. As in Claim 3.7.1, in order to modify $f = [s_0; s_1]$ to be a symplectic Lefschetz pencil, it therefore suffices to modify F on $X \setminus Z(s_0)$. Two local modifications are required: first, it is necessary to modify F so that $|\overline{\partial}_J F| < |\partial_J F|$ everywhere and has non-degenerate critical points (with local holomorphic coordinates), second F must be modified in the neighborhood of base points so that the local model in the definition of topological Lefschetz pencil is satisfied.

For the first modification, the idea is to show that the problem region where $|\partial_J F| \leqslant |\overline{\partial}_J F|$ is localized around the critical points of F, and a modification can be performed in small neighborhoods of these points to resolve this. Thus let $\Gamma \subseteq X \setminus Z(s_0)$ be the set on which $|\partial_J F| \leqslant |\overline{\partial}_J F|$.

Lemma 3.19. *There exists a constant η so that if k is sufficiently large, Γ is contained in the region $\Omega_\eta = \{x \in X \mid |s_0| > \eta\}$.*

To show this, one computes the derivate of F and shows that if both s_1, s_0 are small, then the transversality condition (II) on the pair (s_0, s_1) as a section of $L^k \oplus L^k$ from Theorem 3.7 is violated, if s_0 is small but s_1 is large, then the transversality condition (I) on s_0 alone is violated.

By Lemma 3.19, Γ is bounded away from $Z(s_0)$, and it is defined by a closed condition, hence it is a compact subset of $X \setminus Z(s_0)$. Now denote by $\mathrm{crit}(F)$ the set of critical points, which by the transversality condition $|\nabla_X \partial_J F| > \varepsilon$ are isolated. Since $\mathrm{crit}(F)$ is automatically contained in Γ, it must therefore be a finite set.

Lemma 3.20. *There exists a constant ρ_0 independent of k so that for sufficiently large k the balls of radius ρ_0 centered on points of crit(F) are disjoint and contained in $\Omega_{\eta/2}$. Moreover, for any $\rho \leqslant \rho_0$, after increasing k sufficiently, the set Γ is contained in the union of the balls of radius ρ centered at the point of crit(F).*

Proof. (Sketch) This lemma follows essentially from the implicit function theorem. If x is a point of Γ, then $|\partial_J F| \leqslant |\overline{\partial}_J F| \leqslant Ck^{-1/2}$. Thus if k increases, $|\partial_J F| \to 0$. The transversality condition on $|\nabla_X \partial_J F| > \varepsilon$ ensures that the derivative of $\partial_J F$ is invertible and bounded away from 0. By the inverse function thoerem, ∂F is therefore a local diffeomorphism. One can check, by keeping track of constants in the standard proof of the inverse function theorem, that the local diffeomorphism must be defined on a neighborhood sufficiently large to contain a point $p \in \mathrm{crit}(F)$ i.e. there is a p such that $\partial_J F = 0$ near x. Increasing k further decreases $\partial_J F$, and the point must get closer to x. By choosing k sufficiently large, one can therefore ensures that each point $x \in \Gamma$ is within ρ of a point of $\mathrm{crit}(F)$, completing the lemma. □

At each $p \in \mathrm{crit}(F)$, one has the decomposition $\nabla(\partial_J F) = \partial_X(\partial_J F) + \overline{\partial}_X(\partial_J F)$. The first term is the complex linear part of the Hessian, i.e. a complex quadratic form on $T_p X$ which will now be denoted by H. In local coordinates centered at p, H can be written $H = \sum_{\alpha,\beta} H_{\alpha\beta} z_\alpha z_\beta$. Here, it can be shown that H must be non-degenerate as a complex form, since the transversality condition on $\nabla_X \partial F$ requires H and the anti-linear part part together by non-degenerate as a real form. One then takes a bump function β_p centered at p that is 1 on the ball of radius $\rho/2$ and compactly supported in the ball of radius ρ. Let $w' = F(p) + \delta$, and consider

$$\tilde{F} := \beta_p(w' + H(z)) + (1 - \beta_p)F(z)$$

Lemma 3.21. *For ρ sufficiently small, k sufficiently large, and δ sufficiently small compared to ρ, then on the ball of radius ρ, $\tilde{F}$ has a single critical point at p with local coordinates $(z_1, ..., z_n) \mapsto \sum_i z_i^2$ and satisfies $|\overline{\partial}_J \tilde{F}| < |\partial_J \tilde{F}|$ away from p.*

Proof. This is essentially just a calculation. See [31], Lemma 10. □

The modification of Lemma 3.21 is local, so can be applied separately for each $p \in \mathrm{crit}(F)$ to obtain a new map with isolated critical points conforming to the desired local model and $|\overline{\partial}_J \tilde{F}| \leqslant |\partial_J \tilde{F}|$ satisfied everywhere. Since these modifications are supported away from $Z(s)$, the extension of this map to one $\tilde{f} : X \setminus B \to \mathbb{C}P^1$ is still smooth. The only remaining issue is a local modification around points $b \in B$ that ensures the local model $(z_1, ..., z_n) \to z_1/z_2$ is satisfied there. The details of this final step are essentially linear algebra and are omitted here. Briefly, the proof of this amounts to linear algebra conditions on the symplectic form on the subbundle $TB \subseteq TX$. These conditions are achieved by maps arbitrarily close to f, so a modification of f can be achieved without disrupting the open condition that the tangent spaces of the fibers are symplectic. This completes the proof of Theorem 3.7, hence of Theorem 3.1.

3.6 The Converse Result

In this section, the following converse of Donaldson Theorem 3.1, originally due to Gompf, is proved:

Theorem 3.22. (Gompf, [35]) *Suppose that X is a 4-manifold equipped with a topological Lefschetz fibration $f : X \to S^2$. Let $[F_*] \in H_2(X; \mathbb{Z})$ be the fundamental class of the generic fiber of f. If $[F_*] \neq 0 \in H_2(X; \mathbb{Z})$, then X admits a symplectic structure. An analogous statement holds for Lefschetz pencils, but the homological constraint is automatically satisfied.*

This theorem has important consequences for studying symplectic geometry through Lefschetz pencils. First, it is a purely topological criterion for the existence of a symplectic structure on a 4-manifold, a

question usually in the realm of differential geometry. Second, this result suggests that, in spirit, the data of a symplectic structure and a Lefschetz fibration are equivalent. Using this, symplectic manifolds could, in principle, be classified completely in terms of Lefschetz pencils, and thereby in terms of monodromy in $Mod(F_*)$. This is investigated in greater detail in Section 3.7. First, for completeness, a sketch of the proof of Theorem 3.22 is given. For the detailed proof, there reader is referred to ([16] Theorem 10.2.18).

Proof. The proof relies on the construction of two separate 2-forms. A "vertical" form ω_V that will be non-degenerate on the fibers, and a "horizontal" form ω_H will be non-degenerate in the horizontal directions. Taking

$$\omega = \omega_V + \omega_H$$

will complete the proof. First, the vertical form is constructed.

Lemma 3.23. *There exists a closed, non-degenerate 2-form $\eta \in H^2(X;\mathbb{R})$ so that $\int_F \eta > 0$ for all fibers F.*

This follows immediately from the assumption that $[F_0] \neq 0$: let η be the Poincaré dual of $[F_0]$. The statement that the above integral is non-zero is exactly the conclusion of Poincaré duality. Notice that the singular fibers represent the same homology class as the regular ones, thus the evaluation there remains non-zero (integration taken over the non-closed surface with the critical points removed).

Next, the 2-form η is modified so that it is symplectic along the fibers (it is not, *a priori*, non-vanishing on them). This modification will be ω_V.

First, take a symplectic form ω_y on the fiber $f^{-1}(y)$ for each $y \in S^2$. In a neighborhood of the singularities, take the restriction of the standard form on $\mathbb{C}^2$ in the coordinates in which f has the form $(z_1, z_2) \mapsto z_1^2 + z_2^2$. Around each y, there is a neighborhood U_y such that $W_y = f^{-1}(U_y)$ retracts onto the fiber $f^{-1}(y)$. One obtains a local form ξ_y on each W_y that is the pullback of ω_y under this retraction. Take a finite subcover of the cover provided by the U_y, indexed by $i = 1, ..., n$. By scaling, it can be assumed that $[\xi_{y_i}|_{F_{y_i}}] = [\eta|_{F_{y_i}}]$ for all y_i, hence the difference vanishes in cohomology and so is exact. Let θ_i be so that $d\theta_i = \eta - \xi_{y_i}$ on W_{y_i}. Then, for a partition of unity ψ_i subordinate to U_{y_i} on S^2, one takes

$$\omega_V = \eta + d\left(\sum_i (\psi_i \circ f)\theta_i\right).$$

Now define the horizontal form $\omega_H = f^*(\omega_{S^2})$ for ω_{S^2} the volume form on the sphere. The following lemma then completes the proof.

Lemma 3.24. *The form $\omega := \omega_V + C\omega_H$ is a a symplectic form for sufficiently large $C \in \mathbb{N}$.*

Clearly, the form is closed since d commutes with pullbacks thus it is the sum of two closed forms. One then checks non-degeneracy in both the horizontal and fiber directions.

For the case of Lefschetz pencils, one blows up the initial pencil, keeping track of the information of the exceptional spheres which appear as sections on the fibration. One then repeats the proof and shows that by increasing C even more, these sections are symplectic submanifolds and the blow-down process can be done preserving the symplectic structure. In this case, each fiber intersects all the exceptional spheres non-trivially, hence it cannot be homologically trivial. □

In fact, the proof can be extended to show:

Theorem 3.25. (Gompf, [35]) *The symplectic form ω is canonical up to isotopy, i.e. any two variations on the construction result in symplectic forms connected by a path ω_t of symplectic forms. It is canonical in the sense that if $f : X \setminus B \to S^2$ is a symplectic Lefschetz pencil, applying Theorem 3.22 to the topological Lefschetz pencil underlying f reproduces the same form ω up to isotopy. Moreover, if $f, f' : X \to S^2$ are a pair of equivalent Lefschetz fibrations (in the sense of Theorem 1.45), then applying Theorem 3.22 results in isotopic symplectic forms.*

3.7 Asymptotic Uniqueness

Combined into a single statement, Theorem 3.1 and Theorem 3.22 yield:

Theorem 3.26 (**Donaldson, Gompf**). *Suppose X is a closed 4-manifold. Then X admits a symplectic structure if and only if it admits a topological Lefschetz pencil.*

As mentioned in the previous section, this result already hints that Lefschetz pencils could be used to give a classification of symplectic 4-manifolds in terms of the monodromy of their Lefschetz pencils. This section describes how such a classification could be formulated, and identifies some of the challenges arising in carrying out such a classification scheme. In particular, this involves precisely formulating a uniqueness statement for Lefschetz pencils constructed as in the proof of Theorem 3.1.

The notion of equivalence between different Lefschetz pencils on the same symplectic manifold is rather technical. This is because it is difficult to compare Lefschetz pencils constructed from approximately holomorphic sections s_0, s_1 of L^k for different k. For a fixed (X, ω), let $\mathcal{L}_k(J, C, \varepsilon)$ be as in Definition 3.15. The proof of Theorem 3.1 showed that for sufficiently large k, this set is non-empty, and for each pair the map $f = [s_0; s_1]$ can be modified so that it is a symplectic Lefschetz pencil.

First, one has the following notion of equivalence between topologically Lefschetz pencils.

Definition 3.27. *Two topological Lefschetz pencils $f_0 : X \setminus B_0 \to S^2$ and $f_1 : X \setminus B_1 \to S^2$ are said to be* **isotopic** *if there exist smooth isotopies $F_t : X \times I \to X$ and $\phi_t : S^2 \times I \to S^2$ such that:*

- *Both $F_0 : X \to X$, and $\phi_0 : S^2 \to S^2$ are the identity map.*
- *$F_1(B_0) = B_1$*
- *One has $f_1 \circ F_1 = f_0 \circ \phi_1$ as a map $X \setminus B_1 \to S^2$.*

In particular, two isotopic Lefschetz pencils have the same genus since F_1 takes fibers to fibers, and by Theorem 1.45 yield the same collection of Dehn twists in $Mod(S_g^p)$ up to simultaneous conjugation and Hurwitz equivalence (using Theorem 1.45 for pencils rather than fibrations).

The following result gives a uniqueness statement for Lefschetz pencils constructed as in the proof of Theorem 3.1, up to isotopy.

Theorem 3.28. Asymptotic Uniqueness (Donaldson, [31]) *Let ε, C be fixed and let J, J' be a pair of almost-complex structure on (X, ω). Suppose that $k_i \to \infty$ is an increasing sequence of integers and that for each i, there are symplectic Lefschetz pencils f_i, f_i' resulting from from modifying pairs of approximately-holomorphic sections in $\mathcal{L}_{k_1}(J, C, \varepsilon), \mathcal{L}_{k_1}(J', C, \varepsilon)$ respectively. Then for sufficiently large i, the pencils f_i and f_i' are isotopic.*

This uniqueness statement shows the construction in Theorem 3.1 was, in some sense, canonical, but is quite difficult to work with in practice because it does not provide a description of when two individual Lefschetz pencils are isotopic. Instead, one must consider pencils as part of a sequence of pencils for the increasing parameter k.

Despite this difficulty, the uniqueness theorem 3.28 can be used to give a rough idea of a correspondence between symplectic 4-manifolds and data in the mapping class group. The following discussion is meant to be an intuitive description of this correspondence. For a more technical description, the reader is referred to [36]. Ideally, one could hope to prove a correspondence, in the spirit of Theorem 1.45, that gives an equivalence

$$\left\{ \begin{array}{c} (X, \omega) \\ \text{compact} \end{array} \right\} \Big/ \sim \quad \Longleftrightarrow \left\{ \begin{array}{c} \text{monodromy} \\ \text{data} \end{array} \right\} \Big/ \sim \tag{3.7.1}$$

for two suitable notions of equivalence of the two structures. Here, symplectic manifolds are assumed to have the property, as in the hypotheses of Theorem 3.1, that the cohomology class $[\omega/2\pi] \in H^2(X;\mathbb{R})$ is the reduction of an integral class. The integral lift of $\omega/2\pi$ is denoted $h_\omega \in H^2(X;\mathbb{Z})$. The appropriate notion of equivalence of triples (X,ω,h_ω) is **symplectic isotopy**. That is,

$$(X,\omega,h_\omega) \sim (X',\omega',h'_\omega)$$

if there exists a diffeomorphism $f : X \to X'$ such that $f^*(\omega')$ is a symplectic form on X which is connected to ω through a smooth isotopy ω_t of symplectic forms. In particular a topological Lefschetz pencil $f : X \to S^2$ determines a canonical triple (X,ω,h_ω) up to this equivalence since the form constructed was unique up to isotopy Theorem 3.25. Moreover, if two topological Lefschetz pencils are isotopic as in Definition 3.27, then they determine isotopic symplectic forms (they are isotopic through the forms ω_t constructed by applying Theorem 3.25 to the isotopy of pencils $f_t := \phi_t \circ f_0 \circ F_t^{-1}$).

Now, an appropriate notion of equivalence of monodromy data is required. To each (X,ω,h_ω) one may associate an r-tuple of Dehn twists whose product is the identity in $Mod(S_g^p)$ by considering a Lefschetz pencil. Here, $Mod(S_g^p)$ is the mapping class group of the p-times punctured surface of genus g, where p is the number of points of the base locus. In light of Theorem 1.45 and its accompanying discussion, these tuples of Dehn twists should be considered up to simultaneous conjugation and Hurwitz equivalence. One must, however, also introduce an equivalence relation between this monodromy tuple and monodromy tuples that result from Lefschetz pencils built with different k, from which one obtains r'-tuples of Dehn twists in $Mod(S_{g'}^{p'})$ for r', g', p' not equal to r, g, p. It is therefore necessary to see how replacing a Lefschetz pencil obtained form a pair in $\mathcal{L}_k(J,C,\varepsilon)$ with a pencil obtained for a higher value of the parameter k affects the monodromy. Auroux and Katzarkov gave a topological operation that is equivalent to doubling k, resulting in a formula for the new monodromy.

Theorem 3.29. (Auroux, Katzarkov, [37]) *There exists a stabilization operation on Lefschetz pencils on a 4-manifold X. The stabilization of a Lefschetz pencil f of genus g with p base points and r critical points is a Lefschetz pencil of genus $g' = 2g + p - 1$ with $p' = 4p$ base points and $r' = 4(g + r - 1)$ critical points. The stabilization of f is denote $Sq(f)$.*

There is an explicit formula for the monodromy of $Sq(f)$ in terms of the monodromy of f, though the details are not necessary here [37]. Most importantly, this stabilization gives a topological realization of increasing the parameter k in the construction of symplectic Lefschetz pencils.

Theorem 3.30. (Auroux, Katzarkov, [37]) *Let $f : (X,\omega) \to S^2$ be a symplectic Lefschetz pencil obtained from a pair of approximately holomorphic sections in $\mathcal{L}_k(J,C,\varepsilon)$. Once k is sufficiently large, the monodromy of a pencil obtained from a pair in $\mathcal{L}_{2k}(J,C,\varepsilon)$ is the monodromy of $Sq(f)$ (modulo simultaneous conjugation and Hurwitz equivalence).*

This operation can be used to define an equivalence relation between monodromies that makes the equivalence in (3.7.1) precise. Let $D_{g,p,r}$ be the set of r-tuples of Dehn twists whose product is the identity in $Mod(S_g^p)$, considered up to simultaneous conjugation and Hurwitz equivalence. There is a map

$$Sq : D_{g,p,r} \longrightarrow D_{g',p',r'} \tag{3.7.2}$$

where g', p', r' are as in Theorem 3.29 that takes an r-tuple (which is necessarily the monodromy of *some* pencil by the discussion in Section 1.3) to the r'-tuple that is the monodromy of the stabilized pencil.

The total situation is now the following. For a triple (X,ω,h_ω), let f be a Lefschetz pencil (with g,p,r as before) constructed from a pair of approximately holomorphic sections in $\mathcal{L}_k(J,C,\varepsilon)$ for $k = 2^R$ for some $R \in \mathbb{N}$. Let $\Psi_R \in D_{g,p,r}$ be the r-tuple that is the monodromy of f. One then obtains a sequence of Lefschetz pencils f^ℓ for $\ell \geqslant R$, obtained from pairs of sections in $\mathcal{L}_{2^\ell}(J,C,\varepsilon)$. By Theorem 3.30, these have monodromies $\Psi_\ell = Sq^{(\ell-R)}(\Psi_R) \in D_{\hat{g},\hat{p},\hat{r}}$ where $\hat{g},\hat{p},\hat{r}$ are related to g,p,r by iterating the relations in Theorem 3.29. The stabilization process clearly does not alter the Euler characteristic $\chi = r - 2(2g-2)$ of total space of the Lefschetz pencil (as the total space is unchanged). The initial value of p, which depends on k and the homology class of the fiber, is related to the cohomology class h_ω.

Theorem 3.31. (Donaldson, Auroux, Katzarkov, Gompf, et al. [36]) *Let $\mathcal{X}_{\chi,h} = \{(X, \omega, h_\omega)\}$ be equivalence classes of compact symplectic 4-manifolds up to symplectic isotopy of Euler characteristic χ and $h_\omega = h$. Let $\mathcal{C}_{\chi,p_0}$ be the direct limit of the system of maps of sets (3.7.2) where the initial set has $p_0 = \varphi(h_\omega)$ for some fixed function $\varphi : H^2(X;\mathbb{Z}) \to \mathbb{Z}$. There is an inclusion*

$$Lef \colon \mathcal{X}_{\chi,h} \longrightarrow \mathcal{C}_{\chi,p_0}$$

that associates to each (X, ω, h_ω) (the image in the direct limit of) the monodromy Ψ_f for a symplectic Lefschetz pencil f constructed from a pair of section in $\mathcal{L}_k(J, C, \varepsilon)$ for sufficiently large k.

Proof. Suppose that (M, ω, h_ω) and (M', ω', h_ω) are not equivalent. If X is not diffeomorphic to X', then the monodromies of assoicated pencils cannot agree by Theorem 1.45, hence they are taken to different elements by Lef. In the case that $X = X'$ but $\omega \neq \omega'$, suppose, proceeding by contradiction, that they are mapped to the same. Then there exists a pair of symplectic Lefschetz fibrations f, f' on them constructed as in the proof of Theorem 3.1 with $k = 2^\ell$ for sufficiently large enough ℓ that have the same monodromy tuple in $C_{g,p,r}$ for some g, p, r. Theorem 3.25 ensures that the two symplectic forms, which are the symplectic forms canonically associated to X from the two Lefschetz fibrations, are isotopic. For the details involving how p_0 should relate to the cohomology class h_ω via the function φ, see [36]. □

It is expected, however, that a stronger statement is true:

Conjecture 3.32. *The map*

$$Lef \ : \ \mathcal{X}_{\chi,h} \longrightarrow \mathcal{C}_{\chi,p_0}$$

is a bijection.

This conjecture contains the added assertion that *every* topological Lefschetz pencil on X must necessarily arise as the element of a sequence constructed via Theorem 3.1. It is not at all obvious that this is the case.

The potential of Theorem 3.31 and Conjecture 3.32, should it be true, are significant. These results have reduced the question of the existence of symplectic structures on compact 4-manifolds to questions of pure topology. These results, however, also have significant limitations. First of all, the form of the uniqueness statement (Theorem 3.28) that necessitated the direct limit leaves the object $\mathcal{C}_{\chi,p_0}$ rather intractable. Second, although the question of the existence of symplectic structures has been reduced to pure topology, it is not at all straightforward topology. For high genus surfaces with many punctures, the mapping class group is an extremely complicated object, many aspects of which are still not well-understood. It is suspected, therefore, that significant new insight will be needed if this route is to truly deliver a classification of compact, symplectic 4-manifolds [36].

Even though a complete classification of compact symplectic manifolds using these ideas has remained elusive, Donaldson's theorem has had far-reaching consequences throughout symplectic and contact geometry and smooth topology (as will be seen in the next chapter). In the few years after Donaldson's theorem, these techniques were applied to give many useful constructions of symplectic invariants. The approximately holomorphic techniques developed in the proof were also extended to the odd-dimensional case of contact manifolds, where they were employed to prove many analogous results [38]. Most recently, Lefschetz fibrations have provided enormous insight and computational power in the study of the Homological Mirror Symmetry conjecture [26, 39, 40, 25]. In this last case especially, Lefschetz fibrations continue to produce deep and surprising results in symplectic geometry and their implications appear to be far from being exhausted.

Chapter 4

Broken Fibrations and Morse 2-functions

The existence of Lefschetz fibrations (pencils) on symplectic manifolds naturally led to the question of existence on first near-symplectic and then smooth manifolds. In these two cases, allowing only ordinary "Lefschetz singularities" is insufficient to guarantee the existence of a fibration, as if such a fibration existed, the total space would necessarily be symplectic by Theorem 3.22. It was discovered that considering new types of singularities allows some of the results of the previous chapters to be generalized to arbitrary smooth 4-manifolds. In particular, one must allow fibrations with "round singularities" whose critical locus can include an embedded 1-manifold, i.e. a union of disjoint circles. The existence and essentialness of such singularities therefore provides an obstruction to the total space being a symplectic manifold. In a similar way, (recall Remark 1.46) the number and monodromy of Lefschetz critical points can provide obstructions to the total space being a complex manifold. The question of existence of a Lefschetz fibration on smooth manifolds, and of the number and type of singularities that appear in such a fibration is therefore a question intrinsically linked to the topology and geometry of the manifold. In the last several decades, this link has been exploited to construct many interesting manifolds using Lefschetz Fibrations including ones with exotic smooth structures [41], and whose total space has no complex structure [21]. Much work has also been done, with varying success, to use Lefschetz fibrations to define invariants and show these invariants are independent of the fibration structure, hence depend only on the underlying manifolds.

This chapter is concerned mostly with the existence and uniqueness results of Lefschetz fibrations on smooth manifolds. Sections 4.1 and 4.2 of this chapter provide background and sketch a proof of the existence result. Section 4.3 develops Morse 2-functions, and Section 4.4 uses these to formulate the uniqueness result. The final section describes trisections of 4-manifolds, which are an example of a new potential source of invariants constructed from broken fibrations and Morse 2-functions.

4.1 The Near-Symplectic Case

Throughout this chapter let X (or X^4) denote a smooth, closed, orientable 4-manifold. Recall that a 4-manifold X is **near-symplectic** if it posses a closed 2-form ω such that $\omega^2 \geqslant 0$, and the set on which $\omega^2 = 0$ is an embedded submanifold of dimension 1. The existence of Lefschetz pencils structure on near-symplectic manifolds was shown by Auroux, Donaldson, and Katzarkov, using an extension of the approximately-holomorphic techniques from the previous chapter. This result constitutes an important intermediate step, both logically and historically, between the development of Lefschetz fibration structures on symplectic manifolds and on smooth manifolds. Here, however, the results are only mentioned briefly and the reader is referred to [42] for the details.

The Lefschetz pencil structure in this case will be slightly weaker than that in the symplectic case.

Clearly if the Lefschetz pencil here satisfied the same hypotheses as the symplectic case, Gompf's Theorem 3.22 would show the total space were truly symplectic rather than only near-symplectic. The Lefschetz pencils in the near-symplectic case will be called **singular** or **broken Lefschetz pencils**, and will include a second type of singularity besides the standard Lefschetz singularities modeled on $(z_1, z_2) \mapsto z_1^2 + z_2^2$.

Definition 4.1. *A map $f : X \to S^2$ has* **round** *or* **quadratic** *singularities along a 1-dimensional submanifold L if around each point of L there are local coordinates (t, x_1, x_2, x_3) in which f is locally modeled by*

$$(t, x_1, x_2, x_3) \mapsto (t, x_1^2 \pm x_2^2 - x_3^2).$$

The two main theorems of [42] are extensions of Theorem 3.1 and its converse, Theorem 3.22:

Theorem 4.2. (Auroux, Donaldson, Katzarkov) *Let (X, ω) be a near-symplectic 4-manifold so that ω^2 vanishes along an embedded 1-manifold $L \subseteq X$. Then there exists a map $f : X \to S^2$ such that f has round singularities along L and is a Lefschetz pencil on $X \setminus L$ whose fibers are symplectic submanifolds away from their singular points.*

Theorem 4.3. (Auroux, Donaldson, Katzarkov) *Let X be a 4-manifold equipped with a map $f : X \to S^2$ such that f has round singularities along a embedded 1-manifold $L \subseteq X$ and $f : X \setminus L \to S^2$ is a Lefschetz pencil. Suppose that there is a class $h \in H^2(X; \mathbb{Z})$ such that $h(\Sigma) > 0$ for every component Σ of every fiber of f. Then there exists a near-symplectic form ω on X that vanishes along L such that the fibers of f are symplectic submanifolds away from their singular points.*

The proof of Theorem 4.2 is long and quite technical, but the main idea is rather intuitive. Briefly, it is as follows. Given (X, ω), the construction of Chapter 3 can be repeated almost word for word to obtain a Lefschetz pencil away from a tubular neighborhood of L. On a tubular neighborhood $S^1 \times B^3$ of L, a theorem of Ko Honda [43] shows that there exists the following local model for the symplectic form. On $B^3 \times \mathbb{R}$ consider

$$\Omega = dQ \wedge dt + *(dQ \wedge dt)$$

where $Q(x_1, x_2, x_3) = x_1^2 - \frac{1}{2}(x_2^2 + x_3^2)$, and $*$ is the Hodge star in the standard metric. Quotienting by translation along $\mathbb{R}$ yields a model form Ω on $B^3 \times S^1$. Quotienting by both translation and changes of sign in the B^3 coordinates yields a similar model. The result of Honda shows that L always has a tubular neighborhood where the near-symplectic form has one of these local models. It is not hard to show in these models that $\Omega^2 = (4x_1^2 + x_2^2 + x_3^2)\, dx_1 \wedge \ldots \wedge dt$ vanishes exactly along $(0, t)$.

These local models around the vanishing set L of ω come equipped with the projection to $(-1, 1) \times S^1$ given by $(Q(x_1, x_2, x_3), t)$. Thus one can see that round singularities are defined exactly to be the singularities occurring in this local model. Now there are have two pieces of a Lefschetz pencil: one on a tubular neighborhood νL of the vanishing set of ω given in the local model, and one on $X \setminus \nu L$. The content of the proof of Theorem 4.2 is essentially showing that these two pieces can be patched together. This involves, for example, controlling the behavior of approximately holomorphic sections near the boundary.

4.2 Broken Lefschetz Fibrations

The results of Auroux, Donaldson, and Katzarkov naturally lead to the question of what types of fibrations exist for arbitrary (closed) smooth 4-manifolds. The investigation of the near-symplectic case demonstrates that for an arbitrary 4-manifold one cannot hope to find a fibration structure without allowing round singularities. One can hope, however, that passing from near-symplectic manifolds to arbitrary smooth manifolds does not require the addition of even more types of singularities. This turns out to be true. The existence of such fibrations can already be deduced for a large class of smooth manifolds. In particular, if X^4 is a manifold with a class $[a] \in H^2(X^4; \mathbb{Z})$ having self intersection $[a] \cdot [a] > 0$, then the result for a blow-up of X^4 can be deduced from Theorem 4.2 as follows. For such an X^4, Hodge theory guarantees the existence of a near symplectic form [44]. Choose such a form, apply the theorem to obtain a Lefschetz pencil structure, then forget the form, and blow-up the pencil to obtain a fibration. In this section, Lefschetz fibrations with

round singularities on smooth manifolds are investigated without homological restrictions or reference to the symplectic, near-symplectic, and approximately-holomorphic techniques used thus far.

One may consider fibrations of the following type. Recall that at each point of a smooth map $f : X \to Y$ one can consider the rank of Df, which for maps to S^2 is 0,1, or 2. The rank k locus of f is the set on which Df has rank k.

Definition 4.4. *A* **Broken Lefschetz Fibration** *(BLF) on a smooth 4-manifold X^4 is a map $f : X^4 \to S^2$ whose singular set satisfies the following:*

- *The rank 1 locus of f is an embedded 1-manifold (i.e. a link) $L \subseteq X^4$ whose image $f(L) \subseteq S^2$ is also an embedded 1-manifold, and at points of L there exist local coordinates in which f takes the form $(t, x, y, z) \mapsto (t, \ \pm x^2 \pm y^2 \pm z^2)$.*
- *$f : X^4 \setminus L \to S^2$ is a Lefschetz fibration, i.e. the rank 0 locus of f is a discrete set $A \subseteq X^4$ and around each point of A there exist coordinates in which f takes the form $(z_1, z_2) \mapsto z_1^2 + z_2^2$.*

Notice that at a point of L in coordinates of the above form, the rank 1 locus is $(t, 0, 0, 0) \to (t, 0)$. Thus along the rank 1 locus, f looks locally like a 1-parameter family of 3-dimensional critical points in Morse coordinates. In a slight abuse of terminology, both $L \cup A \subseteq X^4$ and $f(L \cup A) \subseteq S^2$ are called the **critical locus** of f, denoted $\mathrm{crit}(f)$. A single component of the link L will be referred to as a **"round singularity"**. An isolated critical point, which in the previous chapters was the only type of singularity, will now be referred to as a **Lefschetz singularity**.

Away from the critical locus, all points of S^2 are regular values hence the fibers are compact surfaces. A broken fibration is said to be **fiber-connected** if all the fibers are connected, and **indefinite** if each point of L is modeled on an indefinite (index 1 or 2) Morse singularity times an interval, i.e. the chart in Definition 4.4 takes the form $(t, x, y, z) \mapsto (t, x^2 \pm y^2 - z^2)$.

Consider, for a moment, the local behavior when crossing the critical locus at an indefinite round singularity. There are local coordinates in which the map f around the rank 1 locus takes the form $f(t, x, y, z) = (t, x^2 + y^2 - z^2)$ as a map $B^4 \to D^2$.

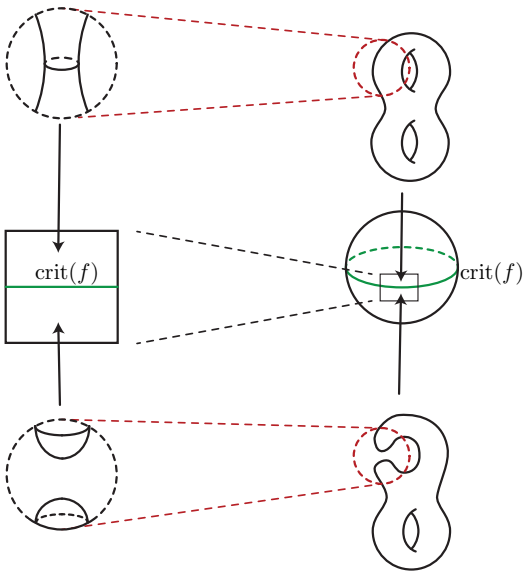

Figure 4.1: The genus of the fiber changing when crossing the critical locus both in the local model (left) and globally (right).

In these coordinates the horizontal axis $(t, 0)$ is the critical locus. In the upper half-plane the fiber in B^4 is the hyperboloid $x^2 + y^2 - z^2 = c$ (Figure 4.1 top left). Moving down, the fiber over $(t, 0)$ is the singular hyperboloid that is two cones put end to end. In the lower half plane the fiber in B^4 is $x^2 + y^2 - z^2 = -c$ which is a union of two disks (Figure 4.1 bottom left). When one considers a region in S^2 intersecting the critical locus as on the right, the $B^4 \subseteq X^4$ in the total space intersects each fiber in an open submanifold (with boundary) that is diffeomorphic to the fiber in the local model. Thus as one crosses the critical locus in S^2, the waist of a cylinder in the fiber of genus $g + 1$ (Figure 4.1 top right) contracts to a single point in a singular fiber above the critical locus, and then separates into two disks on the other side of the critical locus (Figure 4.1 bottom right). Thus **the effect of crossing an indefinite round singularity is to change the genus of the fiber by one**. If f is locally modeled on an index 2 critical point, the direction of the increasing genus is reversed.

Note 4.5. One should notice that a round-singularity has no well-defined index. If there exists a coordinate chart in which the fibration is given by an interval times a standard Morse critical point index k, given by $(t, x, y, z) \to (t, f(x, y, z))$ then composing the chart with the diffeomorphism of the plane $(x, y) \mapsto (x, -y)$ changes f to $-f$, giving a new chart in which the fibration is given by an interval times a standard index $4 - k$ critical point. This change of coordinates flips the coordinate box on the left in Figure 4.1 upside down, making the Morse function f valued on the y-axis turn into $-f$. Thus the index of a round singularity changes depending on which side one approaches it from. One can, however, refer to the index of critical points once a local coordinate chart is chosen, which specifies a single direction as"up". Crossing in direction of increasing genus, a round singularity is always an index 1 critical point, and crossing in the direction of decreasing genus it is index 2. Although the index is not well-defined, it can still be said a round-singularity is of index 0/3 (definite) or of index 1/2 (indefinite).

Examples

In some cases Broken Lefschetz fibrations can be constructed explicitly. The simplest example is constructed by gluing together three pieces. The three pieces are two caps $X^+ \simeq S^2 \times D^2$ and $X^- \simeq T^2 \times D^2$, and a middle piece $W \simeq C \times S^1$ where C is the standard cobordism between T^2 and S^2 which can be visualized as a solid torus with a ball removed (Figure 4.2(a)). W comes equipped with a projection to the annulus given by $(x, \theta) \mapsto (f(x), \theta)$ where $f : C \to [0, 1]$ is a Morse function on the cobordism C with a single critical point. A fibration can be built by gluing the two boundary components of W to the boundaries of X^+, X^- respectively.

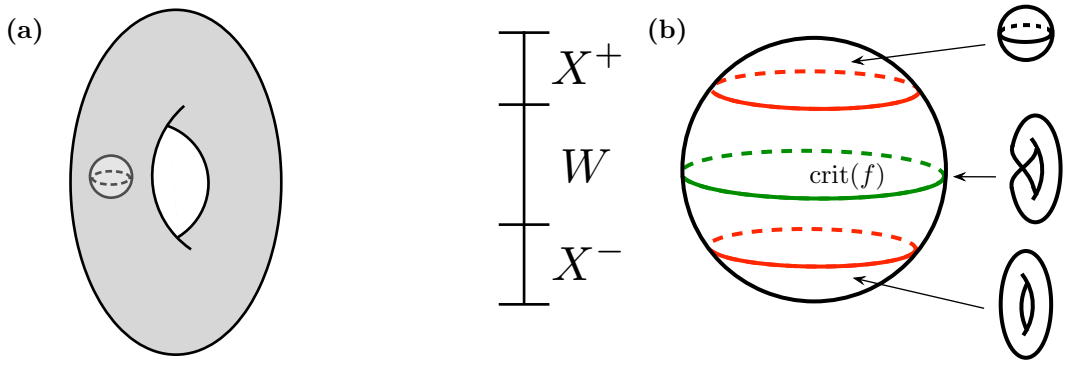

Figure 4.2: (a) the standard cobordism between T^2 and S^2. (b) a fibration obtained from gluing X^+ with its projection to the disk as the northern hemisphere, X^- over the southern hemisphere, and W over the annular region containing the equator. Gluing data must be chosen to glue along the latitudes indicated in red.

The gluing data required are two maps $S^1 \to \text{Diff}(S^2)$ and $S^1 \to \text{Diff}(T^2)$ that glue the fibers above the two circles where disks are glued to the annulus. Of course, the three pieces above and gluing data (up

to isotopy) specifies a 4-manifold uniquely (up to diffeomorphism), as does an analogous construction with multiple annular regions and gluing data. The trick is to know what manifold has been constructed.

Example 4.6. (Trivial Gluings) The simplest example is that when the gluing data is trivial. Even in this simplest possible case, it is quite tricky to identify the 4-manifold, which was originally done in [42]. The first step is to identify $X^- \cup_{id} W$ with a known space. The space turns out to be $S^1 \times S^3 \setminus L$ where $L \subseteq \theta_0 \times \{S^3\}$ is an unknot in S^3 for a fixed value of θ. To see this, consider $S^3 \to D^2$ the projection onto a plane in $\mathbb{R}^4$. Here, the fiber above each point of the interior is a circle, and the fibers above the boundary are single points. It is helpful to visualize composing with the projection of the outer annulus to its circle, to create a new representation of S^3 over the disk with fiber S^1 in the interior and fiber D^2 on the boundary. Taking the product with S^1 obtains $S^1 \times S^3$ projected to the disk with fiber T^2 in the interior and a solid torus on the boundary.

Let θ be a coordinate for the S^1 component, and L be an unknot projecting to the boundary that is transverse to fibers and whose value in the S^1 component is fixed at some θ_0. L intersects each solid torus fiber above the boundary in a single point. Removing a tubular neighborhood of L thus removes a ball from each solid torus, leaving the fibers above the boundary as the standard cobordism C. Extending the projection outward radially by the Morse function f on the cobordism C re-obtains the original abstract fibration $X^- \cup_{id} W$.

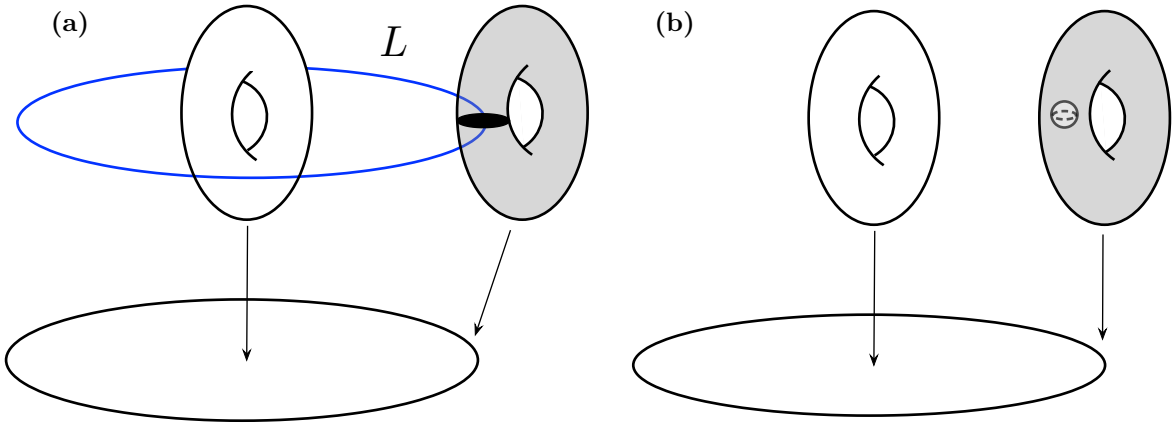

Figure 4.3: (a) A visualization of $S^1 \times S^3$ projected to the disk. Fibers in the interior are tori and fibers on the boundary are solid tori. In both, the "vertical" circle of the tori are the first factor in $S^1 \times S^3$. The knot L (blue) is constant in the S^1 factor and projects to the boundary ∂D^2. (b) the space after removing a tubular neighborhood of L.

To obtain a closed 4-manifold, one glues $S^2 \times D^2$ to the tubular neighborhood of L along their common boundary $S^1 \times S^2$. To see the resulting manifold, consider the decomposition $S^4 = (S^1 \times B^3) \cup_{id} (D^2 \times S^2)$. Gluing $S^1 \times B^3$ to the boundary of $X^- \cup_{id} W$ and $D^2 \times S^2$ to the boundary of X^+ realizes S^4 as a "bridge" between the two pieces, hence the effect of the gluing is connect summing and one concludes the total space where all gluing data is trivial is $(S^1 \times S^3)\#(S^2 \times S^2)$ [42].

Example 4.7. (DAK 4-sphere) If a non-trivial gluing is used, one can obtain the much more familiar manifold S^4. This presentation of the sphere is originally due to Donaldson, Auroux, and Katzarkov. Consider the gluing map of $T^2 \times S^1$ to itself that twists once around one of the loops of T^2. In coordinates, (s, t) on T^2 and φ on S^1 the map is given by $(s, t, \varphi) \mapsto (s, t + \varphi, \varphi)$.

To see the resulting total space, one repeats the construction of $X^- \cup W$ with a new gluing map. The gluing is chosen to rotate once around the coordinate of the S^1 factor of $S^1 \times S^3$. Rotating the boundary T^2 of the solid torus once while circling around the disk, however, is the same as rotating the knot L that was removed. Thus with the new gluing, L twists once around the S^1 factor as it goes around the boundary

of the disk. L then intersects the S^3 factor once for each $\theta \in S^1$, so the effect of removing the tubular neighborhood of L is now to remove a ball from $\{\theta\} \times S^3$ for each $\theta \in S^1$. The resulting total space is $S^1 \times B^3$ with a broken fibration over the disk. Gluing this to X^+ by the identity map on the common boundary $S^1 \times S^2$ is exactly the decomposition $S^4 \simeq (S^1 \times B^3) \cup_{id} (S^2 \times D^2)$.

Example 4.8. (Broken Fibrations on $M \times S^1$) The above presentation of $S^1 \times B^3$ as a broken fibration over the disk allows one to easily give a broken fibration on $M \times S^1$ for any closed 3-manifold M. Let $f : M \to [0,1]$ be a Morse function on M and define a fibration to the annulus by $(x, \theta) \mapsto (f(x), \theta)$. A round singularities appears in the annulus for each critical point of f. See Figure 4.4 (a).

For ε sufficiently small that there are no critical points within ε of the absolute maximum and minimum of f, the preimages $f^{-1}[0, \varepsilon)$ and $f^{-1}(1-\varepsilon, 1]$ are diffeomorphic to B^3. Thus the pre-images of tubular neighborhoods of the boundary circles of the annulus are diffeomorphic to $S^1 \times B^3$. Removing these pre-images and gluing in the fibration of $S^1 \times B^3$ (that was one of the two pieces used to make S^4 in the previous example) over the disk results in a broken fibration over S^2. In this case, a parameterized version of the Morse Lemma can be used to obtain the coordinate charts in the definition.

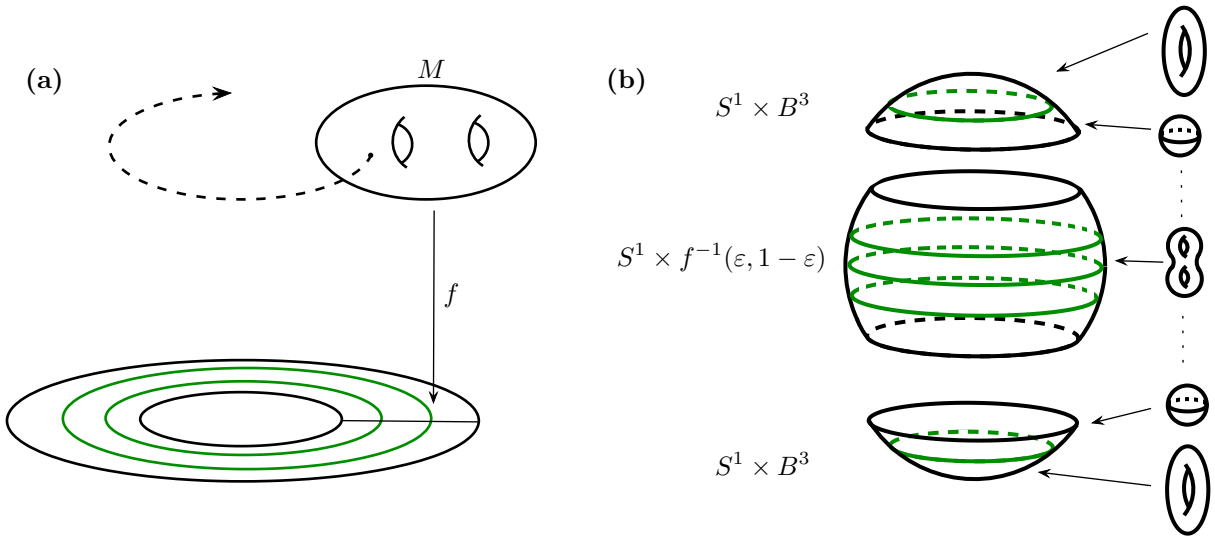

Figure 4.4: (a) a broken fibration of $M \times S^1$ over the annulus with round singularities indicated (green). (b) a broken fibration of $M \times S^1$ over the sphere with the fibers in different regions indicated. Disks around the north and south poles are the fibration on $S^1 \times B^3$. The middle region has a round singularity for each critical point of f (green), and the fibers can be surfaces of higher genus.

Example 4.9. (Definite Singularities) Definite singularities in a broken fibration, i.e. ones whose index in coordinates is 0 or 3, can be rather cumbersome. In particular, they can result is disconnected fibers, and region of S^2 where the fiber is empty. Consider, for a simple example, a three manifold $M = M_1 \sqcup M_2$ that has two connected components each of which is a closed 3-manifold. Let $f : M \to \mathbb{R}$ be a Morse function so that $f^{-1}[0,1] = M_1$ and $f^{-1}[2,3] = M_2$. Consider the same construction as the previous example (4.8) giving a broken fibration of $M \times S^1$ over S^2. In this case, a region around the equator has two round singularities of index 0/3. Along a longitude, these are the maximum on M_1 and the minimum on M_2 (or the reverse in the opposite direction). Along annular regions of increasing latitudes, the fiber is first S^2, then it is empty, then it is again S^2. In particular, there is an annular region with the empty fiber, after which an index 0 critical point begins a new component of the manifold. To avoid situations like this, the condition of being fiber connected and having only indefinite (index 1/2) round singularities is often imposed on broken fibrations.

Handle Attachments

In Section 1.3 a method to obtain a handle-body decomposition from a Lefschetz fibrations was described. In that case, the construction began with the trivial bundle $S_g \times D^2$ of the genus g surface over the disk, and each time the base was expanded to include another Lefschetz singularity, the total space changed by attaching a 2-handle to the vanishing cycle. In the case of broken fibrations, the change to the total space when expanding a fibration to include a round singularity can be described in terms of "round handle attachments".

Definition 4.10. *A* **round k-handle** *on an n-manifold X is a copy of $S^1 \times (D^k \times D^{(n-1)-k})$ attached via a gluing map $S^1 \times \partial(D^k \times D^{(n-1)-k}) \to \partial X$.*

Thus a round k-handle looks like the product of S^1 with a k-handle of one dimension lower. Expanding a Lefschetz fibration to include a round singularity changes the total space by adding a round handle. To see this, take a broken fibration over a disk, and consider extending it by attaching a fibration $f : X \to S^1 \times [0,1]$ over the annulus which contains a single round singularity at $S^1 \times 1/2$. For now, say the inner boundary of the annulus is the lower genus fiber F_g. For each fixed $t \in S^1$, the pre-image of the ray (t, r) for $r \in [0,1]$ is a cobordism C_t between F_g and the high-genus fiber F_{g+1}. The restriction of the fibration to the r-coordinate is a Morse function $f|_t : C_t \to [0,1]$ and has a single (index 1) critical point at $r = 1/2$. In fact, restricting the coordinate chart around the round singularity in which the fibration takes the form $f(t, x, y, z) = (t, x^2 + y^2 - z^2)$ to fixed t gives Morse coordinates on the cobordism. By standard Morse theory, the cobordism C_t is constructed from the product $F_g \times [0,1]$ by attaching a 3-dimensional 1-handle to a pair of points in the the fiber above $r = 1/2 - \varepsilon$ for some small ε. This occurs for all $t \in S^1$, thus the total effect is to add a round 1-handle attached to a pair of knots (K_1, K_2) each of which is a section of the fibration over S^1, i.e. each is transverse to fibers and wraps once around the annulus. The knots (K_1, K_2) intersect each cobordism C_t in the descending sphere of the single critical point of $f|_t$. The story is the same for a round singularity of index 2 (moving outwards) on the annulus: a round 2-handle is attached to the S^1 family of descending spheres. A round 2-handle, however, is just an upside-down round 1-handle, so most of the time it is only necessary to consider round 1-handles.

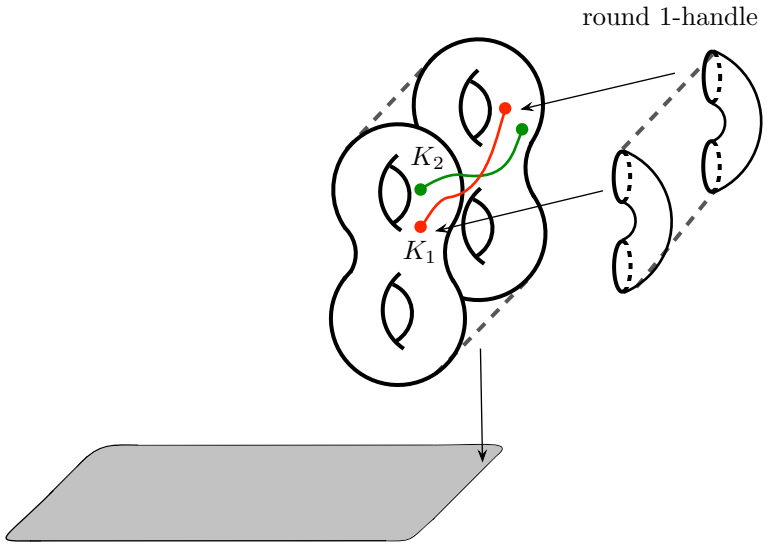

Figure 4.5: A round 1-handle attached to the boundary of a broken fibration along a pair of knots K_1, K_2 (red, green). Along each perpendicular ray, a 3-dimensional 1-handle is attached in the fiber to the intersection of the fiber with K_1, K_2, which is the descending sphere of the Morse function $f|_t$.

Round handle attachments can also be expressed in terms of standard handle attachments. Attaching a round 1-handle is equivalent to attaching a single 4-dimensional 1-handle and a single 4-dimensional two handle. They are attached as follows: first, specify a point on each of (K_1, K_2) and attaches a one handle to these two points making a "bridge" between the two knots, as in Figure 4.6(b). One then attaches the two handle so that the attaching sphere travels around both K_1 and K_2 passing over the bridge twice to go between them. One must remember, however, that the two knots may twist around each other as they go around, which specifies a framing for the two handle.

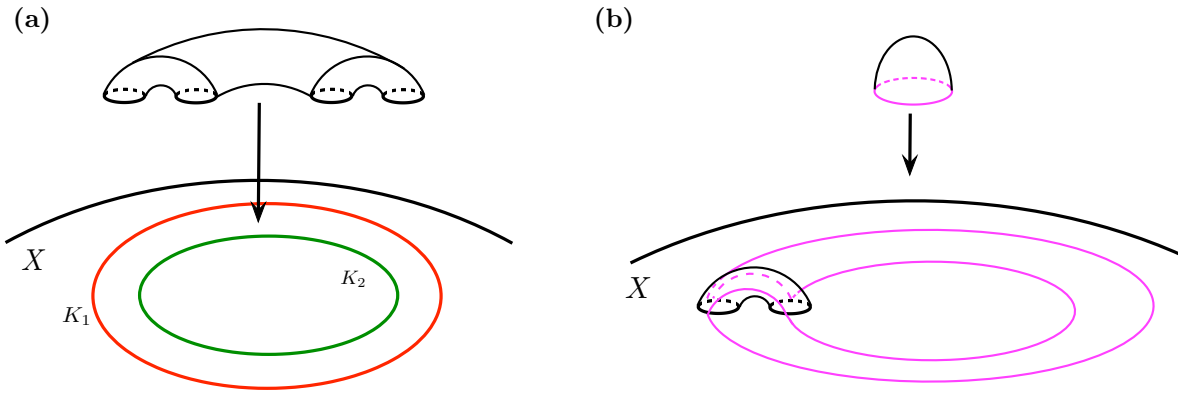

Figure 4.6: (a) Attaching a round 1-handle to a pair of knots K_1, K_2 (red, green). (b) the result of (a) is the same as attaching a 1-handle bridging the two knots and a single 2-handle running along both (magenta).

.

The Existence Theorem

The existence of broken Lefschetz fibrations on closed orientable 4-manifolds was originally proved by Kirby and Gay [45], and later strengthened by Lekili [46].

Theorem 4.11. (Kirby, Gay, Lekili) *Every closed, oriented 4-manifold admits a broken Lefschetz fibration.*

The approach of Kirby and Gay was to construct a broken Lefschetz fibration on a handle-body presentation of a 4-manifold. Briefly, their proof goes as follows.

Let X be a compact 4-manifold, and consider a handle-body decomposition. Let $X^{(1)}$ be the union of B^4 and the 1-handles of X. This 1 handle-body, which is diffeomorphic to $S_g \times D^2$ for some surface S_g of genus g, can be given a Lefschetz fibration over the disk by the projection. One can show that, in general, a broken Lefschetz fibration can be extended over an attached round 1-handle. Recall the above discussion that a round 1-handle can be thought of as a pair of a 1-handle and a 2-handle. The trick is to perform all 2-handle attachments as part of such a pair. Suppose, then, that H is a 2-handle attached to $\partial X^{(1)}$ along a framed knot L. To write H as part of a round handle pair, introduce a canceling 1-2 handle pair near L where the two handle of the pair is attached in a fiber with a framing -1 relative to the fiber (recall the discussion preceding Proposition 1.42). Push L over the 1-handle of the canceling pair so that an arc of L comes out the other side, as in Figure 4.7(b). The result is the same as attaching a round handle along the pair of knots that are L and an unknot nearby, and then attaching the two handle from the canceling pair, as in Figure 4.7(c). The fibration can be extended over the round 1-handle with a round singularity, and over the -1-framed 2-handle with a standard Lefschetz singularity. Introducing a canceling pair of critical points for every 2-handle thus allows one to perform each 2-handle attachment as part of a round 1-handle pair.

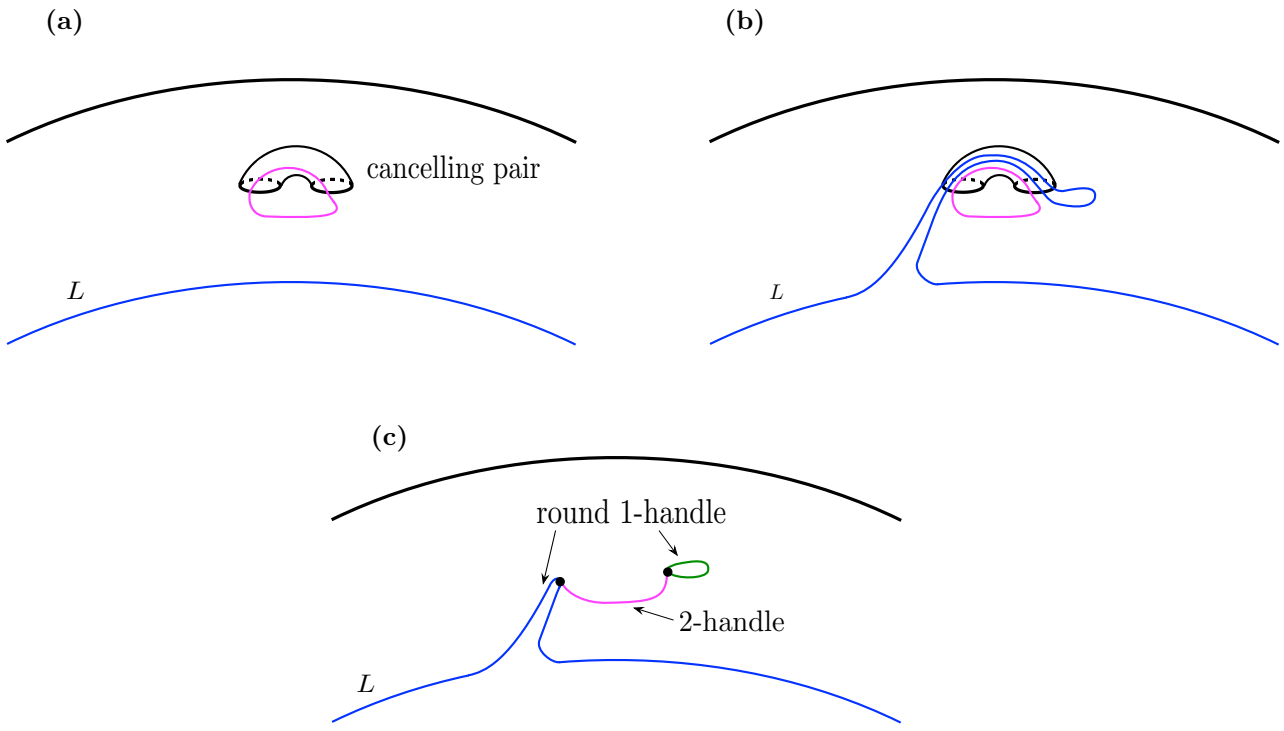

Figure 4.7: (a) attaching a cancelling pair near the knot L (blue). (b) pushing L over the 1-handle of the cancelling pair. (c) the same handle attachments with L now the 2-handle of a round handle pair (blue, green). The remaining 2-handle (magenta) runs over the 1-handle of the round handle pair.

Similar to $X^{(1)}$, there is a fibration over the disk of the handle-body consisting of the union of the 3 and 4-handle of X. These two handle-bodies can be glued along their boundaries to give a complete broken Lefschetz fibration. The details of the proof in many places involves keeping track of the structure of an open book decomposition on the boundary in which the handle attachments occur, and extending this structure over those attachments. For the gluing of the two pieces along their boundaries, some there are subtleties about contact structures on the boundaries that come into play.

Remark 4.12. One should note that Theorem 4.11, in contrast to the existence theorems for symplectic and near-symplectic manifolds, guarantees the existence of a true fibration on X^4, rather than a pencil.

Remark 4.13. The original theorem of Kirby and Gay in fact proves the existence of fibrations allowing"achiral Lefschetz singularities" which are isolated critical points locally modelled on $(z_1, z_2) \mapsto \overline{z}_1^2 + z_2^2$. Thus they consider "broken achiral Lefschetz fibrations" allowing all three types of singularities. It was later proved by Lekili [46] that achiral singularities can be transformed into round and (chiral) Lefschetz singularities by a certain homotopy, thus reducing to the case of (chiral) broken Lefschetz fibrations. An alternative existence proof by Akbulut and Karakurt [47] constructs BLFs on handle-bodies similar to the approach of Kirby and Gay but eliminates the need for achiral singularities from the start.

4.3 Morse 2-functions

Given the above existence theorem for broken Lefschetz fibrations, it is natural to ask when two such fibrations describe the same 4-manifold. Ideally, one would have a correspondence akin to that of Theorem 1.45 giving a correspondence between diffeomorphism classes of 4-manifolds and broken Lefschetz fibrations up to some equivalence. The uniqueness theorem in the next section, due also to Kirby and Gay [48], will

give a result of this form, though not as strong as Theorem 1.45. It turns out that a new but related type of map $X^4 \to S^2$ called a Morse 2-function provides the most natural formulation of the uniqueness theorem. This section, therefore, serves as a primer on Morse 2-functions.

Example 4.8 in the previous section and the local model for round singularities in the definition of broken fibration (Definition 4.4) suggest that considering broken fibrations as local 1-parameter families of Morse functions is a useful perspective. This perspective is already implicitly present in the work of Auroux, Donaldson, and Katzarkov [42], and Kirby and Gay [45], but was first truly exploited by Lekili when considering homotopies of broken Fibrations [46] to remove achiral singularities. Williams [49] extended this result to prove a first uniqueness theorem for broken fibrations. Building on the work of Lekili and Williams, Kirby and Gay isolated the idea of fibrations that are locally families of Morse function, dubbing them Morse 2-functions [48]. Thus Morse 2-function are historically dependent on Lefschetz fibrations, but not logically so since they are defined and studied completely in terms of classical Morse theory and singularity theory that have been well-known for decades. With the language of Morse 2-functions, Kirby and Gay were able to elegantly phrase and strengthen the uniqueness theorem of Williams.

First, it is necessary to recall some known results about homotopies of Morse functions.

Theorem 4.14. (Cerf) *Let $f_1, f_2 : X^4 \to [0,1]$ be two Morse functions with distinct critical values whose gradient flows with respect to a fixed metric g are Morse-Smale. Then there exists a homotopy $f_t : X^4 \times [0,1] \to [0,1]$ between them such that f_t is Morse with distinct critical values and whose gradient flow with respect to g is Morse-Smale at all but finitely many times $t_i \in [0,1]$. Moreover, at these times $t_i \in [0,1]$, only the following behaviors can occur:*

- *(Birth-death) A canceling pair of critical points is born or cancels resulting in a non-Morse function with a single degenerate critical point at $t = t_i$.*
- *(Crossing) Two distinct critical values cross, resulting in a Morse function with non-distinct critical values at $t = t_i$.*
- *(Handle-slide) A flow-line between two critical points of the same index appears at $t = t_i$, resulting in a Morse function whose gradient flow is not Morse-Smale.*

In the third point, such a value t_i results in a handle-slide of the handles of the critical points in question (see [16] Chapter 4-5 for a detailed exposition of handle-slides). The action of such a homotopy can be conveniently visualized by plotting the critical values as a function of t, as shown in Figure 4.8. Such a picture is known as a **Cerf Graphic**. In the graphic, births and deaths appear as left or right cusps respectively, and crossings appear as crossings. Handle-slides must be labelled specifically in the graphic, as no behavior on critical values indicates when one has occurred.

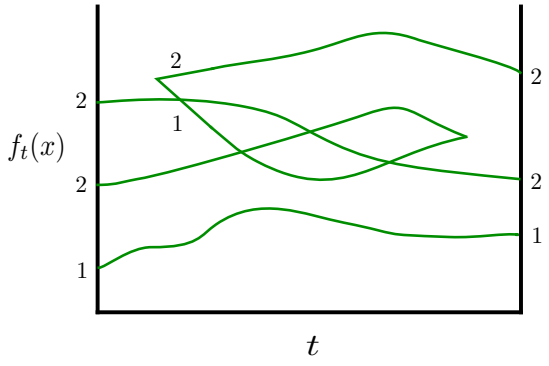

Figure 4.8: A Cerf graphic with critical values (green) labelled with their indices. The horizontal axis is the parameter t, and the vertical axis is the value of the Morse function.

It is helpful to think of this theorem as being a "transversality condition" within the space of smooth functions $C^\infty(X)$. It is well-known that Morse function (with Morse-Smale gradient flows and distinct critical values) form an open, dense set of $C^\infty(X)$. One can imagine the subset on which these are not satisfied as a codimension 1 subset of $C^\infty(X)$. This statement is deliberately left imprecise, as it is only meant to provide intuition. A homotopy f_t is just a path $[0,1] \to C^\infty(X)$ and the above theorem asserts that it can be chosen transverse to this codimension 1 subset, so that it intersects only at finitely many points. This picture moreover suggests that in fact a generic path should satisfy the conditions of Theorem 4.14, and this can be formulated and proved rigorously (although the proof is omitted here).

Theorem 4.15. *Given two Morse functions f_0, f_1 as in Theorem 4.14, there is an open and dense subset of the space of paths $\{g_t : I \to C^\infty(X) \mid g_0 = f_0 \ , \ g_1 = f_1\}$ whose endpoints are f_1, f_2 such that the conclusion of Theorem 4.14 holds.*

Definition 4.16. *A homotopy for which the conclusion of Theorem 4.14 holds is called a* **generic homotopy of Morse functions**.

Now, Morse 2-functions can be defined precisely. Intuitively, these are functions to surfaces that look locally like generic homotopies of Morse functions.

Definition 4.17. *A* **Morse 2-function** *is a smooth map $f : X^4 \to \Sigma$ for some surface Σ (possibly with boundary) such that the following to conditions hold.*

- *$Df \in Hom(TX^4, f^*T\Sigma^2)$ is tranvsere to the rank 0 and 1 loci, thus by counting dimensions the rank 1 locus is an embedded 1-manifold in X^4 and the rank 0 locus is empty.*
- *At each point $p \in \Sigma$ there is a coordinate neighborhood $U \simeq I \times I$ such that $f^{-1}(U) \simeq I \times M^3$ for a 3-manifold M^3 and in these coordinates f takes the form $(t, x) \mapsto (t, f_t(x))$ where f_t is a generic homotopy of Morse functions on M^3.*

As in the case of broken fibrations, the rank one locus (and its image in Σ) is called the critical locus and denote $\text{crit}(f)$. In contrast to broken Lefschetz fibrations, although the critical locus is still embedded in X, the image in Σ need not be. In general, it will be a complicated tangle of immersed circles with cusps and crossings. Most often, Morse 2-functions to $\Sigma = S^2$ are considered, but at times it is also useful to consider the cases of $\Sigma = D^2$ or $I \times I$.

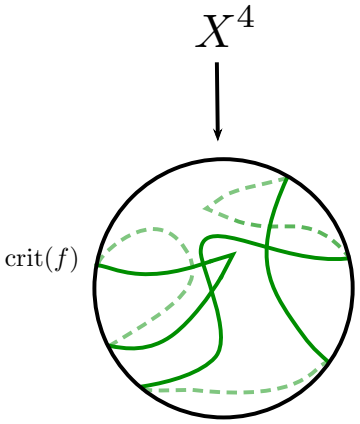

Figure 4.9: A Morse 2-function to S^2 with the critical locus shown (green).

The behavior when crossing the critical locus in the case of Morse 2-function is rather more complicated than in the case of broken fibrations. As in that case, the components of the critical locus do not have a well-defined index, but the index is still well-defined after specifying a normal direction. The adjectives

fiber-connected and indefinite apply to Morse 2-functions as well, meaning the fibers are all connected and the critical locus is absent of index 0/3 components respectively. In each region enclosed by the critical locus, the fiber is a fixed closed surface. If a Morse 2-function is fiber-connected, the fiber in each region can be specified by a labelling of the genus. Across each indefinite component of the critical locus, the genus changes by one. More specifically, an indefinite Morse 2-function has the following local behaviors near cusps, crossings, and embedded regions of the critical locus.

(Embedded regions) Near a point $x \in \text{crit}(f)$ that is neither a cusp nor crossing, there is a local coordinate chart, as in the definition, so that f is modeled by a generic homotopy of Morse function $(t, x) \mapsto (t, f_t(x))$ where $f_t(x)$ has a single critical point. By a parameterized version of the Morse Lemma, one can show there is a coordinate chart in which f takes the form $(t, x_1, x_2, x_3) \mapsto (t,\ x_1^2 \pm x_2^2 - x_3^2)$. The local behavior near x is therefore identical to the case of a Broken Lefschetz fibration: the genus changes by exactly 1 when crossing $\text{crit}(f)$. Crossing $\text{crit}(f)$ in the direction from which the critical locus appears as index 1 always increases the genus. In this direction, the higher genus fiber is obtained from the lower genus one by attaching a 1-handle to a pair of points; in the opposite direction the lower genus fiber is obtained by collapsing a simple closed curve in the fiber. In a coordinate chart $(t, x) \mapsto (t, f_t(x))$, this pair of points and simple closed curve are the ascending and descending spheres f_t respectively. By a slight abuse of terminology, the simple closed curve that collapses is called the **vanishing cycle** at x. See Figure 4.10(a).

(Cusp regions) Near a point $x \in \text{crit}(f)$ where a cusp occurs, there are local coordinates in which f looks like a generic homotopy of Morse functions with a birth-death occurring. Standard singularity theory [48] can be used to show this guarantees the existence of local coordinates in which f takes the form:

$$(t, x_1, x_2, x_3) \mapsto (t, x_1^2 + x_2^3 \pm (t - t_0)x_2 - x_3^2).$$

Locally, the cusp appears as a pair of index 1 and 2 components of crit(f) that meet and annhilate. Because moving into the region enclosed by the cusp must be an index 1 crossing for exactly one of these components, the region inside the cusp is always the region of higher genus. Near the cusp, there are two distinct vanishing cycles for the two components of $\text{crit}(f)$. In a local Cerf graphic $(t, x) \mapsto (t, f_t(x))$, these are the ascending sphere of the index 1 critical point and the descending sphere of the index 2 critical point of the canceling pair. The two vanishing cycles therefore have a single transverse intersection (see Figure 4.10(b)), as this must be the case for the ascending and descending spheres of a canceling pair.

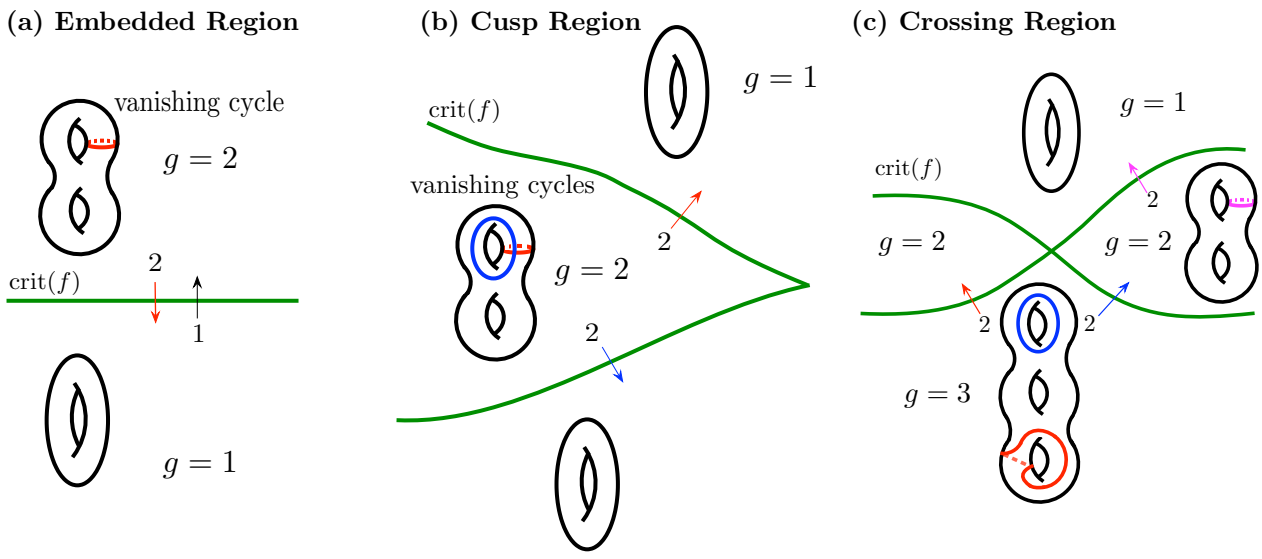

Figure 4.10: The behavior in the three types of regions of the critical locus (green). The genus in each region is labelled. Crossing the critical locus in an index 2 direction decreases the genus by collapsing a vanishing cycle. Vanishing cycles collapse when moving out of high genus region along arrows of the same color.

(Crossing regions) Near a point $x \in \text{crit}(f)$ that is a crossing, a neighborhood in S^2 is separated into four quadrants. One can check the several possible combinations the indices of the two components of $\text{crit}(f)$ that cross to show that at each crossing the four quadrants have genus $g, g+1, g+1$ and $g+2$, with the lowest and highest genus regions being opposite. Moving out from the highest genus region, the vanishing cycles toward the two sides of the crossing need not agree. See Figure 4.10(c).

There is an important subtlety regarding vanishing cycles. Since a Morse 2-function is locally a generic homotopy of Morse functions, handle slides can occur at various isolated points in $\text{crit}(f)$ throughout S^2. The effect of a handle slide is to alter the descending sphere (vanishing cycle) of a critical point by sliding over another (see [16] Chapter 4-5). Since in a Cerf graphic, nothing about the behavior of the critical values can indicate when a handle-slide has occurred, there is no indication from $\text{crit}(f) \subseteq S^2$ when a handle-slide occurs either. It is therefore false, for example, that the vanishing cycle exiting a region at one point must be the same as the vanishing cycle exiting at a nearby point, even if no cusps or crossings occur in between.

Examples

Example 4.18. Any broken fibration with no Lefschetz singularities is automatically a Morse 2-function. In particular, Examples 4.6-4.8 from Section 4.2 are all as such. A standard Lefschetz fibration, however, is a broken fibration but not a Morse 2-function since the rank 0 locus is non-empty.

Example 4.19. (More 2-functions on Cobordisms) A cobordism X between two three-manifolds M_1, M_2 admits a Morse 2-function to the square $I \times I$. Suppose for a second, the cobordism were trivial $I \times M$. Then one could take a generic homotopy of Morse function $f_t : M \to I$ and define $f : I \times M \to I \times I$ by $f(t,x) = (t, f_t(x))$ so that critical locus of f appears in $I \times I$ as the Cerf graphic of f_t. The case where X is a non-trivial cobordism is similar, except the Cerf graphic will have vertical tangencies. In general, if one has a Morse 2-function f on some 4-manifold to $I \times I$, it is possible to check by computing derivatives in the local model guaranteed by the definition, that the projection $\pi \circ f$ to the horizontal coordinate is itself a Morse function, and the critical points occur exactly at the vertical tangencies (see Figure 4.11). One can therefore construct a Morse 2-function on a Cobordism X as follows. Take $g : X \to [0,1]$ a Morse function. This will be the horizontal. Each fiber $M_t := g^{-1}(t)$ is a 3-manifold. Let $f_t : M_t \to I$ be a Morse function on the fiber. It is possible to extend the family f_t to the singular fibers to obtain a smooth function $f : X \to I \times I$ such that the projection to the horizontal is $\pi \circ f = g$ and $f = f_t$ on each level set M_t. The result is that the critical locus of f in $I \times I$ looks like a Cerf graphic for values of t in between the critical values of g, with a vertical tangency appearing at each such critical value, as shown in Figure 4.11.

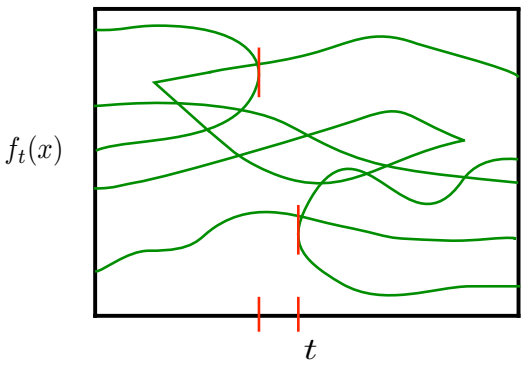

Figure 4.11: The image of a Morse 2-function $f : X \to I \times I$ as in Example 4.19. The vertical tangencies, which are the critical values of the projection $\pi \circ f$, are indicated (red).

Example 4.20. Similar to the case of Cobordisms, a Morse 2-function on an arbitrary 4-manifold X^4 to S^2 can be constructed from the data of a Morse function on X^4 and a Morse function on every level set. Roughly, this process goes as follows (see [50] for the details). First, a Morse 2-function to the plane is

constructed, then it is corrected to one to S^2. Let $g : X^4 \to [0,1]$ be a Morse function with ordered critical values, say $t_1, ..., t_m$. This copy of the interval will be the x-axis in the plane. The fiber $g^{-1}(0)$ is just a point, and projects to the leftmost point in Figure 4.12(a). For $t \in [0, t_m)$ the fiber $g^{-1}(t)$ is a copy of S^3, and can be given a Morse function with exactly 2 critical values. Passing an index 1 critical value t_i changes the fiber of g by attaching a 4-dimensional 1-handle, and the fiber becomes $S^1 \times S^2$, which can be given a Morse function with a single critical point of each index 0,1,2,3. As in the case of cobordisms, the critical point of g appears as a vertical tangency. Continuing this process, one obtains a Morse 2-function of the 1 handle-body of g as in Figure 4.12(a) with one vertical tangency for each index 1 critical point of g.

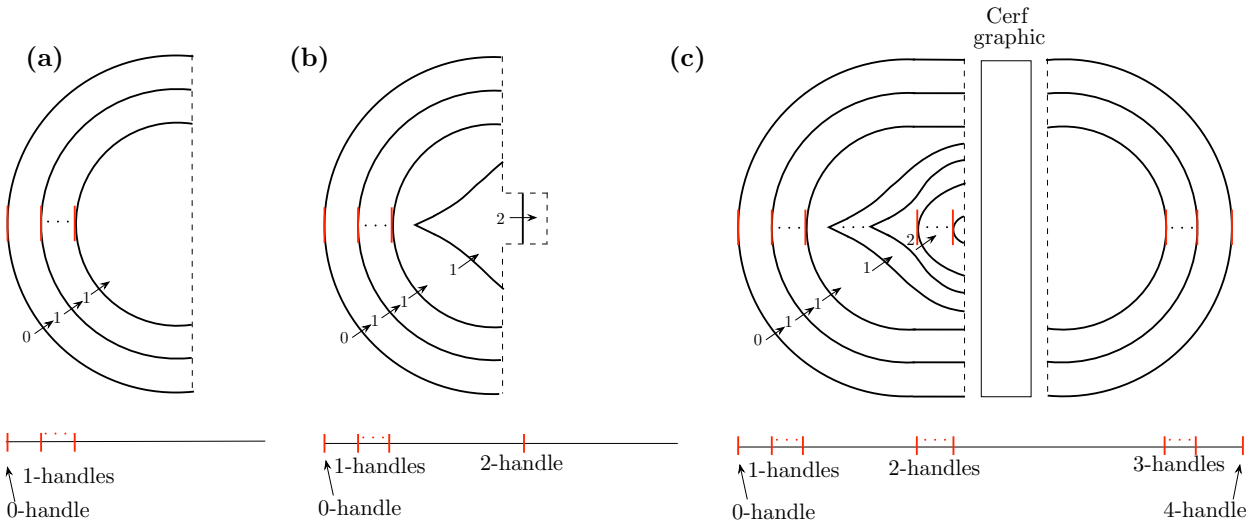

Figure 4.12: The construction of a Morse 2-function to the plane as in Example 4.20. (a) shows the critical locus of f on the 1 handle-body. In (b), a single 2-handle is attached. In (c), all the 2-handles have been attached and the 3 and 4 handle-body in joined on the right.

The next step is to extend the Morse functions on the fibers over the index 2 critical points of g. Attaching a 4-dimensional 2-handle is the same as attaching an interval times a 3-dimensional 2-handle. Thus the 2-handle attachments can be made in this way, and the projection extended over them in a small rectangular offshoot as in Figure 4.12(b). The one subtlety here is that one wants the attaching cirlce to lie in a surface that is a level-set of the vertical Morse function on the rightmost fiber. In the surface the attaching circle may a priori have self-crossings, but this can be avoided by introducing a canceling 1-2 handle pair for each index 2 critical point of g. These canceling pairs appear as arcs with left cusps in Figure 4.12(b). Once all the 2-handles are attached, one obtains a Morse 2-function on the 2-handle-body whose boundary $g^{-1}(t')$ has a fixed Morse function, h'. Then, the same construction as for the 1-handles can be applied to $-g$ to obtain Morse 2-function on the 3 and 4 handle-body of X, whose boundary $g^{-1}(t')$ has a Morse 2-function h''. By choosing a generic homotopy between the Morse functions h', h'' on $g^{-1}(t')$, the two pieces can be joined be a Cerf graphic as in Figure 4.12(c). This gives a Morse 2-function to the plane. To correct this to a Morse 2-function to S^2, notice the outermost ring of the critical locus is index 0 moving in (since the fiber is empty in the outer region of the plane), hence as in Example 4.8, an $S^1 \times B^3$ neighborhood of the outer ring can be removed and replaced with the broken fibration of $S^1 \times B^3$ over the disk used Examples 4.7 and 4.8. This results in a Morse 2-function to the 2-sphere.

Remark 4.21. It is interesting to note there is a clear similarity between the definition of a Morse 2-function and that of a Lefschetz bifibration. One difference is that a Lefschetz bifibration $f : X \to \mathbb{C}^2$ as formulated in Chapter 2 has a second projection of the base to a copy of $\mathbb{C}$, giving a "preferred" direction in along the fibers of this second projection. This was also present in Example 4.20 when the base was simply the disk, as the horizontal projection was a normal Morse function. By either requiring a Morse 2-function to come with a second map $\pi : S^2 \to [0,1]$ so that the composition $\pi \circ f : X^4 \to [0,1]$ is also Morse, or removing the

second map π from the definition of Lefschetz bifibration would allow one to formulate a slight variant on these two structures so that the definitions are identical, up to replacing "smooth" with "holomorphic".

Remark 4.22. It is at first, perhaps, tempting to think that a diagram of S^2 decorated with an immersed link containing only cusps and crossings and with each region labelled with a genus for the fiber above that region specifies a 4-manifold. This is false, and would be akin to a manifold being specified by drawing the interval $[0,1]$ marked with the critical points of a Morse function. In both cases, gluing data is required. In order to reconstruct a closed 4-manifold from the critical locus of a Morse 2-function, one must specify both a genus and gluing data across the boundary of each region. Even then, it is not the case every collection of such data specifies a 4-manifold. The question of what data is needed to reconstruct a closed 4-manifold from the critical locus of a Morse 2-function is answered completely in [51].

4.4 Uniqueness of Broken Lefschetz Fibrations

This section combines the two previous sections to formulate the existence theorem for broken fibrations in terms of Morse 2-functions. This result is rather more complicated than Theorem 1.45, which can be thought of as a uniqueness theorem for standard Lefschetz fibrations, for the following reason. When considering two different broken fibrations that might have the same total space, the critical loci can look very different in S^2, making it not obvious when two are "the same". This problem was hardly present in the case of true Lefschetz fibrations, since isolated points in S^2 can always be rearranged by isotopy. Thus up to an isotopy of S^2 any two true Lefschetz fibrations with the same number of critical points have effectively the same critical locus. In contrast, two broken Lefschetz fibrations can have the same number of components of the critical locus in X^4, but different arrangements of the components that are not isotopic through embedded links in S^2. It is therefore necessary to consider homotopies of broken Lefschetz fibrations that re-arrange the critical locus through functions whose critical locus is not embedded. This naturally leads to Morse 2-functions.

The structure of a Morse 2-function also appears naturally from Lefschetz singularities when considering homotopies of broken fibrations. Lefschetz singularities, while stable under complex perturbations, degenerate into a Morse 2-function configuration under *real* perturbations. Consider the following perturbation of the local model for a Lefschetz singularity:

$$f_s(z_1, z_2) = z_1^2 + z_2^2 + sRe(z_1).$$

Or in real coordinates $z_1 = x + iy$, $z_2 = z + iw$,

$$f_s = (x^2 - y^2 + z^2 - w^2 + sx, 2xy + 2zw).$$

For $s = 0$ the critical locus is the isolated Lefschetz singularity. For $s > 1$, the critical locus degenerates into a circle which projects to a 3-cusped curve as shown in Figure 4.13. To see this, note the differential is

$$Df_s = \begin{pmatrix} 2x+s & -2y & 2z & -2w \\ 2y & 2x & 2w & 2z \end{pmatrix}.$$

For $s > 0$ the differential has rank 1 only where both $w = z = 0$ and the determinant of the first block vanishes, i.e. where $4x^2 + 4y^2 + 2xs = 0$. The solution set can be parameterized by θ as $(-\frac{s}{4}(1 + \cos(\theta)), \frac{s}{4}\sin(\theta), 0, 0)$. The critical locus in S^2 is therefore parameterized by $(\frac{s^2}{16}\frac{(1+\cos\theta)^2}{2} - \frac{s^2\sin^2\theta}{16} - \frac{s^2}{4}(1 + \cos\theta)), -\frac{s^2}{8}\sin\theta(1 + \cos\theta))$ which is the 3-cusped curve in Figure 4.13. It is possible to show, that this three-cusped curve is stable under real perturbations.

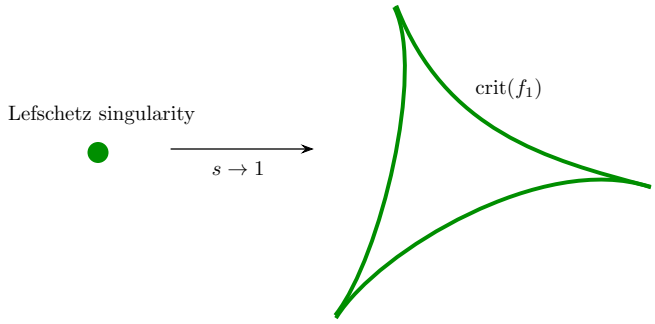

Figure 4.13: Perturbing a Lefschetz singularity.

Akin to the definition of generic homotopies of Morse function, one can define a homotopy of Morse 2-functions to be one that looks locally like a 2-parameter family of Morse functions.

Definition 4.23. *Given two Morse 2-functions $f_1, f_2 : X^4 \to S^2$, a* **homotopy of Morse 2-functions** *is a homotopy $f_s : X^4 \to S^2$ so for each point $p \in S^2$ there exists a neighborhood $U \simeq I \times I$ around p so that $f^{-1}(U) \simeq I \times M^3$ for some 3-manifold M and in coordinates the homotopy is given by*

$$(t, x) \mapsto (t, f_{t,s}(x)) \tag{4.4.1}$$

where f_t for $t \in [0, 1]$ is a generic homotopy of Morse functions for all but finitely many s.

A homotopy of Morse 2-functions is therefore locally just a 2-parameter family of Morse function. One can visualize such a homotopy as a "movie" of Cerf graphics. As s evolves from 0 to 1, the Cerf graphic for $f_{0,t}$ evolves into one for $f_{1,t}$. Each Cerf graphic has a finite number of cusps, crossings, and handle slides. If the two have different numbers of these events, then there must be values of s at which cusps, crossings, or handle slides appear. These are the values of s_0 at which the family $f_{s_0,t}$ is *not* a generic homotopy of Morse functions.

The following is an extension of Cerf's theorem to the 2-parameter case.

Theorem 4.24. (Cerf) *Let $f_{0,t}$ and $f_{1,t}$ be generic homotopies of Morse functions on a closed manifold M. There is an open dense subset of $\{g_{s,t} : I \times I \to C^\infty(X) \mid g_{0,t} = f_{0,t}$ and $g_{1,t} = f_{1,t}\}$ such that for all but finitely many $s_i \in [0, 1]$, the $g_{s,t}$ is a generic homotopy of Morse functions for $t \in [0, 1]$. Moreover, at these finitely many values of s_i only following six events (and their reverses) may occur (shown in Figure 4.14).*

- *(Reidemeister 2 Crossing) Two components of the critical locus that are disjoint at $s = 0$ meet at s_i and have two crossings for $s > s_i$.*
- *(Reidemeister 3 Crossing) A component of the critical locus moves past a crossing of two other components, passing through it at exactly $s = s_i$.*
- *(Legendrian Reidemeister 1 Crossing) A cusp pushes across a component of the critical locus, touching it at exactly $s = s_i$.*
- *(Merge) Two canceling components of the critical locus come together at $s = s_i$, pinching into two cusps for $s > s_i$.*
- *(Eye Birth/Death) Two new canceling components of the critical locus are born for $s > s_i$.*
- *(Swallowtail Birth/Death) Two canceling components are born at $s = s_i$. For $s > s_i$ one of the pair goes on to cancel an existing component.*

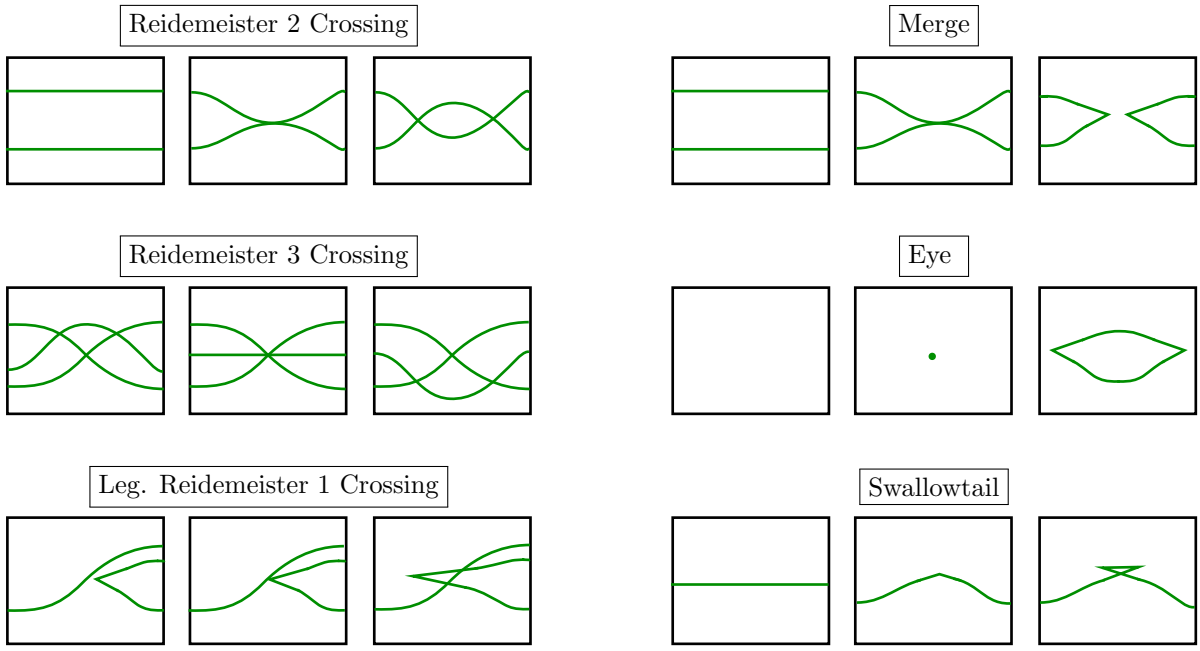

Figure 4.14: The six ways a two-parameter homotopy $f_{s,t}$ can fail to be a generic homotopy for some value $s_i \in [0,1]$. For each event, Cerf graphics of $f_{s,t}$ are shown for fixed $s < s_i, s = s_i$ and $s > s_i$. The first three moves are named because they mimic the Reidemeister moves of knot theory.

Once again, it is helpful to image this theorem as a transversality condition in $C^\infty(X)$. One can imagine the complement of the Morse functions (with Morse-Smale gradient flows and distinct critical values) as a codimension 1 subset of $C^\infty(X)$. Again, this statement is deliberately left imprecise, and only serves to provide intuition. Within this codimension 1 set, there is a higher codimension 2 set of functions that , that are "more" non-Morse. For example, functions with three critical points having the same critical value. With a 1-parameter family of Morse functions, these points are avoided generically. With a 2-parameter family this is no longer the case, and these higher codimension singularities occur at points (s,t) that prevent $g_{s,t}$ from being a generic homotopy of Morse functions for every fixed s.

Definition 4.25. *A 2-parameter family of Morse 2-functions as in Theorem 4.24 is said to be* **generic 2-parameter homotopy of Morse functions**. *Thus a homotopy of Morse 2-functions as in Definition 4.23 is locally a generic 2-parameter homotopy of Morse functions.*

The following theorem is a uniqueness theorem for Morse 2-functions, which will be used momentarily to formulate the uniqueness theorem for broken Lefchetz fibrations.

Theorem 4.26. (Kirby-Gay) *Let $f_0, f_1 : X^4 \to S^2$ be Morse 2-functions. If f_0, f_1 are in the same homotopy class, then there exists a homotopy of Morse 2-functions between them. If f_0, f_1 are both indefinite and fiber connected, then it can be arranged that f_t is indefinite and fiber connected for each t. In particular, the critical locus evolves by a sequence of the moves listed in Theorem 4.24.*

The full proof is given in [48]. While the proof involves nothing more than carefully considering homotopies of Morse functions and the singularities that appear therein, there are many details that must be addressed. Roughly the proof is carried out as follows. First, the theorem is proved locally on $I \times M^3$ with a Morse 2-function that is globally $(t, f_t(x))$ for f_t a generic homotopy of Morse functions on M. In that case, a homotopy of Morse 2-functions exists by Theorem 4.24, and in fact a generic homotopy will be as such. The difficult lies in the second statement, which requires eliminating the definite critical points at each t. Once the local result is proved, a local to global argument is used to prove the result for Morse 2-functions on S^2.

When considering this in the context of broken Lefschetz fibrations, this gives an analogous uniqueness result. In the case of a broken fibration, a small perturbation will immediately cause the broken fibration to degenerate into a Morse 2-function as in Figure 4.13, after which the above theorem will apply. The existence and uniqueness theorems for broken fibrations are summarized in the following theorem.

Theorem 4.27. (Existence and Uniqueness of Broken Lefschetz Fibrations) *Let $[f] \in [X^4 : S^2]$ be a smooth homotopy class of maps. Then $[f]$ can be realized as an indefinite, fiber-connected broken Lefschetz fibration. Moreover, for any two broken Lefschetz fibrations $f_0, f_1 \in [f]$ there is a smooth homotopy $f_t : X^4 \times [0,1] \to S^2$ between them that is a Morse 2-function for all but finitely many values $t \in [0,1]$ (two of which are the endpoints). In particular, after Lefschetz singularities are perturbed as in Figure 4.13, the critical loci $crit(f_0)$, and $crit(f_1)$ differ by a sequence of the moves listed in Theorem 4.24.*

Note the existence statement here asserts the existence of a broken fibration in every homotopy class. This stronger assertion actually follows from the proof of Theorem 4.11, as was first pointed out by Williams in [49]

Theorem 4.27 combines the strongest results on the existence and uniqueness of Lefschetz fibrations known to date in the most general possible case. For several years, research focused on obtaining these results. Now the focus has shifted towards the ultimate goal of using these results to study invariants of smooth 4-manifolds. As mentioned in the introduction to this chapter, several invariants have already been formulated using broken Lefschetz fibrations. Most notably, Tim Perutz introduced invariants of broken fibrations in [52, 53] which he conjectures are the Seiberg-Witten invariants of the underlying 4-manifold. Research in this area continues, using broken Lefschetz fibrations and Morse 2-functions to study invariants of 4-manifolds and to define new invariants altogether. It is hoped that, in the coming years, these ideas will provide new insight into the topology of 4-manifolds.

4.5 Trisections

This section describes a new potential source of 4-manifold invariants resulting from Morse 2-functions. This potential source is a method of decomposing a 4-manifold into three diffeomorphic pieces. These decompositions, which are akin to 3-dimensional Heegaard splittings, are called trisections. It is hoped that they will provide new invariants of smooth 4-manifolds, although so far none have been found definitively. In a larger context, trisections provide an example of how broken Lefschetz fibrations and Morse 2-functions can be applied to study the topology of 4-manifolds. The idea of trisections as they appear in this section is a recent development due mainly to Rob Kirby and David Gay [54].

Heegaard Splittings of 3-manifolds

It will be informative to briefly review the notion of Heegaard splittings on 3-manifolds, since trisections are a quite direct generalization to the 4-dimensional case. For a more detailed explanation of Heegaard splittings, the reader is referred to [55]. As always, all manifolds in this section are closed and oriented.

Definition 4.28. *A* **Heegaard Splitting** *of a 3-manifold M is a decomposition $M = M_1 \cup_\Sigma M_2$ into two submanifolds such that*

$$M_i \simeq \natural^k (S^1 \times D^2)$$

is a solid genus k handle-body, and the two share a common boundary surface $\Sigma \simeq \#^k (S^1 \times S^1)$, called the **Heegaard surface** *of the splitting.*

Choosing diffeomorphisms $\psi_i : M_i \to \natural^k (S^1 \times D^2)$ allows one to express M (up to diffeomorphism) as two genus k handle-bodies glued along their boundary. That is, a Heegaard splitting gives a decomposition

$$M \simeq \natural^k (S^1 \times D^2) \cup_\varphi \natural^k (S^1 \times D^2)$$

where the gluing map is $\varphi = \psi_2^{-1} \circ \psi_1|_{\partial M_1}$. As with all gluings, isotopic gluing maps result in diffeomorphic manifolds.

Example 4.29. The 3-sphere S^1 has a Heegaard splitting

$$S^3 \simeq (S^1 \times D^2) \cup_\varphi (S^1 \times D^2)$$

where $\varphi : T^2 \to T^2$ is (up to isotopy) the diffeomorphism that flips the generators of $H^1(T^2; \mathbb{Z})$. To see this, consider $S^3 \subseteq \mathbb{R}^4$ and project to an $\mathbb{R}^2$ plane. The image is the unit disk D^2 in the plane. The fibers over the interior points of D^2 are circles and the fibers over the boundary are points. Composing with the projection $S^1 \times [1/2, 1] \to S^1 \times \{1/2\}$ on the outer annulus gives a presentation of the 3-sphere above the disk $D^2_{1/2}$ of radius $1/2$ whose fibers above the interior are circles, and whose fibers above the boundary are solid disks. Thus the pre-images of both $\partial D^2_{1/2}$ and the interior are solid tori. These two solid tori are glued along their boundary, and together form S^3. This is called the "standard splitting" of S^3. It can be visualized in $S^3 = \mathbb{R}^3 \cup \{\infty\}$ by taking a solid torus encircling the z-axis, and tube passing through the center of it, that connects at ∞ to form a solid torus.

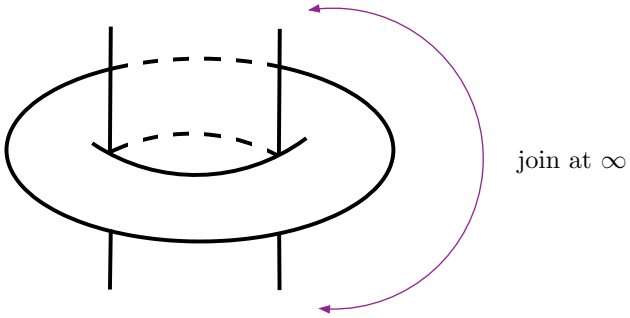

Figure 4.15: A visualization of the standard Heegaard splitting of S^3 into two solid tori. One encircles the vertical axis, the other traces the vertical axis and passes through ∞, hence includes everything outside a compact neighborhood of the origin.

The existence of Heegaard splittings on 3-manifolds is essentially immediate from Morse theory:

Theorem 4.30. *Let M be a closed, oriented 3-manifold. Then M admits a Heegaard splitting.*

Proof. Let $f : M \to [0, 1]$ be a Morse function ordered so that the index 1 critical values fall in (0,1/2), and the index 2 critical values fall in (1/2,1). Say k is the number of index 1 critical points. $f^{-1}[0, 1/2]$ is a solid genus k handle-body with boundary $f^{-1}(1/2) \simeq \Sigma_k$. Considering f upside-down, $f^{-1}[1/2, 1]$ is also a solid handle-body, and must be of the same genus since the boundary is the same. A solid genus k handle-body is $\natural^k(S^1 \times D^2)$ up to diffeomorphism, thus $M_1 = f^{-1}[0, 1/2]$ and $M_2 = f^{-1}[1/2, 1]$ provide a Heegaard splitting of M. □

In general, a Heegaard splitting can be visualized by drawing simple closed curves in a genus k surface. Since M is obtained by attaching 2 and 3-handles to $\natural^k(S^1 \times D^2)$, and there is no choice involved in attaching the capping 3-handle, it suffices to specify the descending spheres of the 2-handles, which will be simple closed curves in the boundary of the 0 and 1 handle-body. Given such a collection of curves, the gluing diffeomorphism with the upside-down handle-body containing the 2 and 3-handles is then given by taking the ascending spheres of the upside-down handle-body to these descending spheres. Thus a drawing of a genus k with k simple closed curves marked as descending spheres specifies a Heegaard splitting. See Figure 4.16. A diagram of a genus k surface with a collection of k simple closed curves specifying a Heegaard splitting in this way is called a **Heegaard diagram**. Note however, that a Heegaard splitting is not uniquely described by a diagram: two Heegaard diagrams describe the same splitting if and only if they differ by handle slides and diffeomorphisms of the surface that rearrange the simple closed curves.

There is another equivalence under which two Heegaard diagrams determine the same 3-manifold. A given 3-manifold admits Heegaard splitting of different genus. Suppose that in the proof of Theorem 4.30, a different

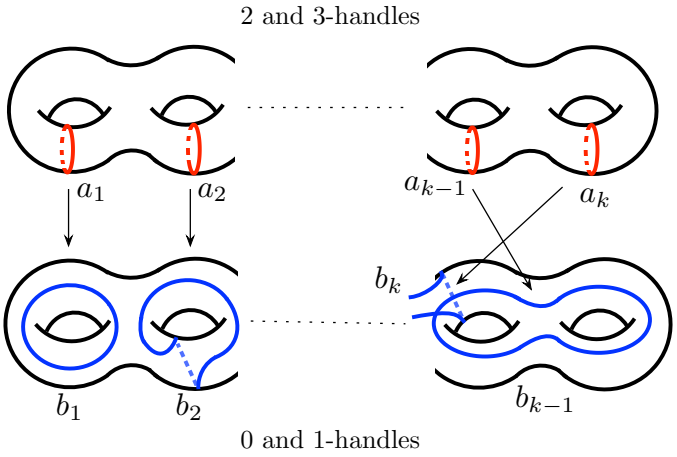

Figure 4.16: A Heegaard splitting on a surface of high genus. The ascending spheres $a_1, ..., a_k$ (red) of the 2 and 3 handle-body are taken to the specified descending spheres $b_1, ..., b_k$ (blue) of the 0 and 1 handle-body. The bottom surface with the blue curves is the Heegaard diagram.

Morse function had been chosen that had an additional pair of canceling critical points. The manifold, of course, does not change, but the genus of the splitting increases by one since there is an additional critical point of each index. Geometrically, the introduction of such a canceling pair of critical points corresponds to connect summing with S^3 with the genus-1 splitting describes above. The corresponding Heegaard diagrams are also connect summed with the standard splitting of S^3 from Example 4.29. This process of introducing a canceling pair of critical points to increase the genus of the splitting is called **stabilization**.

Example 4.31. The following example will be important for trisections. There is a natural splitting of $\#^k(S^1 \times S^2)$. One simply takes $\natural^k(S^1 \times D^2)$ and glues by the identity map. Thus for each cross-sectional disk $\{pt\} \times D^2$ the gluing attaches another disk to the boundary of the first, so the result is $\{pt\} \times S^2$. This decomposition can be stabilized to obtain a decomposition of genus g for any $g \geqslant k$.

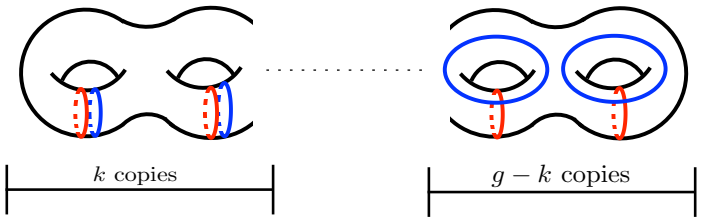

Figure 4.17: The Heegaard diagram for the splitting of $\#^k(S^1 \times S^2)$ of genus g. On the left, k simple closed curve are glued by the identity map, and on the right, $g - k$ copies of the standard splitting of S^3 are joined by connect sum.

It turns out that stabilization is the *only* redundancy in describing 3-manifold by Heegaard splitting. This is made precise by the following theorem.

Theorem 4.32. (Existence and Uniqueness of Heegaard Splittings) *There is a 1-1 correspondence*

$$\{\textit{closed oriented 3-manifolds}\}\Big/\textit{Diffeo.} \xleftrightarrow{\sim} \{\textit{Heegaard Splittings}\}\Big/\textit{Stabilization.}$$

Of course, a similar correspondence holds for Heegaard diagrams when one also quotients out by handle slides and diffeomorphisms of the surface. A complete proof of this result is given in [55].

Trisections of 4-manifolds

Consider for a moment trying to repeat the above construction of Heegaard splittings for a closed, oriented 4-manifold X. Let $f : X \to [0,1]$ be a Morse function with a single 0 and 4-handle. Unlike in the three-dimensional case, X does not easily split into two diffeomorphic pieces. Since a handle-body of X now has 1-handles, 2-handles, and 3-handles, the two handles will have to be divided between the two pieces and there is no reason in general this should be able to be done in such a way that the two pieces are the same.

One can achieve an analogous splitting, however, by allowing three pieces. Let $Z_k \simeq \natural^k(S^1 \times B^3)$. Let $\partial Z \simeq \#^k(S^1 \times S^2) \simeq Y^+_{k,g} \cup Y^-_{k,g}$ be the standard genus g Heegaard splitting of the boundary from Example 4.31.

Definition 4.33. *A* **(g,k)-trisection** *of a 4-manifold X is a decomposition $X = X_1 \cup X_2 \cup X_3$ such that*

- *There are diffeomorphisms $\varphi_i : X_i \xrightarrow{\sim} Z_k$ for $i = 1, 2, 3$.*
- *$\varphi_i(X_i \cap X_{i+1}) \simeq Y^-_{k,g}$ and $\varphi_i(X_i \cap X_{i-1}) \simeq Y^+_{k,g}$ where indices are taken mod 3.*
- *$\varphi_i(X_i \cap X_{i+1} \cap X_{i+2}) \simeq \Sigma_g$ is the Heegaard surface of the splitting $\partial Z_i \simeq Y^-_{k,g} \cup Y^+_{k,g}$ for $i = 1, 2, 3$.*

The three pieces of a trisection can be visualized as fitting together like a disk divided into three equal sectors (see Figure 4.18). Each sector has a boundary represented by two radii. The radial boundary of X_i bordering X_{i+1} represents a piece of the boundary sent by φ_i to $Y^-_{k,g}$, and the radial boundary bordering X_{i-1} is sent to $Y^+_{k,g}$. The three pieces intersect in a surface of genus g which lies in the center.

The pieces are glued together along their boundaries as subsets of X. Alternative, viewing each piece as an abstract copy of Z_k via φ_i, one can think of the three copies of Z_k glued along their boundaries by certain gluing maps. On each Z_k, a piece of the boundary is glued to a piece of each of the other two copies. Specifically, $Y^-_{k,g}$ of the i^{th} copy is glued to $Y^+_{k,g}$ of the next copy $(i+1)^{st}$ copy by the map $\Psi_{i,i+1} = \varphi^{-1}_{i+1} \circ \varphi_i$, and $Y^+_{k,g}$ of the i^{th} copy likewise glued to the $(i-1)^{st}$ copy. Thus, as in the case of Heegaard splittings, a trisection can be given by specifying three maps $\Psi_{i,i+1} : Y^-_{k,g} \to Y^+_{k,g}$. One should note when constructing trisections this way, however, that not all choices of gluing maps will result in a closed 4-manifold. For example, it is necessary for the composition $\Psi_{i,i+1} \circ \Psi_{i+1,i+2} \circ \Psi_{i_2,i}$ to be isotopic to the identity when restricted to the triple intersection Σ_g.

Example 4.34. There is a simple (0,0)-trisection of S^4. It is constructed as follows. Consider $S^4 \subseteq \mathbb{R}^5$ and choose a projection to $\mathbb{R}^2$. The image is the unit disk in the plane. Above each point $(x_1, x_2) \in \mathbb{R}^2$ the pre-images is $\{(x_1, ..., x_5) \mid x_3^2 + ... + x_5^2 = 1 - (x_1^2 + x_2^2)\} \simeq S^2$. Above the boundary points $\{(x_1, x_2) \mid x_1^2 + x_2^2 = 1\}$ the pre-image is a single point $(x_1, x_2, 0, 0, 0)$. Divide the disk into three equal segments that meet in the center. The pre-image of each sector is diffeomorphic to $\natural^0(S^1 \times B^3) \simeq B^4$. The pre-image of the boundary of each sector is a copy of S^3 with the trivial Heegaard splitting $B^3 \cup_{S^2} B^3$ given by the pre-images of the radial lines glued by the fiber above the origin, which is a copy of S^2.

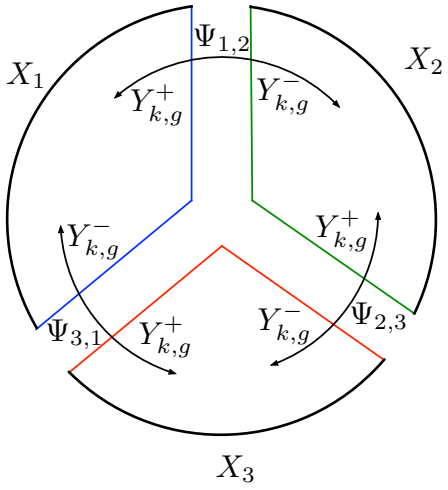

Figure 4.18: A depiction of how the three pieces of a trisection fit together.

Trisections on 4-manifolds can be constructed from Morse 2-functions, just as Heegaard splitting can be constructed from normal Morse functions on 3-manifolds. The projection of S^4 to the disk in the above example is a Morse 2-function. The construction for a general 4-manifold is essentially the same as for S^4: one takes a Morse 2-function to the disk, and the pre-images of three equal sectors provide the three pieces of the trisection.

Theorem 4.35. (Existence of Trisections, [54]) *Let X be a closed, oriented 4-manifold. Then X admits a (g,k)-trisection for some g, k.*

Proof. Choose a Morse 2-function $f : X \to D^2$ to the disk whose critical locus is as in Figure 4.19. Specifically, f should have the following three properties. (1) There is a single definite fold on the boundary of the disk. (2) The critical locus is a series of co-centric circles of index 1 moving in, except in three rectangular regions where arbitrary crossings (but not cusps) are allowed. (3) When D^2 is divided into three sectors, there is at most one cusp per component of $crit(f)$ per sector. Such a Morse 2-function can be constructed by a slight variation on the construction in Example 4.20 (see [54, 50] for the details).

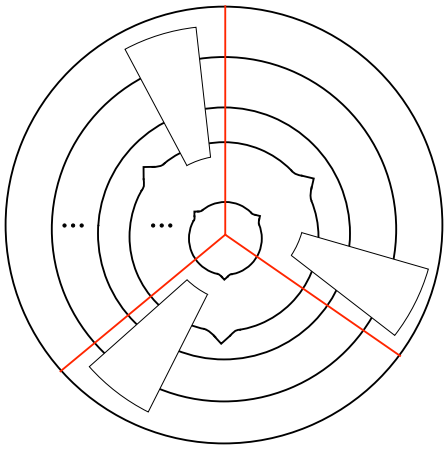

Figure 4.19: The desired critical locus configuration for $f : X \to D^2$. The rectangular boxes can contain arbitrary crossings. The dots denote some arbitrary number of components of crit(f).

Given an f with the desired configuration of $\mathrm{crit}(f)$ the pre-image of each sector $i = 1, 2, 3$ is diffeomorphic to $\natural^{k_i}(S^1 \times B^3)$ where k_i is the number of components of the critical locus with no cusp in sector i. This can be seen as follows. By an isotopy, it may be assumed that the sector is a half disk with a straight vertical boundary. The projection to the horizontal axis is a Morse function with a single critical point at each vertical tangency. Each component without a cusp, of which there are k_i, results in a single critical point of index 1 from its leftmost point which is a vertical tangency. Components with cusps are just pairs of canceling critical points, and have no vertical tangencies so do not affect the total space. In addition, it can be arranged that the crossings in the boxed regions also have no vertical tangencies, hence the crossings do not affect the total space either. Therefore, the pre-image of each sector is a diffeomorphic copy of a handle-body with exactly k_i 1-handles, which is $\natural^{k_i}(S^1 \times B^3)$.

A priori, the three numbers k_i can differ. To remedy this, one can introduce an "eye" in the center of the disk as in Figure 4.20. The eye configuration is familiar as one of the non-generic behaviors from Theorem 4.24. It is the result of introducing a canceling pair of critical points that annihilates immediately. When introducing an eye, it may be arranged by rotating that sector i receives no cusps, while the other two each receive on of the eye's two cusps. The effect is to increase the number of components without cusps in sector i by 1, thereby increasing k_i while keeping k_{i+1} and k_{i+2} fixed. This process can be repeated until $k = k_1 = k_2 = k_3$, in which case the three sectors all have pre-image $\natural^k(S^1 \times B^3)$ as desired.

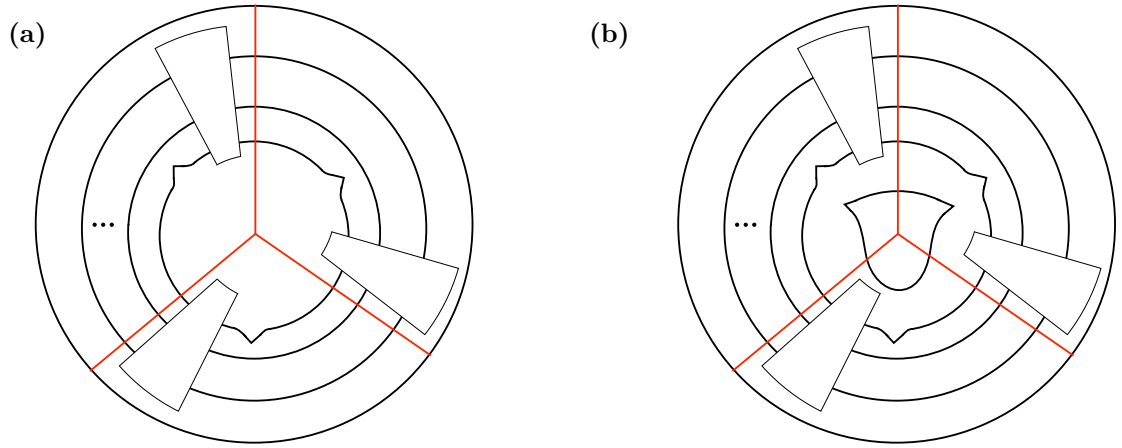

Figure 4.20: Introducing an eye to the critical locus of a Morse 2-function.

□

There is an easy analogue of the stabilization process for trisections. Given a Morse 2-function to the disk, one may always add three eyes in the center so that each second receives three new components two of which have cusps. Since each is a homotopy of a cancelling pair of critical points, the total space is unchanged. This operation gives each sector receives one new component without a cusp, the effect is to increase k by 1. This process is called a **trisection stabilization**. As in the case of Heegaard splittings on 3-manifolds, these stabilizations are the only redundancy in describing 4-manifolds with trisections.

Theorem 4.36. (Kirby, Gay [54, 56]) *There is a 1-1 correspondence*

$$\{\textit{closed oriented 4-manifolds}\}\Big/\textit{Diffeo.} \xleftrightarrow{\sim} \{\textit{Trisections}\}\Big/\textit{Stabilization.}$$

Example 4.37. (Trisection Invariants) By the above theorem, the structure of a trisection is, in some sense, itself an invariant of smooth 4-manifolds. Trisections can also be used to define other invariants of 4-manifolds. One method is to consider the Heegaard diagrams of the three Heegaard splittings in the central

Heegaard surface Σ_g. Thus the surface is decorated with three collections of curves $(\gamma_1, \gamma_2, \gamma_3)$ giving the three Heegaard splittings of ∂X_i.

(1) Considering the pairwise intersection pattern of these collections of curves gives three $g \times g$ matrices, which are an invariant of the four-manifold up to stabilization which direct sums each standard 3×3 blocks.

(2) The vector space $H_1(\Sigma_g; \mathbb{R})$ is symplectic vector space under the intersection pairing. It has three Lagrangian subspaces L_1, L_2, L_3 corresponding to the 3 collections of curves each being the kernel of the map induced on homology by the inclusion $F_g \to \partial X_i$ for $i = 1, 2, 3$. It has been shown that the Maslov index of this triple of Lagrangians is the signature of the 4-manifold [54].

Many additional methods of obtaining invariants from trisections are likely possible. So far, however, no invariants of trisections have been shown to contain anything more than simple homological data.

Example 4.38. (How not to solve the smooth 4-dimensional Poincaré Conjecture [57]) Trisections can be combined with the standard Van-Kampen theorem to obtain a purely group-theoretical statement of the smooth 4-dimensional Poincaré Conjecture [56]. Let

$$S_0 \simeq \pi_1(\Sigma_g, *) \qquad H_g = \langle c_1, ..., c_g \rangle \simeq \pi_1(\#^g(S^1 \times B^2), *) \qquad G_k = \langle d_1, ..., d_k \rangle \simeq \pi_1(X_i, *)$$

be the fundamental groups of the central Heegaard surface, ∂X_i, and X_i respectively. The fundamental group of the surface is $\pi_1(\Sigma_g, *) = \langle a_1, b_1, ..., a_g, b_g \ | [a_i, b_i] = 0 \rangle$, the others are free groups. A trisection gives a commutative cube of inclusions, to which one can apply the Van-Kampen theorem to obtain a commutative cube of the corresponding fundamental groups. Each map is surjective and each face is a pushout square.

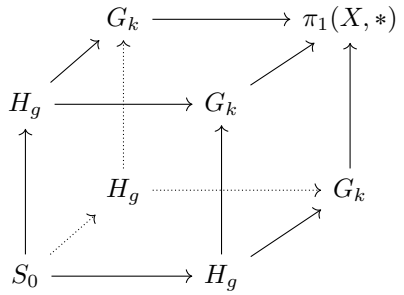

Definition 4.39. *A* **(g,k)-Group trisection** *of a group G is a commutative cube of groups as above with $G = \pi_1(X, *)$ and the groups S_0, H_g, G_k as above. Each homomorphism is required to be surjective and each face a pushout square.*

There is a standard $(3, 1)$-group trisection of the trivial group, which can be described simply in terms of generators [56]. A **group stabilization** is to take the free product with the (3,1)-trisection of the trivial group. One can show that the effect of a trisection stabilization on X results in a group stabilization of the fundamental groups, thus there is a 1-1 correspondence between group trisections up to isomorphism and stabilization and 4-manifold trisections up to diffeomorphism and stabilization. Applying this in case of $\pi_1(X, *) = 0$ results in the following statement.

Proposition 4.40. *The following two statements are equivalent:*

(I) *Any any compact, connected, orientable 4-manifold with trivial fundamental group is diffeomorphic to S^4.*

(II) *Any group trisection of the trivial group is stably equivalent to the trivial trisection of the trivial group.*

Statement (I) is of course the smooth 4-dimensional Poincaré conjecture, while (II) is a statement only about groups. Though as David Gay has pointed out in the talk after which this example was named, statement (II) seems rather more intractable than the conjecture itself.

Bibliography

[1] J. Lee, *Smooth Manifolds*, Springer, 2003.

[2] J .Milnor, *Morse Theory*, Princeton University Press, 2016.

[3] M. Audin and M. Damian, *Morse theory and Floer homology*, Springer, 2014.

[4] J. Vick, *Homology Theory: an Introduction to Algebraic Topology*, Springer, 2012.

[5] S. Kobayashi and K. Nomizu, *Foundations of Differential Geometry. Vol. 1*, New York: Wiley, 1969.

[6] J. Morgan and G. Tian, *Ricci Flow and the Poincaré Conjecture*, A.M.S., 2007.

[7] S. Smale, *Generalized Poincaré's conjecture in dimensions greater than four*, Annals of Math. **74** (1961), 391–406.

[8] S.K. Donaldson and P. Kronheimer, *The Geometry of Four-manifolds*, Oxford University Press, 1990.

[9] E.J.N. Looijenga, *Cohomology and intersection homology of algebraic varieties*, in *Complex Algebraic Geometry at Park City*, A.M.S., 1997, p. 221–263.

[10] K. Lamotke, *The topology of complex projective varieties after S. Lefschetz,* Topology, **20** (1981), 15–51.

[11] P. Griffiths and J. Harris, *Principles of Algebraic Geometry*, Wiley, 2014.

[12] B. Farb and D. Margalit, *A Primer on Mapping Class Groups*, Princeton University Press, 2011.

[13] D. Auroux, Lecture 14 in Lecture notes for the MIT course *Topics in Geometric Topology*, Spring 2006.

[14] L. Nicolaescu, *An Invitation to Morse Theory*, Springer, 2011.

[15] J. Milnor and J. Stasheff, *Characteristic Classes*, Princeton University Press, 2016.

[16] R.E. Gompf and A. Stipsicz, *4-manifolds and Kirby Calculus*, A.M.S., 1999.

[17] S. Akbulut, *4-Manifolds.* Oxford University Press, 2016.

[18] B. Moishezon, *Complex surfaces and connected sums of complex projective planes*, Springer Lecture Notes in Mathematics, vol. 603, Springer, 2006.

[19] A. Kas, *On the handlebody decomposition associated to a Lefschetz fibration*, Pacific Jour. Math., **89** (1980), 89–104.

[20] Y. Matsumoto et al. *Lefschetz fibrations of genus two-a topological approach*, in *Proceedings of the 37th Taniguchi Symposium on Topology and Teichmüller Spaces*, ed. Sadayoshi Kojima et al., World Scientific, 1996, p. 123-148.

[21] N. Hamada, R. Kobayashi, and N. Monden, *Non-holomorphic Lefschetz fibrations with* (-1)*-sections*, preprint, arXiv:1609.02420, 2016.

[22] D. Auroux, V. Muñoz, and F. Presas, *Lagrangian submanifolds and Lefschetz pencils*, Jour. Sympl. Geom. **3** (2005), 171–219.

[23] P. Seidel, *Fukaya Categories and Picard-Lefschetz Theory*, European Math. Soc., 2008.

[24] M. Zaidenberg, *Lectures on exotic algebraic structures on affine spaces*, preprint, math/9801075, 1998.

[25] R. Casals and E. Murphy, *Legendrian fronts for affine varieties*, preprint, arXiv:1610.06977, 2016.

[26] A. Keating, *Homological mirror symmetry for hypersurface cusp singularities*, preprint, arXiv:1510.08911, 2015.

[27] A. Cannas Da Silva, *Lectures on Symplectic Geometry*, Springer, 2001.

[28] D. McDuff and D. Salamon, *Introduction to Symplectic Topology*, Oxford University Press, 1998.

[29] V.I. Arnol'd, *Mathematical Methods of Classical Mechanics*, Springer, 2013.

[30] S.K. Donaldson, *Symplectic submanifolds and almost-complex geometry*, J. Diff. Geom. **44** (1996), 666–705.

[31] S.K. Donaldson, *Lefschetz pencils on symplectic manifolds*, J. Diff. Geom. **53** (1999), 205–236.

[32] W.P. Thurston, *Some simple examples of symplectic manifolds*, Proc. of the AMS, **55** (1976), 467–468.

[33] D. Auroux, *Asymptotically holomorphic families of symplectic submanifolds*, GAFA **7** (1997), 971–995.

[34] R. Bott and L.W. Tu, *Differential Forms in Algebraic Topology*, Springer, 2013.

[35] R. Gompf, *Symplectic structures from Lefschetz pencils in high dimensions*, Geom. & Topology Monographs **7** (2004), 267–290.

[36] S.K. Donaldson, *Lefschetz fibrations in symplectic geometry*, in *Proc. of the I.C.M.* vol. 2, Berlin, 1998., p. 309–314.

[37] D. Auroux and L. Katzarkov, *A degree doubling formula for braid monodromies and Lefschetz pencils*, Pure Appl. Math. Quarterly **4** (2008), 237–318.

[38] F. Presas, *Geometric decompositions of almost contact manifolds*, in *Contact and Symplectic Topology*, Springer, 2014, p. 137–172.

[39] P. Seidel, *Homological mirror symmetry for the genus two curve*, preprint, arXiv:0812.1171, 2008.

[40] M. McLean, *Lefschetz fibrations and symplectic homology*, Geom. & Topology **13** (2009), 1877–1944.

[41] R.I. Baykur and M. Korkmaz, *Small Lefschetz fibrations and exotic 4-manifolds*, Math. Annalen **367** (2016), 1–29.

[42] D. Auroux , S.K. Donaldson and L. Katzarkov, *Singular Lefschetz Pencils*, Geom. &Topology, **9**(2005), 1043–1114.

[43] K. Honda, *Local properties of self-dual harmonic 2-forms on a 4-manifold*, J. reine angew. Math. **577** (2004), 105–116.

[44] D. Gay and R. Kirby, *Constructing symplectic forms on 4–manifolds which vanish on circles*, Geom. &Topology **8** (2004), 743–777.

[45] D. Gay and R. Kirby, *Constructing Lefschetz-type fibrations on four-manifolds*, Geom. & Topology **11** (2007), 2075–2115.

[46] Y. Lekili, *Wrinkled fibrations on near-symplectic manifolds*, Geom. & Topology **13** (2009), 277–318.

[47] S. Akbulut and C. Karakurt, *Every 4-manifold is blf*, preprint, arXiv:0803.2297, 2008.

[48] D. Gay and R. Kirby, *Indefinite Morse 2-functions; broken fibrations and generalizations*, Geom. & Topol **19** (2015), 2465–2534.

[49] J. Williams, *The h–principle for broken Lefschetz fibrations*, Geom, & Topology **14** (2010), 1015–1061.

[50] Robion Kirby, Topology seminar at the University of Edinburgh, YouTube Lecture, `https://www.youtube.com/watch?v=UpyJRXuuUHg&t=2321s`, November 2012.

[51] D. Gay and R. Kirby, *Reconstructing 4–manifolds from Morse 2–functions*, Geom. & Topology Monographs **18** (2012), 103–114.

[52] T. Perutz, *Lagrangian matching invariants for fibred four-manifolds: I*, Geom. & Topology **11** (2007), 759–828.

[53] T. Perutz, *Lagrangian matching invariants for fibred four-manifolds: II*, Geom. & Topology **12** (2008), 1461–1542.

[54] D. Gay and R. Kirby, *Trisecting 4–manifolds*, Geom. & Topology **20** (2016), 3097–3132.

[55] M. Scharlemann. *Heegaard splittings of compact 3-manifolds*' preprint, math.GT/0007144, 2000.

[56] A. Abrams, D. Gay and R. Kirby, *Group trisections and smooth 4-manifolds*, preprint, arXiv:1605.06731, 2016.

[57] D. Gay, *How not to prove the smooth 4-dimensional Poincaré conjecture*, Boston Graduate Topology Seminar, Sep. 24, 2016.